

**ROLE OF FUNGI IN THE BIOFILTRATION OF LIVESTOCK HOUSING AND
MANURE STORAGE EMISSIONS**

A Dissertation

SUBMITTED TO THE FACULTY OF
UNIVERSITY OF MINNESOTA

BY

Jason Paul Oliver

IN PARTIAL FULFILLMENT OF THE REQUIREMENTS
FOR THE DEGREE OF
DOCTOR OF PHILOSOPHY

Jonathan S. Schilling

August 2015

© Jason Paul Oliver, 2015

ACKNOWLEDGEMENTS

Funding for this project was provided by grants from the United States Department of Agriculture, National Institute of Food and Agriculture, Agriculture and Food Research Initiative (USDA/2010-85112-20520 & USDA/2012-69002-19880) and the USDA, NIFA McIntire-Stennis Project (#MIN-12-074). I would like to thank my advisor Dr. Jonathan S. Schilling for his mentorship, open door, and the space he created for learning; my committee Drs. Kevin A. Janni, Larry D. Jacobson, Paige J. Novak and Robert A. Blanchette, for their thoughtful guidance; Brian Hetchler for his hands-on expertise and insight; members of the Schilling laboratory for their research support; Justin Kaffenberger for thoughtful feedback; Zewei Song for help with molecular work; Gerry Presley and the others at the University of Minnesota Mycology Club for their fun fungal energy; and the United States Forest Service Laboratory in Grand Rapids, MN for use of laboratory equipment.

DEDICATION

I dedicate this dissertation to my future wife, Amy T. Fox, for her love, support and patience; to my bored dogs, Goldberry and Esau, for tolerating my attention to work instead of them; and to the hope for long-term sustainability of agricultural systems and rural economies.

ABSTRACT

Biofilters use porous media colonized by microbial biofilms to capture and degrade odorous, hazardous and greenhouse gases making them well-suited for livestock housing and manure storage emissions. Fungi are abundant in these biofilters though their dynamics, degradation of media, community shifts, and functional roles have not been well-investigated. To explore spatial and temporal fungal dynamics in full-scale woodchip biofilters treating swine barn emissions, a novel monitoring approach was developed. Using wooden baits and microbial measures optimized to target biofilms biofilter fungi were characterized and shown to tolerate media desiccation. Additionally, successional patterns at the taxa and guild level were studied, and the development of a dominant fungal community was identified. To address the practical question of media longevity, a litter bag study was deployed in the same full-scale biofilters. Decay rates of various media types were identified, and microbial decay was dependent on media quality, nitrogen, and emissions levels. Using a lab-scale biofilter system, fungi were shown to improve the capture of methane, particularly after periods of low-concentration inlet emissions. Using a chromatographic isotherm the ability of fungi to sorb methane gas was verified for the first time. Collectively, this work showcases dynamics and potential abilities of fungi in biofilters treating livestock production emission and may be used to guide subsequent efforts to connect fungi to biofilter function. If these processes can be understood and controlled, there is the potential to improving biofilter performance, better protect air quality and improve farming system sustainability.

TABLE OF CONTENTS

List of Tables	vii
List of Figures	viii
1. Introduction and Literature Review	1
1.1. Impact of modern livestock production on air quality	1
1.2. Controlling livestock emissions	5
1.2.1. Biofilter design and function	6
1.2.2. Understanding biofilter microbial ecology	8
1.2.3. Potential roles of biofilter fungi	10
2. Research Objectives	13
3. A New Approach for Assessing Biofilm Microbial Communities on Organic Media Used for Gas-Phase Biofiltration	14
3.1. Summary	14
3.2. Introduction	15
3.2.1. Focused microbial ecology can guide and improve biofilter performance. 15	
3.2.2. Full-scale field monitoring is needed to link real-world biofilter performance to microbial communities	16
3.2.3. Monitoring microbes in full-scale biofilters should be high-throughput and target biofilm communities	18
3.2.4. Aims	19
3.3. Materials and methods	20
3.3.1. Study site, biofilter design, conditions & performance	20
3.3.2. Wood baits for optimized biofilm sampling	21
3.3.3. Microbial biomarkers	25
3.3.4. Confocal microscopy	27
3.3.5. Statistical analyses	27
3.4. Results	28
3.4.1. Targeting biofilm communities	28
3.4.2. Biofilm sample size requirements	31
3.4.3. Biofilm fungi in full-scale biofilters	33
3.5. Discussion	37
3.5.1. Wood baits were effective and isolating biofilms improved measurement precision	37
3.5.2. The effect of biofilm sample weight on the extraction of microbial biomarkers	40
3.5.3. The fungal:total microbial ratio was greatest in biofilms harvested from drier biofilter media.	41
3.6. Conclusions	44
4. Fungal Dynamics in a Full-Scale Biofilter	46
4.1. Summary	46
4.2. Introduction	47

4.2.1. Inherent complexity of biofiltering systems	47
4.2.2. Assessment of microbial variability and community shift are needed	47
4.2.3. Fungi are potential keystone species in biofilters	49
4.2.4. Aims	49
4.3. Methods.....	50
4.3.1. Study site.....	50
4.3.2. Biofilm monitoring	50
4.3.3. Fungal succession monitoring.....	52
4.3.4. Statistics	54
4.4. Results.....	55
4.4.1. Consequences of microbial growths on biofilter media and its variability	55
4.4.2. Variability of microbial measures on biofilter media	57
4.4.3. Fungal communities in a livestock emission biofilter	59
4.5. Discussion	65
4.5.1. Microbial dynamics and variability in a full-scale biofilters	65
4.5.2. Successional patterns of fungi in a biofilter.....	67
4.6. Conclusions.....	68
5. Linking Media Decay with Traits to Better Predict Biofilter Longevity.....	70
5.1. Summary	70
5.2. Introduction.....	70
5.3. Methods.....	73
5.3.1 Biofilter media, litter bags, and field site.....	73
5.3.2. Media characterization.....	75
5.3.3. Nitrogen treatment tests	76
5.3.4. Statistics	78
5.4. Results.....	79
5.4.1. Decay rates of various biofilter media	79
5.4.2. Predictors of biofilter media longevity	82
5.4.3. Effect of N loading on decay of biofilter media	84
5.4.4. Influence of livestock production emissions on decay rates.....	86
5.5. Discussion	87
5.5.1. Media decay patterns were distinct.....	87
5.5.2. Media quality predicted decay	90
5.5.3. N enrichment altered decay rates	92
5.5.4. Recommendations for biofilter end-users.....	93
5.6. Conclusions.....	94
6. Potential Role of Biofilter Fungi in CH ₄ Capture.....	96
6.1. Summary	96
6.2. Introduction.....	96
6.3. Methods.....	100
6.3.1. Lab-scale biofilter	100
6.3.2. Screening the potential of fungi to improve CH ₄ biofiltration.	101

6.3.3. Effect of fungal biomass on CH ₄ biofiltration.....	103
6.3.4. Chromatographic isotherm - Sorption of CH ₄ by fungal materials	103
6.3.5. Statistical analyses	105
6.4. Results.....	106
6.4.1. Ability of fungal biofilters to mitigate CH ₄	106
6.4.2. Increased <i>P. ostreatus</i> biomass improved CH ₄ biofiltration.....	107
6.4.3. Fungal sorption of CH ₄ in a chromatographic isotherm	109
6.5. Discussion	111
6.5.1. Fungi improved CH ₄ biofiltration at lab-scale.....	111
6.5.2. Fungi can sorb CH ₄	113
6.5.3. Interactions of fungi and methanotrophs	114
6.6. Conclusions.....	115
7. Conclusions.....	116
8. Bibliography	117
9. Appendixes	133

LIST OF TABLES

Table 3.1 Summary of inlet emissions and biofilter performance measured by bag sampling. Year one emissions, measured semi-continuously, can be found in Janni et al. (2014).	21
Table 4.1 The 5 dominant fungal OTUs in each sample and their percent abundance....	65
Table 5.1 Mean and (standard deviation) of initial physiochemical traits of tested biofilter media (n=3 per analysis).	77
Table 5.2 Means and (standard deviations) of decay rate constants (yr^{-1}) for the first 3 mo. ($k_{3\text{mo}}$), for losses from June 2012-June 2013 ($k_{\text{year 1}}$), for losses from June 2013-2014 ($k_{\text{year 2}}$), and for the full 27mo. of decay ($k_{27\text{mo}}$) for both the treatment and control biofilter locations (n=5).	82
Table 5.3 Significant simplified models for predicting biofilter media weight loss for early (3 mo.) and long-term (27 mo.) decay for each biofilter location (control & treatment) noting the intercept, coefficient values, degrees of freedom (df) and the coefficients of determination (R^2). Long-term models using only C and N as predictors are also included.	83
Table 5.4 Means and standard deviations of decay rate constants (yr^{-1}) for the N treated birch and SYP media for both the treatment ($k_{\text{Treatment}}$) and the control (k_{Control}) biofilter locations.	85
Table 6.1 Statistical differences in CH_4 capture of microbial treatments during peak emissions.	107

LIST OF FIGURES

Figure 1.1 Percentage of total U.S. livestock inventory produced on concentrated animal feeding operations.	2
Figure 1.2 U.S. anthropogenic NH ₃ emissions by source.	3
Figure 1.3 U.S. anthropogenic CH ₄ emissions by source.	5
Figure 3.1 a) Photograph and microbial sampling locations (schematic) in the full-scale biofilter treating exhaust air from a swine nursery. The air plenum was subdivided so that each exhaust fan delivered air to a separate part of the biofilter. See Janni et al. (2014) for details. Monitoring was focused on the biofilter area fed by a continuous running pit fan. Inlet emissions were measured in the plenum (C _i), while outlet emissions were measured shallow in the biofilter, between microbial sample points (C _o). b) Schematic of wood wafers used as microbial biofilm baits. Wafers were sub-sectioned for the measurement of moisture content and microbial biomarker extraction was conducted on sample fractions to separate biofilm from microbial growth inside the wood.	22
Figure 3.2 The effect of sample fractioning on extraction of microbial biomarkers from baits incubated 8 mo. in a biofilter microcosm. For each biomarker (n=10) tested subsamples included baits with an attached biofilm left whole (<i>attached whole</i>), or milled (<i>attached ground</i>), biofilms (<i>detached biofilm</i>), biofilm-free wood left whole (<i>wood whole</i>), or milled (<i>wood ground</i>), and the sum of paired biofilm and wood fractions (<i>sum</i>). Non-incubated treatments (<i>controls</i>) (n=5) were also tested. Means with different letters are significantly different ($\alpha = 0.05$). Boxplots depict the media, 1st and 3rd quartiles, and quartile values plus or minus the interquartile range times 1.5. Circles represent outliers.	30
Figure 3.3 The effect of biofilm sample weight on the extraction of microbial C, ergosterol (n=10) and total DNA (n=6). For each biomarker, means with different letters are significantly different ($\alpha=0.05$).	32
Figure 3.4 Regressions average coefficient of variation (CV) for dry weight normalized total microbial C (CFE), total ergosterol (ERG) (n=10), and total DNA (DNA) (n=6) and the biofilm sample weight.	33
Figure 3.5 Boxplots depicting total fungal:total microbial biomass ratios (measured as mass normalized total ergosterol to total microbial C) of biofilter sampling locations for biofilm (light grey) and wood substrates (dark grey). On the second axis is the mean sample moisture content (% dry weight) of biofilter sampling locations (black diamonds), standard deviation represented by the error bars (n=6). Means with different letters are significantly different ($\alpha = 0.05$).	34
Figure 3.6 Linear model of the total fungal:total microbial biomass ratio (measured as mass normalized total ergosterol to total microbial C) and sample moisture content (% dry weight) indicating the ability of fungi to tolerate drier conditions. Location variable affects were tested and found to be not significant.	35

Figure 3.7 Boxplots depicting fungal:bacterial biomass ratio (Ct Fungi: Ct Bacteria) of biofilter sampling locations for biofilm samples based on qPCR results.	36
Figure 3.8 a) Photograph of a bait from the far-shallow location after the moisture content subsection was removed. A fungal dominant biofilm can be seen growing on the bait surface. b) Cross section of the bait showing drill holes used to sample internal microbial biomass. Aerial hyphae can be seen extending out from the biofilm and wood degradation is evident below the biofilm. The black box indicates the approximate location of the confocal image. c) An unmixed, stitched confocal micrograph of biofilm and bait section showing fungal hyphae (stained with WGA-TMR, excited with a 561 laser) growing aerially (white arrow) and connected to mycelial growths in and across wood cells. The dashed line indicates the surface of the bait.....	37
Figure 4.1 Spatial and temporal media moisture content and mass loss of baits collected from the north and south biofilters.....	56
Figure 4.2 Coefficient of variation of moisture content and mass loss at the final 3 year harvest date. Levels of comparison include chips of the same bait (chips), baits of the same location (baits), chips for an entire sample location (location), and all the sampled chips of a biofilter (biofilter).	57
Figure 4.3 Average ergosterol and fungal biomass ratios over time in the north and south biofilters.	58
Figure 4.4 Coefficient of variation of microbial C and ergosterol biomass at the final 3 year harvest date. Levels of comparison include subsamples of the same biomass pool (subsample), biomass pools of separate chips from the same bait (chips), chips for an entire sample location (location), and all the sampled chips of a biofilter (biofilter).	59
Figure 4.5 Shannon alpha diversity metrics for biofilter sample communities. Similar letters note measures that are not significantly different (n=3).	60
Figure 4.6 Phylum and class level fungal community structure by sample of the 50 most abundant OTUs.	61
Figure 4.7 Identifiable guilds of the biofilter fungal communities.	62
Figure 4.8 Nonmetric multidimensional scaling (NMDS) ordination of sample biofilter community data showing the influence of the vector time.	63
Figure 4.9 Similarity based on Bray-Curtis of year 1 and 3 communities to the initial communities of either time0 media or the manure.	64
Figure 5.1 Mass loss of biofilter media incubated in the treatment location (n=5).	80
Figure 5.2 Mass loss of biofilter media incubated in the control location (n=5).	81
Figure 5.3 Mass loss of N-amended birch media incubated in the treatment and control locations of the biofilter for 12 mo. (n=10). Different letters note means that are significantly different ($\alpha=0.05$).	84
Figure 5.4 Mass loss of N-amended SYP media incubated in the treatment and control locations of the biofilter for 12 mo. (n=10). Different letters note means that are significantly different ($\alpha = 0.05$).	85

Figure 6.1 Schematics of a) the single biofilter column, b) the lab-scale biofilter assembly, and c) a photograph of the installed system.	100
Figure 6.2 a) Schematic of the isotherm column, and a photo of b) the column, and c) the column installed into the GC.	105
Figure 6.3 Capture of manure storage CH ₄ by biofilter columns with various microbial inocula.	106
Figure 6.4 CH ₄ capture by lab-scale biofilter columns packed with increasing amounts of <i>P. ostreatus</i> fungal biomass.	108
Figure 6.5 Boxplot of CH ₄ capture by <i>P. ostreatus</i> at day 3 (n=4). Different letters note statistically different means ($\alpha=0.05$).	108
Figure 6.6 SEM images of sand mixed with a) ascomycete and b) basidiomycete fungal spores. Insert photos show the spores at higher magnification.	109
Figure 6.7 Overlay of chromatographic outputs of a sand control and a sand/basidiospore test sorbent.	110
Figure 6.8 Peak area of control and test sorbents for various levels (w/w) of basidiomycete (Basid) or ascomycete (Asco) fungal materials (n=20). Different letters denote significantly different mean values ($\alpha=0.5$)	111

1. INTRODUCTION AND LITERATURE REVIEW

1.1. Impact of modern livestock production on air quality

Globally, livestock production is growing (Ilea, 2009). In developed nations, production gains are the result of increased usage of efficient, consolidated farming systems called concentrated animal feeding operations (CAFOs). These farms are large herd size animal feeding operations on small production land areas where livestock, feed and excrement are all held (US-EPA, 2015b; US-EPA, 2015c). In the United States, the use of these farming systems has significantly increased over the last 50 years (Figure 1.1). Unfortunately, alongside the production gains of consolidated animal agriculture are an associated degradation of water and air resources (Jacobson et al., 2011; Steinfeld et al., 2006).

Only in the last 20 years has the impact of livestock production on the atmosphere received serious scientific attention (NAS, 2003). This was prompted by public and health professional concerns over the increased concentration and generation of untreated odorous wastes from modern farming systems (APHA, 2003; Trabue et al., 2010). CAFO emissions are now understood to be complex mixtures of odorants, volatile organic carbons (VOCs), hazardous gases, greenhouse gases (GHGs), particulate matter and bioaerosols that change in composition with animal type, age, diet, housing, manure management and production system. In fact, hundreds of odorous VOC types can be emitted by a single farm (Lo et al., 2008; Schiffman et al., 2001).

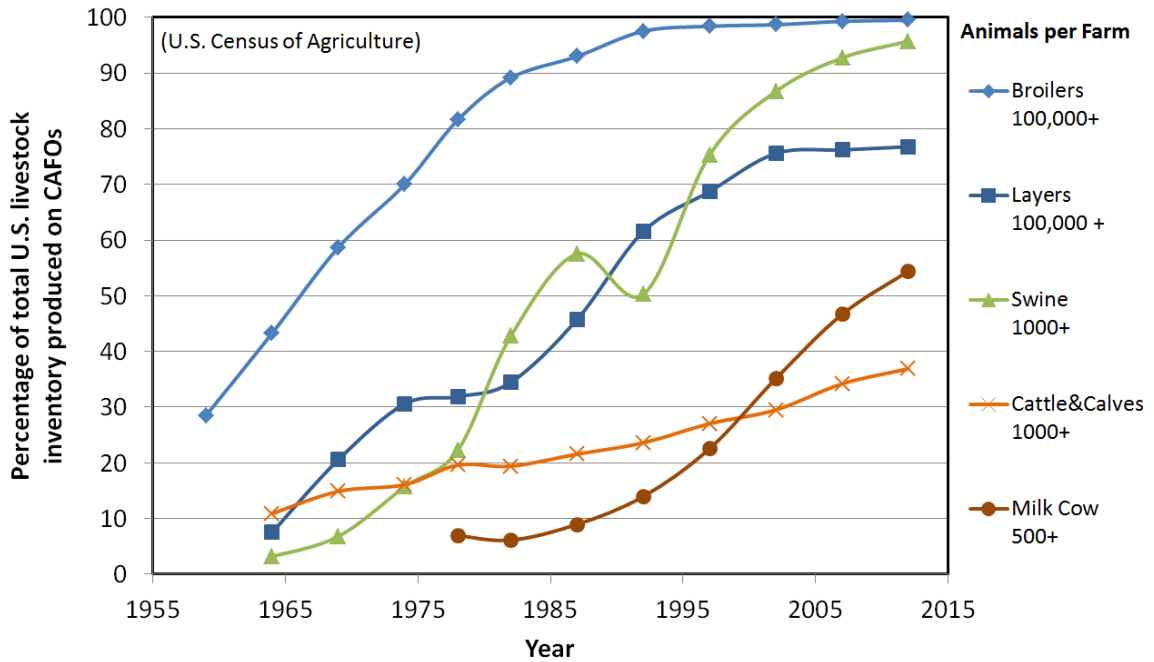


Figure 1.1 Percentage of total U.S. livestock inventory produced on concentrated animal feeding operations.

Odorous emissions from animal agriculture negatively impact property values (Edwards & Massey, 2011; Isakson & Ecker, 2008), the well-being of near-by residences (Cole et al., 2000; O'Connor et al., 2010), and can seriously impair health. In farmers, chronic exposure to farm generated VOCs and gases has been linked to increased respiratory illness and decreased lung function (May et al., 2012; Szadkowska-Stanczyk et al., 2010). These emissions similarly harm the health of neighboring communities (Donham et al., 2006), with possible disproportionate effects on underrepresented, low-income communities (Wilson et al., 2002; Wing et al., 2000), though these findings have been difficult to substantiate (O'Connor et al., 2010). Livestock is also affected, with reduced pulmonary function and growth rates linked to hazardous farm emissions (Holland et al., 2002).

Noteworthy hazardous livestock production emissions include hydrogen sulfide (H_2S) and ammonia (NH_3). Hydrogen sulfide is a potent odorant generated from anaerobic manure storages (Jacobson et al., 2006) which is hazardous at high concentrations, with acute exposures sometimes fatal (CDC, 2006). Ammonia, also odorous, is generated directly from ammoniacal-N in urine or from the transformation of urea in manure (Jacobson et al., 2004; Liang et al., 2006). Like H_2S , NH_3 is life-threatening at concentrated levels and can impair respiratory functions at low concentrations (CDC, 2004; NYS-DOH, 2004). Livestock production is the most significant source of NH_3 in the U.S., emitting >70% of the total national anthropogenic emission of the gas (US-EPA, 2012a) (Figure 1.2).

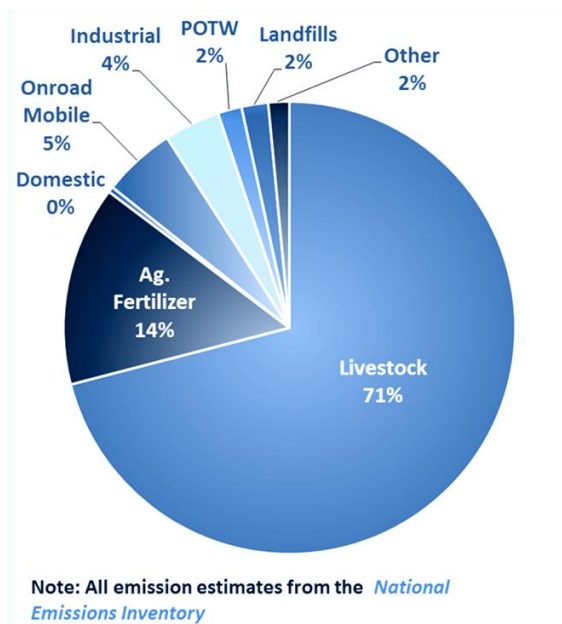


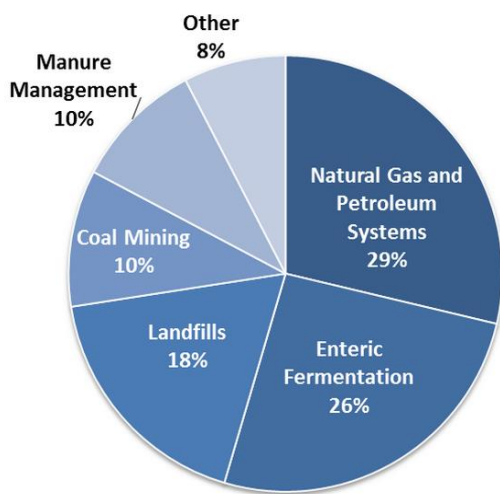
Figure 1.2 U.S. anthropogenic NH_3 emissions by source.

Emissions from livestock production systems also significantly impact the environment. For example, H_2S reacts with atmospheric oxygen and water to form sulfuric acid, a significant contributor to regional acid deposition. Due to a short

atmospheric residence time, NH_3 is deposited near farms leading to localized eutrophication of surface waters (Hristov et al., 2011; Ritz et al., 2004). Ammonia can also impact the environment at greater distances by reacting with acid gases in the atmosphere to form fine particulate matter, a haze-producing secondary pollutant (US-EPA, 2004). Particulate matter formed by this reaction or emitted directly by farms can lead to cloud formation and radiative forcing, altering climate (IPCC, 2007). More directly contributing to climate change, however, are the GHGs carbon dioxide (CO_2), methane (CH_4) and nitrous oxide (N_2O); CH_4 and N_2O having $\sim 25\times$ and $300\times$ times the heat trapping effect of CO_2 , respectively (IPCC, 2007). Livestock production accounts for 9%, 35-40% and 65% of global anthropogenic emissions of CO_2 , CH_4 , and N_2O , respectively, equal to 18% of total GHG emissions (Steinfeld et al., 2006). While most U.S. GHG emissions are from fossil fuel combustion (Jacobson et al., 2011), livestock production is the primary source of anthropogenic CH_4 (Figure 1.3).

Methane is a particular emission of concern for both its significance and the potential benefits of its mitigation. Generation of CH_4 from enteric fermentation and anaerobic manure storage in the U.S. has increased $\sim 15\%$ in the last 10 years. While only 3.1% of total U.S. anthropogenic GHG production (as CO_2 equivalents), U.S. CH_4 emissions (as CO_2 equivalents) exceed the GHG releases of some industrialized countries (US-EPA, 2013; US-EPA, 2012b) and thus can be considered a significant emission. Mitigating farm produced CH_4 can help keep global warming below dangerous thresholds and reduce near-term climate change impacts. This is due to the significant

warming potential and relatively short atmospheric residence time (~10 y versus ~100 y for CO₂) of CH₄ (IPCC, 2007). As the benefits of CH₄ mitigation can be realized in decades, not centuries, both scientist and politicians have called to quickly reduce anthropogenic emissions of the GHG (Montzka et al., 2011; Shindell et al., 2012; U.S. Department of State, 2010; UNEP & WMO, 2011; White House, 2014).



Note: All emission estimates from the *Inventory of U.S. Greenhouse Gas Emissions and Sinks: 1990–2013*.

Figure 1.3 U.S. anthropogenic CH₄ emissions by source.

1.2. Controlling livestock emissions

Complete reduction of livestock emissions like NH₃ and CH₄ will require both primary and secondary control. Primary, or source control, uses improved diet (Hayes et al., 2004; Meda et al., 2011; Satter et al., 2002; Sutton et al., 1999) and animal productivity (Capper et al., 2009), additives (Guarino et al., 2007; McCrory & Hobbs, 2001), and changes to housing, bedding and ventilation to control emissions. While these efforts can reduce emissions, livestock physiology limits the potential for total elimination and makes secondary control measures essential.

Many secondary air pollution control technologies are available (Vallero, 2008), though biotechnologies, like biofilters, are best suited for the low-concentration, mixed-composition emissions of livestock production (Delhomenie & Heitz, 2005). Additionally, biofilters can be constructed by end-users, operated at ambient temperatures, power for pollutant removal is supplied by the catabolism of heterotrophic microorganisms, and pollutant breakdown minimizes secondary treatment and handling requirements. These attributes keep construction and operational costs low and further suit biofilters for farm applications.

1.2.1. Biofilter design and function

Biofilters can remove > 90% of H₂S and NH₃, 75-90% of odor, and 50% of CH₄ from livestock emissions, in addition to other VOCs and particulates (Chen et al., 2008b). Removal efficiencies at both lab- and field-scale are quite variable, however, due to limited system knowledge and process unpredictability (Chen et al., 2009). To date, models based on simplified, laboratory biofiltration systems have been insufficiently robust for widespread use (Devinny & Ramesh, 2005). As a result, full-scale biofilter design in the U.S. are based on empirical experience and ‘rule of thumb’ measures (Schmidt et al., 2004). The fundamental design parameter is empty bed contact time (EBCT) which relates biofilter size to effluent flow rate:

$$EBCT = \frac{V_f}{Q} \quad (1.1)$$

where V_f = volume filter bed media (m^3), and Q = air flow rate ($m^3 s^{-1}$). A 5 to 10 s EBCT is used for manure storage odor (Schmidt et al., 2004) and existing vent fan specifications determine Q enabling calculation V_f .

Media, sometimes called packing material, is the foundation of a biofilter. It provides physical structure that must be porous enough to facilitate air flow and minimize pressure drop, but high enough in surface area to maximize microbial attachment and reaction sites. Media must also have high water holding capacity to limit desiccation and maintain the optimal 40-60% moisture content (Chen et al., 2008a; Goldstein, 1999; Nicolai & Lefers, 2006; Nicolai et al., 2006). Recalcitrant, engineered media are being developed to optimize these attributes (e.g. synthetic foam cubes, biochar), but their high cost and poor availability have limited their use by U.S. livestock producers. Instead, low-cost organic media is typically used, such as peat, soil, compost, wood chips, and mulch (Chen & Hoff, 2009), with agricultural by-products promising alternatives (Akdeniz et al., 2014; Ramirez-Lopez et al., 2003). Additionally, organic media provide carbon and nutrients for microbial growth and have indigenous microbial populations that may participate in the biofiltration process. The main drawback of these media is their degradation, compaction and resulting performance loss, which necessitates semi-regular replacement. The useful life of media is estimated at 3-5 years (Chen & Hoff, 2009), though longevity will depend on media type and the abiotic and biotic conditions of the biofilter. These drivers of media degradation have not been thoroughly explored, though such work could improve replacement frequency and cost estimates.

The performance of a biofilter is often assessed by its removal efficiency (RE), defined as the fraction of contaminant removed:

$$RE = \frac{C_{\text{inlet}} - C_{\text{outlet}}}{C_{\text{inlet}}} \times 100 \quad (1.2)$$

where C_{inlet} = inlet gas concentration (ppm), and C_{outlet} = outlet concentration (ppm). Successful biofiltration is dependent on both physiochemical and biological processes. Initially, emissions are captured from the passing air by the biofilm and media. Once condensed, the pollutant moves along concentration gradients in the biofilm to microbial oxidation sites where they are degraded (Deviny & Ramesh, 2005). Seemingly a straightforward process, actual dynamics are complex. Firstly, adsorption onto media and microbial cells, and absorption into extracellular material and free water is not always fast or permanent and can be rate limiting with these high velocity effluents. Secondly, pollutant transport and oxidation is governed by a concert of metabolisms and microbial ecological processes which remain opaque, difficult to model and control.

1.2.2. Understanding biofilter microbial ecology

Linking microbial ecology to system function is an active research area in both natural and engineered environments. Discerning these relationships in biofilters offers the potential to improve design, operation and pollutant targeting for enhanced performance. In biofilters, we know prokaryotic and fungal communities are assembled into complex, 3-dimensional congregations, called biofilms, which are fixed together and to the surface of biofilter media by extracellular substances. However, we lack a

comprehensive understanding of how variable these biofilms are, how to effectively sample them, and of what importance some taxa may have to the biofiltration process.

We do know the function of some biofilm microbes, however, such as the NH_3 oxidizing bacteria and Archaea which oxidize NH_3 , the colorless sulfur bacteria which oxidize H_2S (Madigan et al., 2009), and the methanotrophs which oxidize CH_4 (Semrau et al., 2010). As a result, correlating the presence of these groups to pollutant removal has been a common approach to study biofilter ecology, particularly in laboratory systems. Though functionally relevant, such an approach is narrowly focused and may overlook other microbial groups with significant influence on performance. Work by Juhler et al. (2009) illustrates this point, where NH_3 oxidizing bacteria populations were not clearly correlated to NH_3 concentrations, as breakdown products and competition for oxygen by more prolific VOC degrading heterotrophs were found to restrict their growth. Thus, VOCs had to first be removed to enable NH_3 oxidation to improve, and only by investigating a more complete community was this ascertained.

Full community analysis is another approach used to improve our understanding of biofilter microbial ecology, though complex results and contradictory patterns can limit taxa based approaches (Cabrol & Malhautier, 2011). For example, both stable and dynamic microbial communities have been associated with stable biofilter function (Cabrol et al., 2012a; Friedrich et al., 2003; Sakano & Kerkhof, 1998) and fluctuating pollutant loading (Cabrol et al., 2012b), with incompletely resolved influences of operational history (Cabrol et al., 2009). Though the uses of these powerful approaches

are improving our understanding of biofilter communities, new functional measures of these communities are needed to fully understand biofilter dynamics (Briones & Raskin, 2003; Franklin & Mills, 2006).

Diversity based measures can be quite informative, however, when studying microbial succession and biofilter startup. Biofilters often lag in performance following construction, controlling emissions only once an appropriate dominant microbial community has established. Both media amendments (Vergara-Fernandez et al., 2011) and inoculum acclimation strategies (Elias et al., 2010) have been investigated to reduce this performance lag time. In lab-scale studies, large shifts from the diversity inherent in the organic media (Ding et al., 2008) and inoculum (Steele et al., 2005) have been reported, even with optimized inoculum (Falk et al., 2009), resulting in an adapted dominant community (Steele et al., 2005). This is the result of strong environmental selection, microbial competition and the seeding of novel microbial cells from aerosolized effluent (Ho et al., 2008). Diversity changes following construction have not been thoroughly investigated in the field or over long periods, and have rarely addressed the fungal community. Such research efforts would greatly add to the understanding of biofilter microbial acclimation and may help target efforts to develop inoculum and reduce lag time.

1.2.3. Potential roles of biofilter fungi

When the research focus is connecting full-scale biofilter performance to biofilm communities, functional measures focused broadly on the major microbial groups - fungi

and bacteria - rather than on specific oxidation processes can help initiate the study of these large, heterogeneous, complex bioreactors. In soils for example, the fungal:bacterial ratio is a useful indicator of soil fertility and health (Strickland & Rousk, 2010) and can support the study of large-scale below-ground biodiversity-ecosystem functional patterns (Fierer et al., 2009). This same potential exists for biofilters, though fungi and their interactions with other biofilm microbes have largely been overlooked (Ralebitso-Senior et al., 2012). From the relatively few studies of biofilter fungi, several unique attributes are identifiable which give them unique potential to affect biofilter performance. These include: 1) tolerance to desiccation (Kennes & Veiga, 2004) and low-pH conditions (Devinny et al., 1999), both common stresses to stable biofilter performance; 2) their filamentous (hyphal) growth which can extend into media pore space to increase the effective surface area in contact with the polluted airstream (Arriaga & Revah, 2005; van Groenestijn, 2001); and 3) the unique coatings of extracellular proteins on hyphae (Wosten, 2001) that provide desirable physiochemical surface properties that may enable improved capture of emissions, such as hydrophobic industrial VOCs (Cox et al., 1997; Estevez et al., 2005a; Jorio et al., 2009; Spigno et al., 2003). In the presence of VOCs, fungal biomass has been shown to increase in hydrophobicity and surface area (Vergara-Fernandez et al., 2006), a potential capture increasing response that may be harnessable for some poorly soluble livestock emissions. The physical, not oxidative, process of pollutant capture (which is often rate limiting) makes measurement of this distinct microbial biomass functionally relevant.

The presence of fungi in livestock emission biofilters has not been thoroughly studied, particularly in full-scale systems despite their noted abundance (Cardenas-Gonzales et al., 1999; Kristiansen et al., 2011a; Xue et al., 2013). Developing fungal biofilm sampling approaches suitable for these systems, discerning measurement and environmental variability, and exploring fundamental spatial/temporal dynamics are all needed first step to begin characterizing the potential biofiltration capacity of fungi. Broad initial characterization of these keystone decay organisms can help target focused, follow-up analyses in full-scale biofilters and improve knowledge of biofilter microbial ecology (Cabrol & Malhautier, 2011). By contributing knowledge about the ecology of an understudied, yet potentially important, biofilter microbial population (i.e. fungi), our understanding of biofilter function can be advanced, leading to potential improvements in biofilter design, operation and capability.

2. RESEARCH OBJECTIVES

This dissertation has four main research objectives:

- 1) To develop a biofilm targeted approach for the measurement of fungal biomass in biofilters treating livestock production emissions.
- 2) To apply the developed approach to generate baseline information on fungal dynamics in full-scale biofilters treating livestock production emissions.
- 3) To test the ability of media types to resist microbial degradation in a full-scale biofilter and identify predictors of this decay to enable biofilter end-users to better assess media longevity and cost tradeoffs.
- 4) To explore the specific role of fungi in the biofiltration and capture of CH₄.

3. A NEW APPROACH FOR ASSESSING BIOFILM MICROBIAL COMMUNITIES ON ORGANIC MEDIA USED FOR GAS-PHASE BIOFILTRATION

3.1. Summary

Gas-phase biofilters are effective pollution control bioreactors for agricultural effluents, but sampling and measuring the microbial communities responsible for pollution mitigation is needed to better control performance. In this study, we developed a wood bait and optimized microbial biofilm sampling for monitoring microbial biomarkers (microbial C, ergosterol, DNA) in a full-scale biofilter. Results indicated biofilms were best targeted by their removal prior to biomarker extraction. We identified a sampling threshold for these biofilms of ≥ 100 mg for accurate and low variability biomarker measurement. Using this approach in a full-scale biofilter revealed that the fungal contribution (as ergosterol) to total microbial biomass was greatest in the most desiccation-prone area of the biofilter. This observation is in line with results from previous lab-scale studies and could be due, in part, to connectivity between fungal hyphae growing in biofilms and the wood baits, shown by confocal microscopy. Quantitative PCR results were unable to detect this shift, due potentially to inadequate sample sizes and DNA extraction efficiencies. This work provides a targeted sampling strategy for microbial biofilms in gas-phase biofiltration, adaptable to other pollution control bioreactors and that can be used to study microbial community dynamics in full-scale systems.

3.2. Introduction

3.2.1. Focused microbial ecology can guide and improve biofilter performance

Bioreactors are an efficient alternative to traditional physical and chemical pollution control technologies (Delhomenie & Heitz, 2005), but understanding the community structure-function relationships that underpin stable performance remains a challenge (Briones & Raskin, 2003; Cabrol & Malhautier, 2011). Unlike other pollution control technologies, bioreactors harness microbial communities to capture and degrade pollutants. The use of a diverse microbial consortium enables the simultaneous treatment of pollutant mixtures of variable concentrations, giving bioreactors great promise for aqueous (Schipper et al., 2010) and gaseous agricultural effluents (Nicolai et al., 2008).

Biofilters are bioreactors that utilize microbial growths and their extracellular products on the surfaces of stationary reactor media (biofilms) to capture and degrade pollutants from a passing effluent (Mudliar et al., 2010). In gas-phase applications, biofilters are capable of reducing odorous volatile organic compounds, hydrogen sulfide and ammonia emissions from livestock building and manure storages by more than 90% (Chen & Hoff, 2009). Biofilters may also effectively treat greenhouse gas emissions, including methane (Veillette et al., 2012). Given their performance potential, low-cost and adaptability, biofilters are considered the most promising pollution control technology for livestock facility emissions by waste management experts in the United States (Liu et al., 2014) and Europe (Hamon et al., 2012; Ubeda et al., 2013). Despite this potential, however, biofilter deployment has been hampered by unpredictable

performance fluctuations and suboptimal emissions control (Chen & Hoff, 2009). This inability to predict fluctuations in biofilter performance, particularly under field conditions, is attributed to an inadequate understanding of the microbial communities active in the system (Devinny & Ramesh, 2005). To improve and control performance (i.e. pollutant sorption and oxidation), monitoring these active microbial communities, both bacterial and fungal, under field conditions is essential (Malhautier et al., 2013). With inlet and outlet emissions of a full-scale biofilter easily measurable, development of a complementary biofilm monitoring approach will also enable the use of biofilters as a model for studying microbial community structure and system function relationships (Cabrol & Malhautier, 2011).

3.2.2. Full-scale field monitoring is needed to link real-world biofilter performance to microbial communities

Simple lab-scale reactor designs and stable operational parameters are typically used to study the effects of microbial community structure on biofilter performance (Malhautier et al., 2013). In most cases, the microbial communities in these systems are monitored indirectly by pollutant and metabolite measurements (Maia et al., 2012a; Maia et al., 2012b), or by targeting oxidative bacteria (Hayes et al., 2010; Posmanik et al., 2014). Although such approaches have correlated specific lab-scale microbial groups to the biofiltration of particular emissions, system performance in full-scale systems may depend on more complex microbial interactions. For example, nutritional sharing between microbial populations (cross-feeding) is an essential component of natural (Seth

& Taga, 2014) and applied microbial communities (Jagmann & Philipp, 2014). Synergistic/antagonistic community effects can also affect bioreactor performance (Guo et al., 2014). Thus, the study of individual parts of a community may oversimplify and not represent its whole. By monitoring the response of a more complete microbial community to stable (Cabrol et al., 2012a; Chung, 2007; Ding et al., 2006) and perturbed emissions loading (Cabrol et al., 2012b), patterns have emerged for community succession, functional redundancy and perturbation resistance/resilience responses.

To date, few microbial studies have been conducted on full-scale, gas-phase biofilter systems, although field studies have led to significant advances in the control of aqueous bioreactor systems (Sipma et al., 2010). Similar to laboratory-scale studies, full-scale biofilter microbial investigations have mostly targeted specific bacterial oxidative groups in highly-controlled systems (i.e. biotrickling filters) under relatively stable operations (Juhler et al., 2009; Kristiansen et al., 2011b; Xue et al., 2013; Xue et al., 2011). While these works are significant contributions to the field, our understanding of microbial responses to real-world perturbations in the complex, organic media biofilters used most commonly by United States livestock production facilities is still limited. Data are particularly lacking for fungi in these systems, despite their potential importance to biofilter stability (Ralebitso-Senior et al., 2012). To enable such investigations, an adaptable biofilm microbial monitoring approach is required, tunable to various full-scale designs and heterogeneous organic media types.

3.2.3. Monitoring microbes in full-scale biofilters should be high-throughput and target biofilm communities

Comprehensive monitoring of biofilter microbial communities demands high throughput, in order to enable detection of small spatial/temporal changes in large, heterogeneous bioreactors. Biofilter heterogeneity can be attributed to bioreactor size, fluctuations in emission loading, but also to non-uniform organic media and its impact on abiotic and microbial conditions. Wood mulch is one of the most widely used media in US livestock production emission biofilters (Chen & Hoff, 2009). It is preferred for its low-cost, wide availability, moisture holding capacity, bulk porosity, and ability to support a diverse microbial community (Schmidt et al., 2004). Although wood mulch promotes robust biofilm formation, its heterogeneity complicates microbial sampling (Cabrol et al., 2010), and large sample numbers are required to ensure representativeness.

Furthermore, monitoring strategies must target the surface biofilm communities where effluents and biocatalysis are at an interface. Unlike biofilms on uniform, solid media, biofilms on wood mulch are accompanied by microbial populations degrading and growing within the media. Thus, while some members of this wood mulch microbial community are significant to biofiltration (i.e. facilitating pollutant sorption, actively biodegrading pollutants, supporting/antagonizing growth of biocatalytic groups), the significance of others inside the wood may be less direct (i.e. wood-degrading saprobes). With the functional significance of many microbial groups poorly resolved (Peay, 2014) and the role of some biofilter taxa, such as fungi, particularly understudied (Ralebitso-

Senior et al., 2012), it is important to examine the entire biofilter microbiota. By separating the biofilm and wood microbiota, the independent impacts of their growths on pollutant biocatalysis as well as their interactions can be better assessed.

One rapid, low-cost microbial monitoring approach suitable for high-sample numbers and biofilms is the detection of microbial biomarkers. Like any measure of microbial structure, biomarkers are not free of caveat and can only minimally resolve complex microbial consortia, but they do provide relevant functional information and have been used widely in natural systems (Joergensen & Wichern, 2008). Moreover, rapid biomarker sampling to complement or target other microbial community assessments as has been demonstrated in lab-scale biofilter research (Cabrol et al., 2009; Prenafeta-Boldú et al., 2012b).

3.2.4. Aims

There were three main intentions of this research. Our first objective was to design a bait system that would provide a relevant substrate for monitoring bacterial and fungal biofilms colonizing biofilter packing media. Our second objective was to optimize the harvest and sampling strategies for these baits to ensure repeatable, low variability extraction of biofilm microbial biomarkers. Our third objective was to evaluate the approach in a full-scale biofilter to verify our ability to track key biofilter microbes in the field. By sampling in various areas of a biofilter, our design was geared to capture biofilm variability across biofilter packing. Biomarkers (microbial carbon (C), ergosterol, DNA) were chosen for monitoring bacterial and fungal dynamics in biofilters for their

functional significance in other systems, low cost, and their potential to target more detailed molecular assessments.

3.3. Materials and methods

3.3.1. Study site, biofilter design, conditions & performance

For the field component of this work, we used the NE up-flow, flat-bed biofilter constructed in 2011 on a 288 piglet swine nursery with deep-pit manure storage at the University of Minnesota West Central Research and Outreach Center in Morris, MN (Figure 3.1 a). Non-inoculated, fresh birch (*Betula papyrifera*) chips which passed a 5 cm mesh were used as biofilter media. We focused on a portion of the biofilter (L: 3.5 m, W: 1.25 m, H: 0.35 m) treating air from a continuously running pit fan with an airflow rate $\sim 0.3 \text{ m}^3 \text{ s}^{-1}$; 6 s empty bed contact time was the design target. Initial media porosity was $52.9 \pm 1.6 \%$ and media density was $187 \pm 6 \text{ kg m}^{-3}$ measured according to Schmidt et al. (2004). For the first year of operation, inlet and outlet air were semi-continuously sampled using an automated instrument trailer (Janni et al., 2014). Subsequently, inlet and outlet emissions were collected in duplicate into 50 L FlexFoil® bags similarly to Akdeniz et al. (2011) (Figure 3.1 b). Hydrogen sulfide (H_2S) was measured with a Model 45C Thermo Fisher Scientific analyzer (Franklin, MA, USA) while ammonia (NH_3), carbon dioxide (CO_2), methane (CH_4) and nitrous oxide (N_2O) were measured with an INNOVA Model 1412, LumaSense Technologies multi-gas monitor (Ballerup, Denmark). Standard cylinder gas was used to set correction factors for analyzers. Performance was calculated as removal efficiency (Table 3.1).

Table 3.1 Summary of inlet emissions and biofilter performance measured by bag sampling. Year one emissions, measured semi-continuously, can be found in Janni et al. (2014).

		<u>NH₃</u>	<u>H₂S</u>	<u>CO₂</u>	<u>CH₄</u>	<u>N₂O</u>
Statistic		ppm	ppb	ppm	ppm	ppb
Inlet	Mean	5.2	119	1034	95	1064
	SD	3.5	197	737	89	899
	Max.	11.9	616	2612	223	2649
	Min.	0.8	11	304	14	428
RE (%)	Mean	30	69	-21	31	-95
	SD	17	32	42	38	254
	Max.	50	99	9	84	2
	Min.	-2	15	-125	-10	-771

Footnote: Negative values indicate generation of a gas by the biofilter

3.3.2 Wood baits for optimized biofilm sampling

Similar to the “coupon” baits used to monitor biofilms in aqueous systems (Deines et al., 2010), wood baits were developed to enable uniform biofilm sampling in the heterogeneous biofilter media. Baits consisted of 3 birch (*Betula papyrifera*) wafers (6.5 × 2.0 × 0.5 cm) cut with the largest face tangential, strung to a numbered aluminum tag with fishing line (Figure 3.1 b). The wafer dimensions resembled the average biofilter media size distribution, and replicate wafers enabled paired biomass measures.

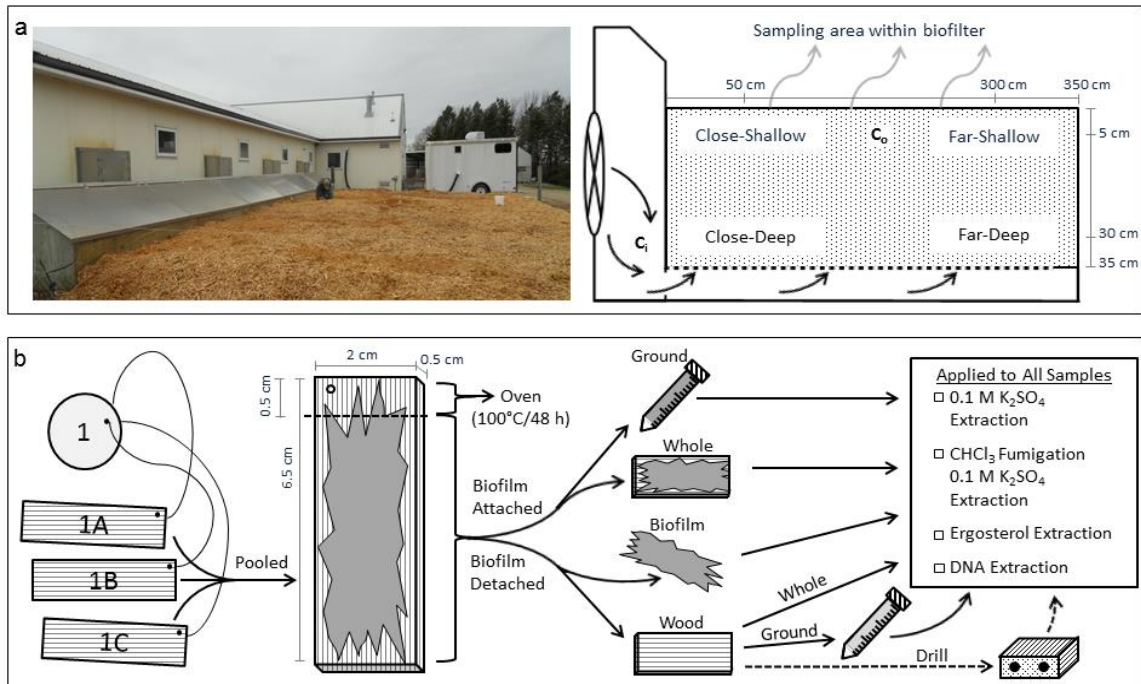


Figure 3.1 a) Photograph and microbial sampling locations (schematic) in the full-scale biofilter treating exhaust air from a swine nursery. The air plenum was subdivided so that each exhaust fan delivered air to a separate part of the biofilter. See Janni et al. (2014) for details. Monitoring was focused on the biofilter area fed by a continuous running pit fan. Inlet emissions were measured in the plenum (C_i), while outlet emissions were measured shallow in the biofilter, between microbial sample points (C_o). **b)** Schematic of wood wafers used as microbial biofilm baits. Wafers were sub-sectioned for the measurement of moisture content and microbial biomarker extraction was conducted on sample fractions to separate biofilm from microbial growth inside the wood.

To optimize the use of wood baits for biofilm sampling, we needed to know 1) if we could accurately assess the biofilm community by extracting whole baits, or if separation of the biofilm from the substrate was required, and 2) how much biofilm was needed for low-variability, accurate biomarker measurement. To do this, a collection of wood mulch media from a 6 year old biofilter treating swine odor was sieved through a 1 cm mesh, and spread into a gas-tight plastic tub. This microcosm was plumbed to a 55 gal swine manure storage which generated a polluted effluent for a lab-scale biofiltration

system (Appendix 3.1). Average inlet emissions were 23.5 ± 13.5 ppm NH₃, 565 ± 660 ppb H₂S, 518 ± 53 ppm CO₂, 38 ± 26 ppm CH₄, and 404 ± 80 ppb N₂O (n > 500). Baits were incorporated into the tub and the contents were mixed and watered weekly to promote homogenous biofilm growth and to maintain wood moisture content between 40-60% dry wt., determined by comparing pre- and post-drying (100°C, 48 h).

Baits were harvested from the microcosm at 8 mo. and subsampled aseptically into 5 pieces using a sterile chisel. One subsample (0.5 × 2.0 × 0.5 cm) was used for measuring moisture content (% dry wt.), and the remaining 4 subsamples (1.5 × 2.0 × 0.5 cm) were used for sample process testing. Of these subsamples, the 1st was left intact with biofilm attached (designated as *attached whole*), the 2nd was aseptically ground in a Midas Rex® Electric Bone Mill (Medtronic Inc., Minneapolis, MN, USA) with modified blades sharpened to an angle (*attached ground*), the biofilm of the 3rd was scraped free using a sterile single-edge razor blade (*detached biofilm*), leaving a biofilm-free bait (*wood whole*), and the 4th was similarly scraped but the bait was ground (*wood ground*). Ten replicates were immediately used for each microbial measure and 5 replicates of non-deployed baits were used as controls (Figure 3.1 b).

To test biofilm sample size requirements, a large pool of biomass had to be generated and homogenized to ensure uniformity. To do this, >30 g of biofilm was scraped from the microcosm baits into a sterile blender containing 100 mL of sterilized Type I water. The slurry was mixed for 30 s, transferred to a sterile glass petri dish, and the added water was evaporated by the sterile stream of air in a laminar hood. Intensive

sample homogenization is required for the detection of cells in aggregates, but also liberates microbial C and introduces error in microbial biomass measurement (Jenkinson & Powlson, 1976). To minimize this error, active cells were allowed to reabsorb the microbial C liberated by sample mixing by incubating the homogenized biofilm 2 d at 22°C. Microbial biomarkers (microbial C, ergosterol, DNA) were then measured on biofilm subsamples of 10, 30, 50, 100, 150, and 200 g. Ten replicates were used for microbial C and ergosterol, 6 for DNA, and empty extraction vials were used as controls.

For a field test, baits were placed at 4 locations in the media at the time of biofilter construction: 50 and 300 cm from the fan inlet (*near* and *far*, respectively), and 5 and 30 cm from the biofilter surface (*shallow* and *deep*, respectively) (Figure 3.1 a). After 20 mo., 10 baits were collected from each location, stored in sterile plastic baggies, and returned to the laboratory on ice. Baits were subsampled for moisture content, biofilm material was harvested aseptically using a sterile razor blade, then pooled for each location into a sterile 15 mL centrifuge tube, and gently mixed. Baits were then sectioned aseptically using a sterilized chisel. Similar to the sampling method by (Jasalavich et al., 2000), a drill fitted with a sterile 2 mm dia. titanium bit was used to collect wood shavings from inside the bait, through the sectioned face (Figure 3.1 b, **Figure 3.8**). Wood shavings were also pooled in a sterile 15 mL centrifuge tube and gently mixed. Drilling was used instead of milling to improve targeting of internal wood communities and to speed aseptic sampling. Pooled biofilms and drillings were subsampled (n=6) for microbial biomass determinations.

3.3.3. Microbial biomarkers

Total microbial biomass was determined by chloroform fumigation extraction (CFE) (Needelman et al., 2001), with sample moisture content raised above 50% for dry samples to enable maximal C flush (Ross, 1989). Samples were extracted in 0.1 M K₂SO₄ (12.5 mL dry g⁻¹) with orbital shaking (100 rpm) for 1 h, then filtered and stored at -20°C. Extracts were later thawed, diluted 1:20 with Type I H₂O, and analyzed for non-purgeable organic C on a Shimadzu (Kyoto, Japan) TOC-VCPH analyzer. Extractant salinity was lowered to 0.1 M K₂SO₄ as no statistically difference with the recommended 0.5 M solution was observed (Appendix 3.2) and the less saline extractant, in addition to sample dilution, helped minimized analyzer error and maintenance.

Fungal biomass was measured chromatographically as total ergosterol (Tank & Webster, 1998). Free ergosterol was extracted from samples stored at -20°C in 5 mL methanol by a 2 h, 65°C reflux. Samples were then saponified and refluxed an additional 30 min to solubilize esterified ergosterol components. Samples were centrifuged, the supernatant was removed, residual solids were rinsed in methanol, the samples were again centrifuged and the supernatants combined. Total ergosterol was separated from alkaline methanol by 3 pentane phase separations and extracts were combined and evaporated. Ergosterol was re-dissolved in methanol, filtered and measured with high performance liquid chromatography (HPLC) on an Agilent Technologies (Minnetonka, MN, USA) 1200 series HPLC using a methanol mobile phase, 1 mL min⁻¹ flow rate and Phenomenex™ (Torrance, CA, USA) 4μ Hydro-RP 80a column at 40°C, using 7-

dehydrocholesterol as an internal standard. These extraction methods were optimized for high yield and recovery.

DNA was extracted by a modified CTAB extraction (Song et al., 2014). Samples were extracted in 800 μ l of CTAB extraction buffer (2% CTAB, 2% PVP-40, 0.5% β -mercaptoethanol) and incubated 1 h at 65°C. Impurities were removed by phase separation with phenol/chloroform/isoamyl alcohol (25:24:1) then with chloroform/isoamyl alcohol (24:1). DNA was precipitated with isopropanol, washed with 70% ethanol and dissolved in nuclease-free H₂O. DNA extracts were purified using the QIAquick® PCR purification spin column kit (Qiagen Sciences, Germantown, MD, USA), dissolved in nuclease-free H₂O and quantified using a Qubit® Fluorometer (Life Technologies, Grand Island, NY, USA) then stored at -20°C for later use.

Quantitative real-time PCR (qPCR) was used to quantitatively amplify gene copy numbers of fungal and bacterial rDNA from biofilm samples. An ABI Prism™ 7900HT sequence detection system (Life Technologies, Grand Island, NY, USA) was used. Optimized thermal cycling conditions were 95°C for 10 min. then 40 cycles of denaturation at 95°C for 1 min, annealing at 53°C for 30 s and extension at 72°C for 1 min. Samples, non-template DNA blanks, and 10 \times dilutions of template DNA used to determine reaction efficiency were all run in triplicate. Each 15 μ L reaction contained, 7.5 μ l of iTaq™ SYBR® Green Supermix with ROX (Bio-Rad Laboratories, Hercules, CA, USA), 0.6 μ L (400 nM) of forward and reverse primers, 5 μ L (~5 ng) of template

DNA, and 1.3 μL RNase free water. The respective forward and reverse primers were ITS-1 and ITS-4 for fungi and Eub 338 and Eub 518 for bacteria (Fierer et al., 2005).

3.3.4. Confocal microscopy

Confocal microscopy was used to visualize fungal hyphae in the biofilm and wood bait, similar to the methods of Schilling et al. (2013). Baits were tangentially sectioned (15 μm) with a Damon-IEC Minotome microtome cryostat (International Equipment Company, Chattanooga, TN, USA) after tissue freezing medium (TFMTM) (Triangle Biomedical Sciences, Durham, NC, USA) infiltration and storage at -20°C . Sections were mounted onto a slide, stained in the dark with 10 $\mu\text{g mL}^{-1}$ wheat germ agglutinin-tetramethylrhodamine in $1\times$ PBS (pH 7.4) (WGA-TMR, excitation 555 nm, emission 580 nm, Invitrogen, Calsbad, CA, USA) for 30 min, then rinsed with $1\times$ PBS. Stained sections were then imaged using a Nikon A1si confocal system (Nikon Instruments Inc., Tokyo, Japan), equipped with a 32-channel PMT spectral detector, mounted on a Nikon Ti2000E inverted fluorescence scope. The 561 and 405 laser bands were used to excite and separate fungal and wood tissues. Emissions were collected and NIS Elements imaging software (Nikon Instruments Inc., Tokyo, Japan) was used to unmix selected spectra. ImageJ 1.47 (National Institute of Health, Bethesda, Maryland, USA) was used to prepare images for publication.

3.3.5. Statistical analyses

All statistical analyses were conducted with R 3.0.1 (GNU Project). Normal distribution of data was verified by Shapiro-Wilk normality testing and differences in

biomarker measures were determined by one-way ANOVA. A separate ANOVA was run for each biomarker response. With the sample fractioning experiments, where highly variable ranges in measurement were being compared, data could not be normalized through transformation and the Kruskal-Wallis test was used to test differences in biomarker measures. A separate Kruskal-Wallis test was run for each biomarker response. Tukey HSD was used post-hoc to test differences in means. The alpha level was set to 0.05 for all analyses. Coefficient of variation (CV) was used as an index of measurement variability.

3.4. Results

3.4.1. Targeting biofilm communities

Comparison of sample fraction biomarker values revealed that microbial biomass within the wood matrix contributed significantly to biofilm assessments, and therefore required a sampling approach (scraping) to isolate biofilms from substrate microbiota (Figure 3.2, Appendix 3.3). For both total microbial biomass, measured as microbial C, and total fungal biomass, measured as ergosterol, mean values for *attached whole* fractions exceeded extractable biomarker values for *detached biofilm* fractions. The range and standard deviation of *attached whole* biomarker values for total microbial and fungal biomass were also larger than *detached biofilm* fractions. With total DNA, there was no significant difference between the mean values for *attached whole* and *detached biofilm* fractions, but the range and standard deviation of the *detached biofilm* fractions were

smaller than other fractions. *Detached biofilm* fractions routinely had the smallest biomarker values of all the fractions tested.

Extraction of *attached whole* fractions overestimated *detached biofilm* microbial biomass, and in some cases better represented maximum extractable microbial biomass of the sample measured as *attached ground*, or approximated by the *sum* of surface and wood biomarkers. For all mean biomarker values, there was no statistical difference between *attached ground*, the *sum of detached biofilm + wood whole*, and the *sum of detached biofilm + wood ground*. Exhaustiveness of the biofilm scrape was verified by the lack of difference between these values, and confirmed by confocal observations (data not shown). For total microbial and fungal biomass mean values, *attached whole* was also not statistically different from the *attached ground* baits. Unlike the other biomarkers, however, the mean total DNA value for *attached whole* samples was significantly less than the *attached ground* mean. Variability was generally higher in samples that were ground. Range and deviation of values were significantly greater for *attached ground* versus *attached whole* fractions for microbial C and DNA and for *wood ground* vs. *wood whole* fractions for all biomarkers.

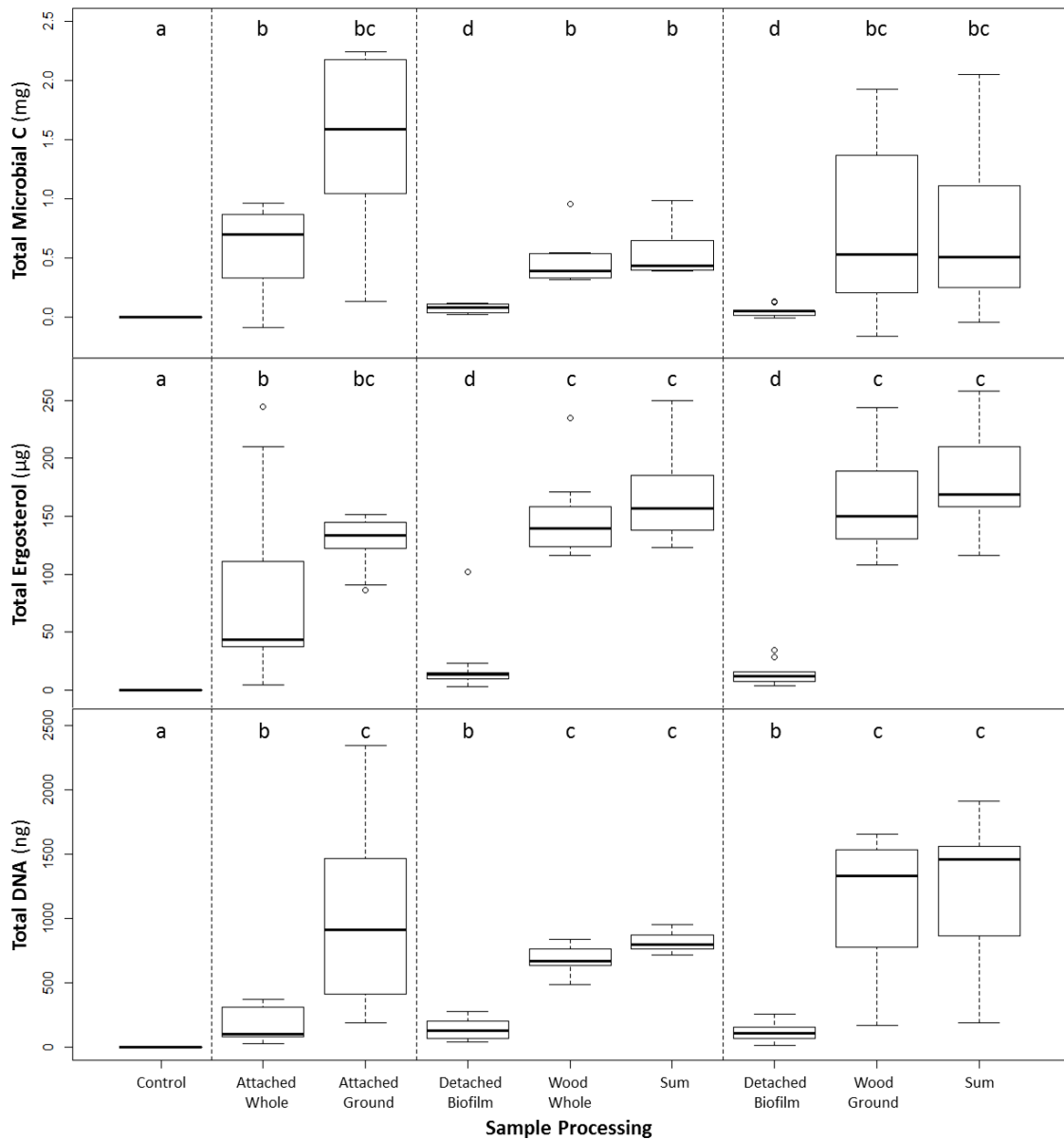


Figure 3.2 The effect of sample fractioning on extraction of microbial biomarkers from baits incubated 8 mo. in a biofilter microcosm. For each biomarker (n=10) tested subsamples included baits with an attached biofilm left whole (*attached whole*), or milled (*attached ground*), biofilms (*detached biofilm*), biofilm-free wood left whole (*wood whole*), or milled (*wood ground*), and the sum of paired biofilm and wood fractions (*sum*). Non-incubated treatments (*controls*) (n=5) were also tested. Means with different letters are significantly different ($\alpha = 0.05$). Boxplots depict the media, 1st and 3rd quartiles, and quartile values plus or minus the interquartile range times 1.5. Circles represent outliers.

3.4.2. Biofilm sample size requirements

Results indicate that variability was generally higher for small sample sizes, and generally declined for all biomarkers when larger samples were used. Accurate biomarker detection required ≥ 100 mg of biofilm per extraction (Figure 3.3, Appendix 3.4). Microbial C and ergosterol mean values generally plateaued as sample size increased. Variability stabilized at threshold sample weights between 50 and 150 mg depending on the biomarker (Figure 3.3), with increasing biomass sample weight correlating well with the reduction in CV for both microbial biomarkers (**Figure 3.4**). Patterns with DNA were more variable and not significant due either to the use of fewer replicates or to extraction issues.

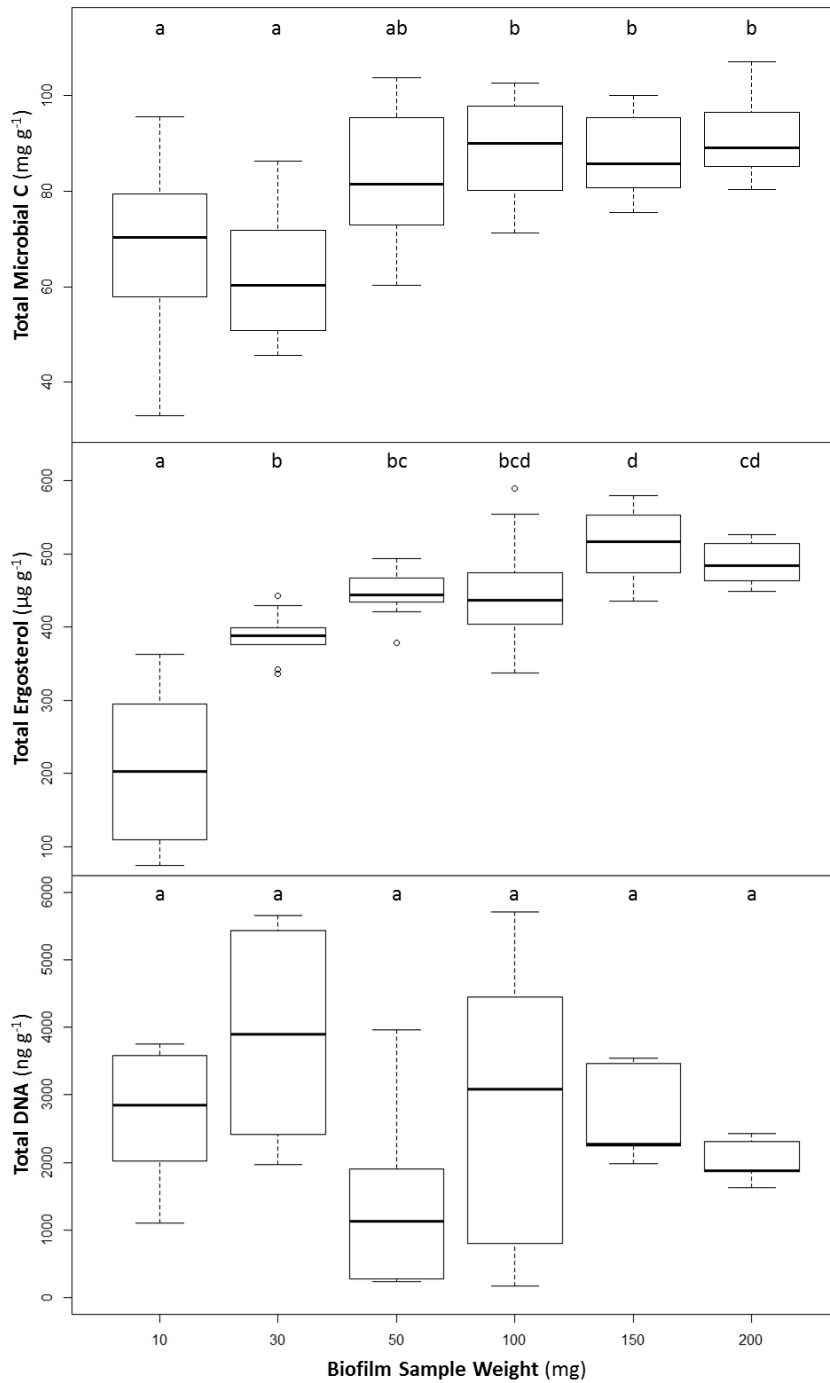


Figure 3.3 The effect of biofilm sample weight on the extraction of microbial C, ergosterol (n=10) and total DNA (n=6). For each biomarker, means with different letters are significantly different ($\alpha=0.05$).

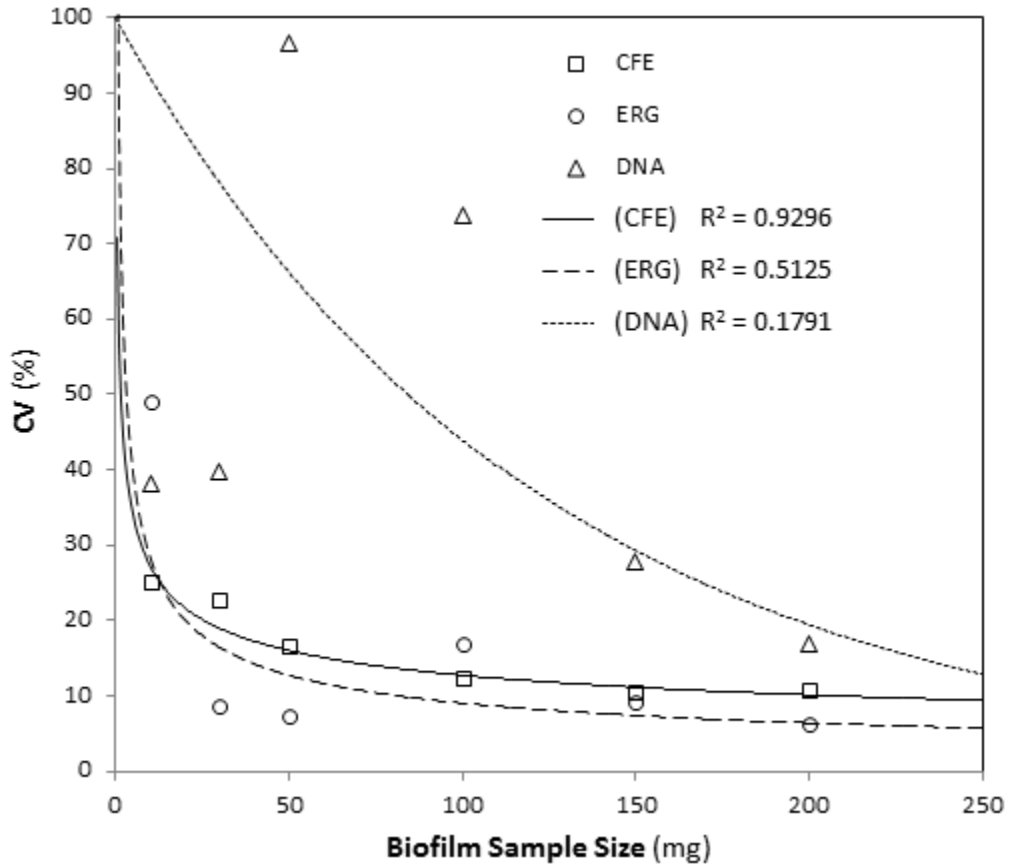


Figure 3.4 Regressions average coefficient of variation (CV) for dry weight normalized total microbial C (CFE), total ergosterol (ERG) (n=10), and total DNA (DNA) (n=6) and the biofilm sample weight.

3.4.3. Biofilm fungi in full-scale biofilters

In the pooled biofilm samples, a significantly higher total fungal:total microbial biomass ratio was measured on baits in the far-shallow location than in the other locations (Figure 3.5, Appendix 3.5). The shift in this ratio was not driven by an increase in fungal biomass, which remained stable, but by a significant loss in total microbial biomass. The greatest microbial growths were measured in the far-deep biofilm samples where mean values of chloroform labile-C and total ergosterol were both significantly elevated. Homogenized samples of wood drillings from the full-scale, flat-bed biofilter

showed no difference in the ratio of total fungal:total microbial biomass using our protocol (Figure 3.5, Appendix 3.5). Microbial biomass was more concentrated in biofilms than in wood drillings. An inverse relationship between the mean biofilm fungal:total microbial ratio and the associated moisture content of each sample area was also apparent (Figure 3.5, Appendix 3.5). This negative correlation was consistent when biofilm ratios were compared to sample moisture content, regardless of the sample location (Figure 3.6).

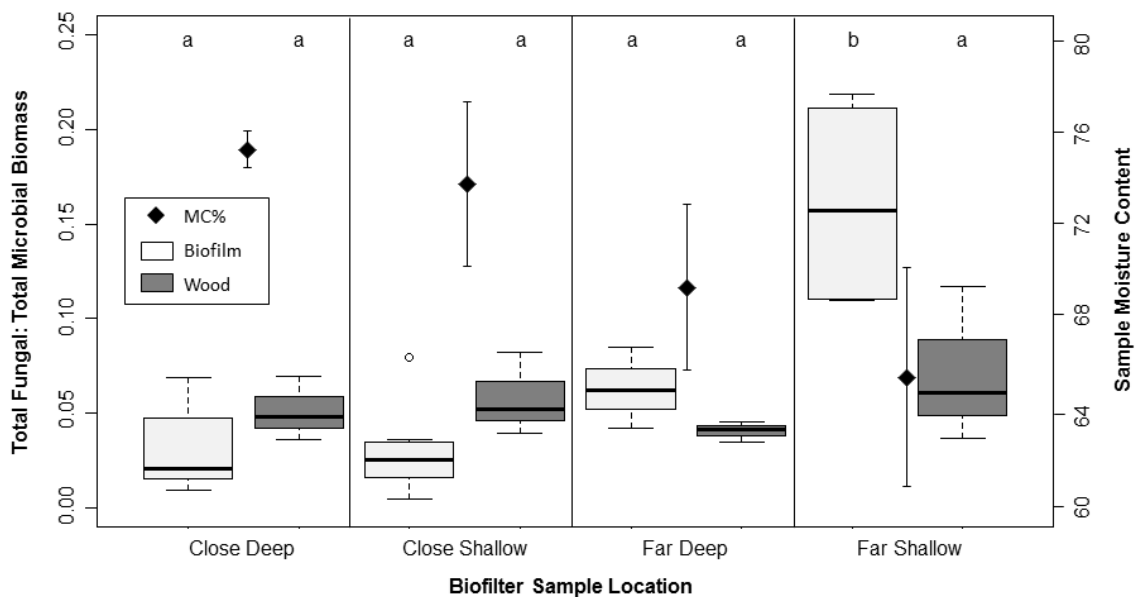


Figure 3.5 Boxplots depicting total fungal:total microbial biomass ratios (measured as mass normalized total ergosterol to total microbial C) of biofilter sampling locations for biofilm (light grey) and wood substrates (dark grey). On the second axis is the mean sample moisture content (% dry weight) of biofilter sampling locations (black diamonds), standard deviation represented by the error bars (n=6). Means with different letters are significantly different ($\alpha = 0.05$).

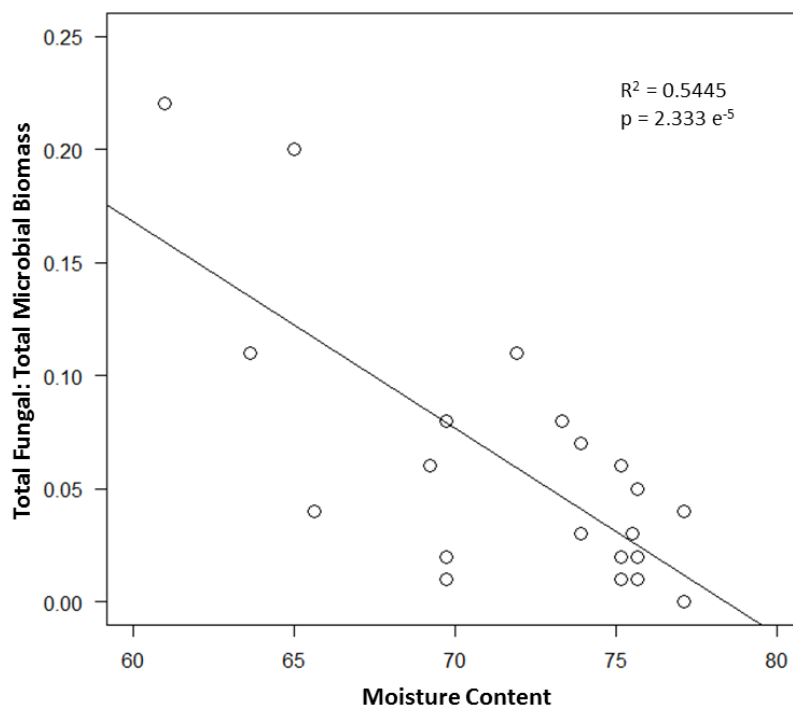


Figure 3.6 Linear model of the total fungal:total microbial biomass ratio (measured as mass normalized total ergosterol to total microbial C) and sample moisture content (% dry weight) indicating the ability of fungi to tolerate drier conditions. Location variable affects were tested and found to be not significant.

The qPCR based fungal:bacterial ratios, used to complement total fungal:total microbial ratios based on ergosterol and microbial C, showed similar results for biofilm samples (**Figure 3.7**, Appendix 3.6). Again, there was no significant difference between the close-deep, close-shallow, and far-deep locations, but the fungal:bacterial ratio for the far-shallow location was not significantly higher as was noted previously. Similar to the ergosterol and microbial C data, however, the far-shallow location also resulted in markedly more measurement variability than other locations.

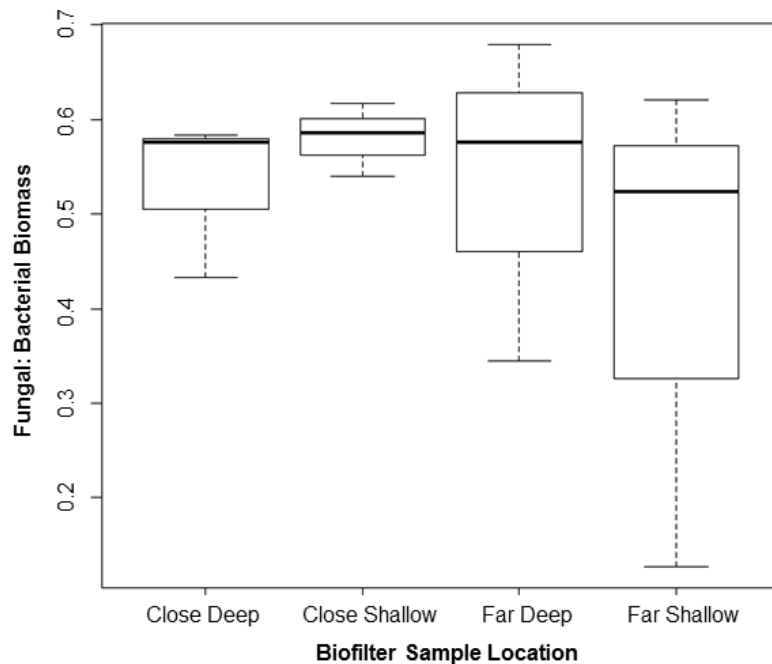


Figure 3.7 Boxplots depicting fungal:bacterial biomass ratio (Ct Fungi: Ct Bacteria) of biofilter sampling locations for biofilm samples based on qPCR results.

In the far-shallow location, biofilms were typically variable with reduced thickness, compared to the thick, more uniform biofilms from locations like far-deep. On the more desiccated samples, typical of the far-shallow location, biofilms were quite variable and were often observed with scattered growths of fungal aerial hyphae (**Figure 3.8 a, b**), perhaps explaining this variability. Confocal micrographs show connectivity between these aerial tufts of hyphae and the filamentous growth of fungal inside the wood matrix (**Figure 3.8 c**), suggesting an inoculum reserve below the surface in these porous wood media.

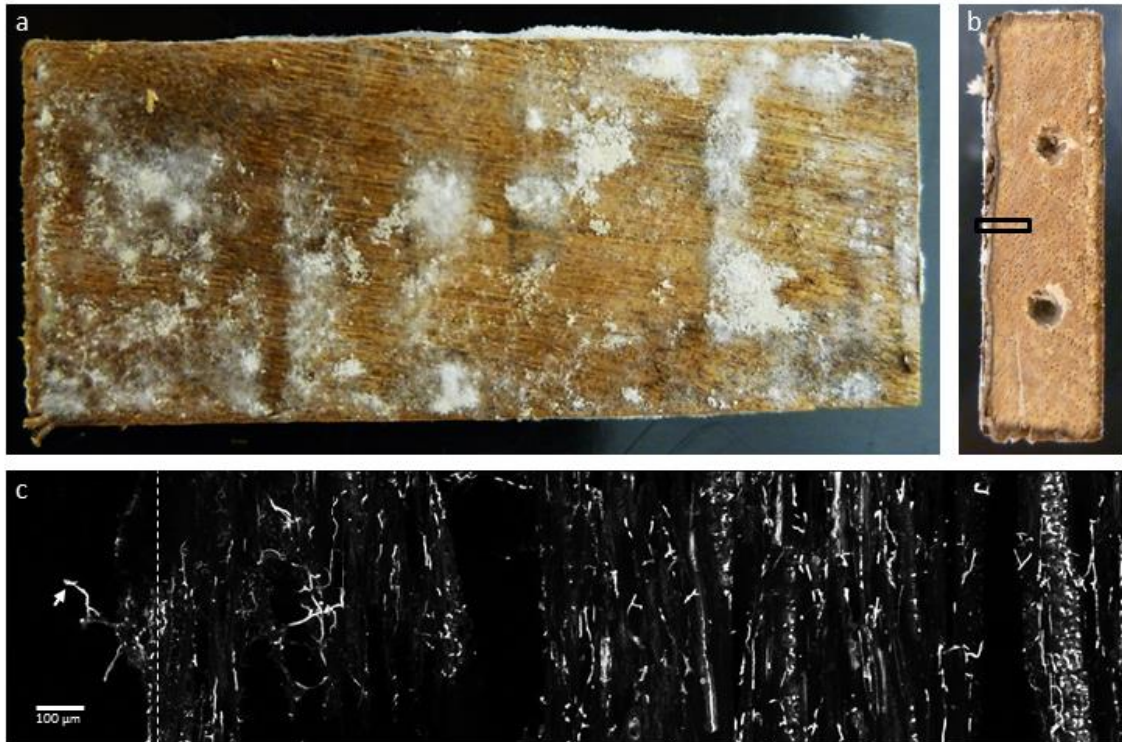


Figure 3.8 a) Photograph of a bait from the far-shallow location after the moisture content subsection was removed. A fungal dominant biofilm can be seen growing on the bait surface. b) Cross section of the bait showing drill holes used to sample internal microbial biomass. Aerial hyphae can be seen extending out from the biofilm and wood degradation is evident below the biofilm. The black box indicates the approximate location of the confocal image. c) An unmixed, stitched confocal micrograph of biofilm and bait section showing fungal hyphae (stained with WGA-TMR, excited with a 561 laser) growing aeriually (white arrow) and connected to mycelial growths in and across wood cells. The dashed line indicates the surface of the bait.

3.5. Discussion

3.5.1. Wood baits were effective and isolating biofilms improved measurement precision

Wood baits were effective for sampling biofilter microbiota, and the biofilms on these baits were successfully targeted by their removal prior to biomarker measurement. Biofilm baits for aqueous systems, known as “coupons”, have been successfully used

since the 1990s to monitor microbial biofilm communities in aqueous bioreactor systems (Deines et al., 2010). These field studies have significantly improved aqueous bioreactor stability (Sipma et al., 2010). While these coupons are typically made of piping materials, wood baits have been used similarly for monitoring biofilms in natural stream systems (Tank & Webster, 1998). To our knowledge, this is the first use of a wood bait to sample microbial biofilms in gas-phase bioreactors. Like the use of coupons in aqueous systems, the use of biofilm baits in gas-phase biofilters facilitated precision sampling of natural biofilms growing in a complex, heterogeneous environment.

Scraping the biofilms free from bait surfaces prior to analysis was necessary for low-variability, targeted microbial assessment. Small discrepancies between the mean values for summed fractions (*biofilm + wood*) and the entire sample (*attached ground*) were the likely result of milling artifacts and their impact on measurement accuracy. With the exception of the *attached ground* ergosterol measurement, milling increased biomarker variability for both *attached biofilm* and scraped samples. Effective sampling of wood microbiota and complete biomarker extraction depends on effective pulverization of the wood matrix. However, this intensive processing can also degrade microbial cellular components and has been shown to increase measurement error for all biomarkers tested (Cabrol et al., 2010; Jenkinson & Powlson, 1976; Newell et al., 1988). Although sampling microbial biomass in wood will always require some sample processing, scraping biofilms from the bait circumvented issues with milling and resulted here in small biomarker measurement variability.

Extraction of *attached* samples unsuccessfully targeted biofilms, and differences in biomarker extraction capacities complicate comparative analyses. When *attached whole* samples were extracted, biomarker measures were more variable and typically did not approximate detached biofilm fractions. Differences in the ability of extraction protocols to dissociate biofilms and penetrate the wood matrix may explain why DNA extracted from attached whole samples approximated biofilm measures, while other biomarker measures of unfractionated samples overestimated the biofilm. Biofilms are a protective microbial growth strategy (Hall-Stoodley et al., 2004) with an improved resistance to antimicrobial agents (Mah & O'Toole, 2001). Work in biofilter systems has shown extraction of microbial DNA from active biofilms is problematic (Cabrol et al., 2010), so it is plausible that the attached biofilm limited extraction of basal microbial cells and left wood microbiota protected. With the other biomarker extraction techniques, which utilize hot solvents, fumigants, and additional/longer cell disruption steps, this biofilm protection was presumably overcome and wood microbiota was susceptible to biomarker extraction.

Sample storage further affected biomarker analysis, particularly for ergosterol. In an accompanying methods development experiment, extractable ergosterol from attached whole fractions increased with length of storage time, eventually reaching levels not statistically different from attached ground fractions (Appendix 3.7). This additional source of variability might explain the unique result of greater measurement variability for attached whole fractions than for attached ground fractions. In the accompanying

experiment, where degradation was standardized by use of a single fungal strain, milled sample variability was greater than whole sample variability. It is possible that the biofilm and bait test material conditions generated here were more varied, as a consortium inoculum was used. As a result, inconsistent solvent diffusivity through attached whole samples may have contributed more to measurement variability than milling where a well-mixed, uniform sample enabled uniform biomarker extraction. Selecting storage time or extraction conditions that would limit over-estimation of biofilm biomarkers would be difficult with variable biofilm and bait field conditions. Biofilm scraping is therefore a more standardizable approach for targeting biofilms and is suitable for various biomarkers, environmental condition, and avoids the limitations encountered when directly sampling bulk, heterogeneous field biofilter media.

3.5.2. The effect of biofilm sample weight on the extraction of microbial biomarkers.

Sample size relationships indicated a threshold requirement of ≥ 100 mg of biofilm for stable, low variability measurement of biomarkers. Based on biofilter sampling experiences from this study, approximately 1 mg of wet biomass was harvested on average from each 1 cm² of wood bait surface. Thus, at least 100 cm² of surface area was required per microbial measure. In our study, adequate sample size was achieved by pooling scrapes from smaller baits, as baits with a 100 cm² surface area would have under represented actual biofilter media dimensions and airflow exposures. Pooling also ensured sample representativeness, as some collected biofilm growths had wet weights an order of magnitude smaller (desiccated and early time collections) or larger (wetted and

later collections) than the mean biofilm size. High variability of biofilm thickness in response to abiotic conditions is not uncommon (Deshusses, 1997; Wäsche et al., 2002). Although pooling may mask some microbial populations in soil (Manter et al., 2010) and biofilm microbial communities (Nyvad et al., 2013), no significant difference was seen between microbial populations of individual and pooled composite soil samples (Osborne et al., 2011), and bioreactor studies have shown pooling reduces sampling bias and variability (McIlroy et al., 2009). With biofilm growths variable within and across systems, we report our findings on a mass basis to facilitate adaptation and pooling optimization for other pollution control bioreactor study systems. Once optimized for a new system, the use of baits allows microbial biomarkers to be normalized more relevantly by surface area.

3.5.3. The fungal:total microbial ratio was greatest in biofilms harvested from drier biofilter media.

As could be done for emissions reductions, the optimized monitoring approach successfully correlated a full-scale biofilm community shift across a same spatial scale to abiotic conditions. Specifically, microbial biomass inside the wood was shown to remain stable across sample locations while fungi dominated the biofilms in drier areas of the biofilter. The greatest microbial biomass, fungal and total, was in the far-deep location, an inlet area of the biofilter less affected by solar and wind drying. More stable temperature and moisture conditions support vigorous microbial growth, and reported cell densities in the laboratory are usually greatest at biofilter inlets where emissions

loading is highest (Cabrol & Malhautier, 2011). The use of baits corroborated those findings in a field-scale biofilter. When the proportions of biomass were investigated, however, fungi were found to dominate biofilms from drier samples, such as those collected in the more exposed far-shallow location. Biomarker data suggested that greater total fungal:total microbial ratios in these biofilms were the result of significant losses in total microbial biomass and not additional fungal biomass. It is plausible that bacterial susceptibility and fungal tolerance to the rapid and frequent drying drove these shifts, supporting other lab-scale observations of fungi better tolerating periodic biofilter desiccation (Kennes & Veiga, 2004).

Quantitative PCR did not confirm increased fungal presence in the dry, far-shallow location of the biofilter, due potentially to the differences in biomarkers targets, but more likely to environmental and analytical variability. Despite DNA purification efforts, reaction optimizations, primer set testing and Pearson correlation coefficients (R^2) of the standard curves for both targets greater than 0.990, the qPCR amplification efficiencies (147% and 105% for ITS and 16S rRNA, respectively) and the standard curves slopes (-3.198 and -2.542, respectively) indicate an issue with fungal qPCR sampling. Differential melting of double-stranded fungal DNA was observed in the dissociation curves (Appendix 3.8). This is indicative of heteroduplexes (double stranded DNA comprised of complementary strands from different sources), the potential result of heterozygosity in the original samples and hybridization of near-complementary strands. As reaction efficiency and heteroduplex issues were unique to fungal measures and not

encountered for bacterial targets, it is likely that variability in the ITS target region and environmentally-mediated changes in fungal gene copy number (Manter & Vivanco, 2007; Song et al., 2014), along with inadequate DNA extraction efficiencies (Cabrol et al., 2010), were responsible. Further optimization for biofilter communities and a greater sample size may thus be required to reduce variability of molecular measures, a counterintuitive finding given the detection limits for DNA. This may particularly be true in areas of a biofilter where sample moisture content and biofilm growth is variable and heterogeneous, such as the far-shallow location, where the greatest variability was observed by all biomarker measures. Although qPCR has been used successfully as a biomass measure in lab-scale biofiltration systems (Prenafeta-Boldú et al., 2012a), these results suggest caution, with optimization of sample size and detection a requirement during experimental design.

The potential tolerance of fungi to drier media observed in this study may be explained by the fungal production of hydrophobins and to their unique hyphal growth form. Once secreted, hydrophobins assemble into surface membranes on hyphal and spore surfaces (Linder, 2009). Work with a pathogenic fungal system has shown this protein coating facilitates spore desiccation tolerance (Klimes & Dobinson, 2006). Perhaps hydrophobin assembly on biofilter hyphae also creates an impervious barrier to moisture loss, in addition to their known facilitation of hyphal protrusion into the air from aqueous biofilms (Wosten, 2001). Fungal morphology may also help explain tolerance to biofilter media desiccation. As shown in our confocal micrograph, there is connectivity

between the biofilm and hyphal reserves inside the wood. This connectivity may provide fungi a “harbor” of inoculum and allow them to conduit water from the wood to drying surface growths, as fungi have well documented capacities to translocate water and nutrients (Cairney, 1992). In biofilters, fungal hyphae are recognized to increase the effective capture area in contact with the effluent (Arriaga & Revah, 2005; van Groenestijn, 2001), and enhance the removal efficiencies of particular emissions (Kennes & Veiga, 2004; Prenafeta-Boldú et al., 2012a; Rene et al., 2013). These desiccation tolerant fungal biofilms may also support and anchor other microbial growths and play a significant role in maintaining biofilter performance during drier periods. The reserves of fungal growth inside the wood may also speed performance recovery when media is rewetted, as rapid growth from within the wood may again help anchor a rejuvenating biofilm. Though abundant in organic (Cardenas-Gonzalez et al., 1999) and synthetic media biofilters (Kristiansen et al., 2011a; Xue et al., 2013), fungi are not routinely measured in biofilter studies and should be assessed in terms of improving biofilter control (Ralebitso-Senior et al., 2012). With the challenge of moisture management in full-scale biofilter operations (Chen & Hoff, 2009; Chen et al., 2008a; Nicolai & Lefers, 2006), this resilience potential is promising for engineers aiming to stabilize and control performance.

3.6. Conclusions

Here we have detailed an optimized wood ‘bait and scrape’ monitoring technique that can be used to explore the patterns and potentials of bacterial and fungal biofilm

growths in gas-phase biofilters. A sampling threshold of ≥ 100 mg of microbial biofilm was identified for repeatable, low variability biomarker measurement, but larger sample sizes may be required for effective DNA measurement and use. Through field testing, we have evidence of fungal tolerance to media moisture stress, and suggest further investigation of fungi for their role in biofilter desiccation tolerance. Overall, this targeted biofilm sampling approach enabled full-scale microbial monitoring of biofilters and can be optimized to facilitate more detailed downstream analyses.

4. FUNGAL DYNAMICS IN A FULL-SCALE BIOFILTER

4.1. Summary

Microbial dynamics and consequences were studied in two full-scale livestock emission biofilters. Wooden chip baits were used to follow changes in media moisture content and decay and to sample biofilm growths that were harvested for microbial monitoring. Average media moisture contents and mass losses were dependent on biofilter and sample location with variability seen among chips. Spatial and temporal variability and fluctuations were also recorded using the microbial biomarkers, labile-C and ergosterol. By identifying operational variability future media sampling and biofilm monitoring efforts can be of greater use. Sequence-based characterization of the fungal communities in a single biofilter showed both initial media and storage manure influenced the development of climax biofilm communities. Dominant fungal taxa were identified with unique saprobic capabilities that may play important roles in biofilter function. Identifying inoculum sources, characterizing biofilm succession, and classifying the climax biofilter community improves our knowledge of biofilter media colonization. With this information, efforts to speed and control establishment of microbial populations in biofilters can be supported. Through such efforts, initial performance lag time might be avoided and microbial communities with robust biofiltration capacities may be more utilizable.

4.2. Introduction

4.2.1. Inherent complexity of biofiltering systems

Biofilters are treatment systems that use complex microbial communities naturally established on organic media to manage complex gaseous emissions. Biofilters treating livestock production emissions can be made from a range of woody and compost materials (Mudliar et al., 2010), including agricultural by-products (Akdeniz et al., 2014; Ramirez-Lopez et al., 2003), though mulch is most commonly used (Chen & Hoff, 2009). The primary roles of these media are to provide surfaces for microbial attachments and act as a carbon and water reservoir to support these microbial growths. Diverse microhabitats suitable for microbial colonization are created by the inherent variability of media size, condition, and age. The media also acts as an inoculum, delivering its own resident microbial groups to the system. The media, along with unmanageable abiotic conditions and variable emission compositions and concentrations act as selective pressures and dictate microbial community development. While some members of the developed microbial community are directly involved in the biofiltration process, others likely have only indirect or indiscernible associations with system performance. These complex ecological interactions make connecting microbial communities to system performance a challenge, particularly under full-scale conditions.

4.2.2. Assessment of microbial variability and community shift are needed

Resolving these ecological patterns, however, must be overcome to improve biofilter control and performance predictability. To help guide targeted microbial

investigations, it is first important to characterize system variability so that adequate sampling is ensured. This includes monitoring abiotic conditions that control, and are consequences of, microbial systems, as well as the microbial dynamics themselves. Large sampling efforts and high-throughput, but functional relevant microbial measures should be used for such initial characterizations (Joergensen & Wichern, 2008), which can focus taxa based metrics of biofilters that are not always correlated to system performance (Cabrol & Malhautier, 2011).

Community based measures do have utility in the detailing biofilter microbial succession and identification of high-performing climax communities (Steele et al., 2005). When a biofilter is first deployed, there is a typical lag period of inefficient performance which has been linked to the time required for a high-performing, dominant community to establish (Cabrol & Malhautier, 2011). While both media amendments (Vergara-Fernandez et al., 2011) and inoculum strategies (Elias et al., 2010) have been explored, enhanced establishment of a high-performing dominant communities often fails (Falk et al., 2009; Steele et al., 2005). This is due to the influence of microbes present in the media and those selected for by the environment. If community shifts in full-scale biofilters were better characterized, there may be an opportunity to improve inoculum development or enrichment measures to more rapidly establish high performing microbial communities and reduce system lag.

4.2.3. Fungi are potential keystone species in biofilters

The succession of fungal communities in biofilters have been particularly understudied (Ralebitso-Senior et al., 2012). Fungi can be thought of as keystone species in biofilter decay systems since their community dynamics 1) govern biochemical cycling and wood media breakdown (Hiscox et al., 2015), 2) affect translocation of water and nutrients which may facilitate the growth of other microbial consortia (Cairney, 1992), and 3) their biomass can increase effective capture area (Arriaga & Revah, 2005) and control emissions capture rates of some emissions (Kennes & Veiga, 2004). Despite these capacities, almost nothing is known about fungal populations in full-scale biofilters, particularly their successional patterns and the composition of dominant taxa. As keystone organisms and principle agents of decay, improved knowledge of fungal dynamics might enable improved effort to establish top performing biofilter communities.

4.2.4. Aims

There were two main objectives of this research. The first was to parameterize system variability using a spatial and temporal sampling of two full-scale biofilters, paired with measurement of biotic and abiotic variables. The second was to study the successional pattern of fungi in a single full-scale biofilter over a 3 year period to identify the dominant taxa as well as the potential origin of these communities.

4.3. Methods

4.3.1. Study site

Two up-flow, flat-bed biofilters at the University of Minnesota West Central Research and Outreach Center in Morris, MN were investigated. The northeast (referred to as *north*) biofilter was constructed of fresh birch (*Betula papyrifera*) chips < 5 cm in diameter, the southeast (*south*) biofilter of birch chips < 10 cm in diameter. Both biofilters treated exhaust air from swine nurseries (288 piglets) which shared a deep-pit manure storage. Monitoring was focused on a portion of each biofilter (L: 3.5 m, W: 1.25 m, H: 0.35 m) that treated air from a continuously running pit fan with an airflow rate $\sim 0.3 \text{ m}^3 \text{ s}^{-1}$; a 6 s empty bed contact time was the design target. For more information about biofilter designs and media characteristics see Janni et al. (2014).

4.3.2. Biofilm monitoring

Chip baits for biofilms, consisted of 3 birch (*Betula papyrifera*) wafers ($6.5 \times 2.0 \times 0.5 \text{ cm}$) cut with the largest face tangential, were strung to a numbered aluminum tag with fishing line (Figure 3.1, Appendix 4.1). The wafer dimensions resembled the average biofilter media size distribution, and replicate wafers enabled paired biomass measures. Initial chip masses of the baits were recorded and baits were placed in both biofilters at 4 locations at the time of biofilter construction: 50 and 300 cm from the fan inlet (*near* and *far*, respectively), and 5 and 30 cm from the biofilter surface (*shallow* and *deep*, respectively) (Figure 3.1). Ten baits were collected from each biofilm monitoring location after 16, 29, 42, 63, 99, 134, 198, 409, 591, 785 and 1132 days of incubation and

returned to the laboratory in sterile bags on ice. Sample mass was recorded, biofilm material was harvested aseptically using a sterile razor blade, replicate biofilms were pooled, baits were subsampled for moisture content, and mass loss was calculated.

Microbial biomass measures were made on a subset of biofilm collections: day 409 (year 1), day 785 (year 2), and day 1132 (year 3). Fresh homogenized biofilms were subsampled for microbial biomass measures and the remaining pooled biofilms were frozen at -20°C for later DNA extraction. Total microbial biomass was determined by chloroform fumigation extraction similarly to the approach of Needelman et al. (2001), with sample moisture content raised above 50% for dry samples to enable maximal C flush (Ross, 1989). Samples were extracted in 0.1 M K_2SO_4 ($12.5 \text{ mL dry g}^{-1}$) with orbital shaking (100 rpm) for 1 h, then filtered and stored at -20°C . Extracts were later thawed, diluted 1:20 with Type I H_2O , and analyzed for non-purgeable organic C on a Shimadzu TOC-VCPH analyzer (Shimadzu Corp., Kyoto, Japan).

Fungal biomass was measured chromatographically as total ergosterol similarly to the approach of Tank and Webster (1998). Free ergosterol was extracted from samples stored at -20°C in 5 mL methanol by a 2 h, 65°C reflux. Samples were saponified and refluxed 30 min to solubilize esterified ergosterol components. Samples were centrifuged, the supernatant was removed, residual solids were rinsed in methanol, the samples were again centrifuged and the supernatants combined. Total ergosterol was separated from alkaline methanol by 3 pentane phase separations and extracts were combined and evaporated. Ergosterol was re-dissolved in methanol, filtered and measured with high

performance liquid chromatography (HPLC) on an Agilent 1200 series HPLC (Agilent Technologies, Minnetonka, MN, USA) using a methanol mobile phase, 1 mL min⁻¹ flow rate and Phenomenex™ 4μ Hydro-RP 80a column (Phenomenex Co., Torrance, CA, USA) at 40°C, using 7-dehydrocholesterol as an internal standard. These extraction methods were optimal for high yield and recovery (Appendix 4.2).

4.3.3. Fungal succession monitoring

A next generation sequencing approach was used to investigate fungal community succession and origin in the north biofilter. For successional monitoring, DNA was extracted from the north biofilter far deep (*deep*) and far shallow (*shallow*) locations of the day 409 (*Yr1*) and day 1132 (*Yr3*) biofilm collections. To explore potential sources of fungal inoculum, DNA was also extracted time zero media (*time0* media) and a time zero manure sample from the deep-pit storage (*manure*) which also had been stored at -20°C. Three replicates of all samples were used. DNA was extracted by a modified CTAB procedure (Song et al. 2014). Samples were extracted in 800 μl of CTAB extraction buffer (2% CTAB, 2% PVP-40, 0.5% β-mercaptoethanol) and incubated 1 h at 65°C. Impurities were removed by phase separation with phenol/chloroform/isoamyl alcohol (25:24:1) then with chloroform/isoamyl alcohol (24:1). DNA was precipitated with isopropanol, washed with 70% ethanol and dissolved in nuclease-free H₂O. DNA extracts were purified using the QIAquick® PCR purification spin column kit (Qiagen Sciences, Germantown, MD, USA), dissolved in nuclease-free H₂O and quantified using a Qubit® Fluorometer (Life Technologies, Grand Island, NY, USA).

For sequencing, the fungal specific ITS1 region was amplified in a 25 μ L PCR reaction (12.5 μ L Roche 2X FastStart, 1.5 μ L MgCl₂ (25mM), 0.25 μ L BSA(50 μ g/ μ L), 0.45 μ L of each barcoded primer (ITS1F & ITS2), 2 μ L DNA (diluted 1:10), 7.85 μ L molecular grade water). Reaction conditions included an initial denaturation step (95°C, 10 min), then 30 cycles of (denature 95°C, 30 s; anneal 50°C, 20 s; elongate 72°C, 30s), followed by a final elongation (72°C, 8 min). Amplification was verified on an electrophoresis gel with 1X TAE buffer. Amplicons were purified using the Agincourt AMPure XP PCR purification kit (Beckman Coulter Inc., Brea, CA, USA), DNA concentration was quantified with a Qubit® Fluorometer (Life Technologies, Grand Island, NY, USA), and combined in equimolar concentrations (25 ng) into a single pool for Illumina MiSeq sequencing (250 base pair end) at the University of Minnesota Biomedical Genomics Center.

Cutadapt was used to trim primer sites, adapter sites, and low quality ends of reads (< q20) from forward MiSeq Illumina reads (match error rate of $e = 0.2$). Both ends of reads were trimmed (quality threshold set at 20) and reads less than 125 bp were filtered. USEARCH was then used to de-replicate and discard singletons, and then chimeras were filtered and sequences were clustered at 97% similarity using the UPARSE algorithm to generate an operational taxonomic unit (OTU) list, a proxy for species list. The OTU list was then filtered against the Basic Local Alignment Search Tool (BLAST) database (National Center for Biotechnology Information, Bethesda, MD, USA) to remove low match length sequences. Using QIIME, OTUs with over 97%

similarity to BLAST entries were assigned a taxonomical label and samples were rarefied to an equal sampling depth of 20,000 sequences. A mock community of representative biofilter fungi was used to verify the integrity of the pipeline similar to the methods of Nguyen et al. (2015). FUNGuild was used to identify guilds of the sequenced taxa.

4.3.4. Statistics

For the first objective, coefficient of variation was used as the metric of biotic and abiotic variability. Using the final sample collection (day 1132), variability was measured between chips of the same bait, between replicate baits, between all chips for a location, and between all chips of a single biofilter. Variabilities were averaged for each level of comparison and deviations of this variability were calculated.

For the second objective, the R (version 3.1.3) package ‘vegan’ was used for diversity and statistical analyses. Alpha diversity, or the community diversity within a sample, was measured using the Shannon-Wiener index. ANOVA and Tukey HSD were used to compare the diversity measures between samples. Beta diversity, or the differential diversity between samples, was measured using Bray-Curtis dissimilarity. The dissimilarity matrix was used to plot a nonmetric multidimensional scaling and the envfit function was used to fit the variable time onto the ordination. Betadisper was used to test distance of points to their centroid and permutest was used to test if these centroid distances were different for different sample replicates. A pairwise permutation was run to test if sample communities were distinct from one another. For OTU and guild

summaries, OTUs with like taxonomic labels were first condensed and counts were made based on this updated OTU table.

4.4. Results

4.4.1. Consequences of microbial growths on biofilter media and its variability

Average media moisture content of the north and south biofilters ranged from 30-60% and 40-70%, respectively (Figure 4.1). In the north biofilter, the shallow locations were generally wettest while no locational effect was measured in the south biofilter. A slight rise in average moisture content was measured in later south biofilter collections, while no clear temporal change was measured in the north biofilter. In both biofilters, sample moisture content could range > 60% within a single time collection, though not equally for all locations.

Average mass loss for both biofilters increased steadily over time with decay slightly faster in sampling sites closer to the barn (Figure 4.1). Generally, mass loss was higher in the south biofilter where average losses after 3 year were 44.07%, 41.33%, 39.76%, and 43.76% for the close deep, close shallow, far deep, and far shallow locations, respectively. Mass losses were quite variable between bait chips in this biofilter, ranging over 80% at the final collection. Average mass losses in the north biofilter were 27.83%, 31.50%, 26.10%, and 21.69% for the close deep, close shallow, far deep, and far shallow locations, respectively. Mass loss was less variable in this biofilter, typically ranging ~40% at the final collection with the exception of the far shallow location where chip variation was around 60%.

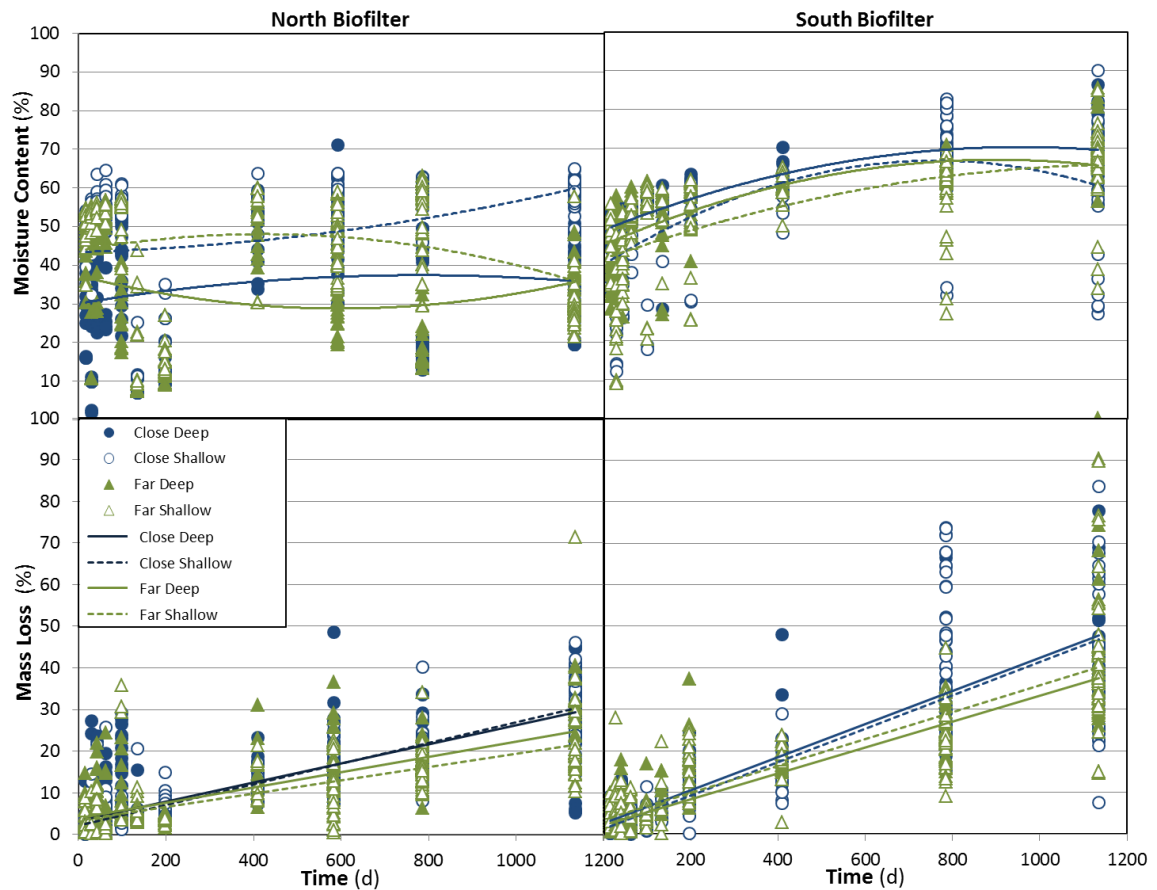


Figure 4.1 Spatial and temporal media moisture content and mass loss of baits collected from the north and south biofilters.

Measured moisture content and mass loss variability increased but stabilized with increased sampling. With moisture content, there was the least variability between chips of the same bait and the greatest variability between the neighboring biofilters (Figure 4.2). In contrast, the average deviation of this variability was greatest between chips, ~22%, but was smallest when biofilters were compared, ~3%. Mass loss measurements were less variable than moisture content (Figure 4.2), but similarly increased with the distance between samples. Unlike moisture content, however, the deviation of this variability also increased with distance between samples.

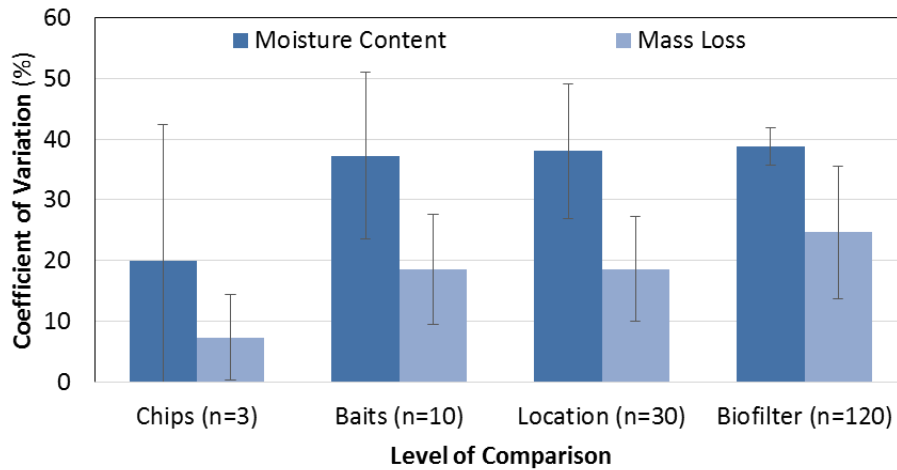


Figure 4.2 Coefficient of variation of moisture content and mass loss at the final 3 year harvest date. Levels of comparison include chips of the same bait (chips), baits of the same location (baits), chips for an entire sample location (location), and all the sampled chips of a biofilter (biofilter).

4.4.2. Variability of microbial measures on biofilter media

Fungal biomass, measured as ergosterol, ranged from 0.2 to 4.6 mg g⁻¹ of dry biomass over the 3 years of biofilter sampling (Figure 4.3). Ergosterol rates increased over time in the north biofilter and exceeded south biofilter rates, which were more stable and ~ 1 mg g⁻¹ of dry biomass across the sampling. The fungal biomass ratio, measured as ergosterol:microbial C, ranged from 0.08 to 0.85. For many sample locations, this ratio increased slightly over time, while a more pronounced increase was measured for the shallow locations of the north biofilter.

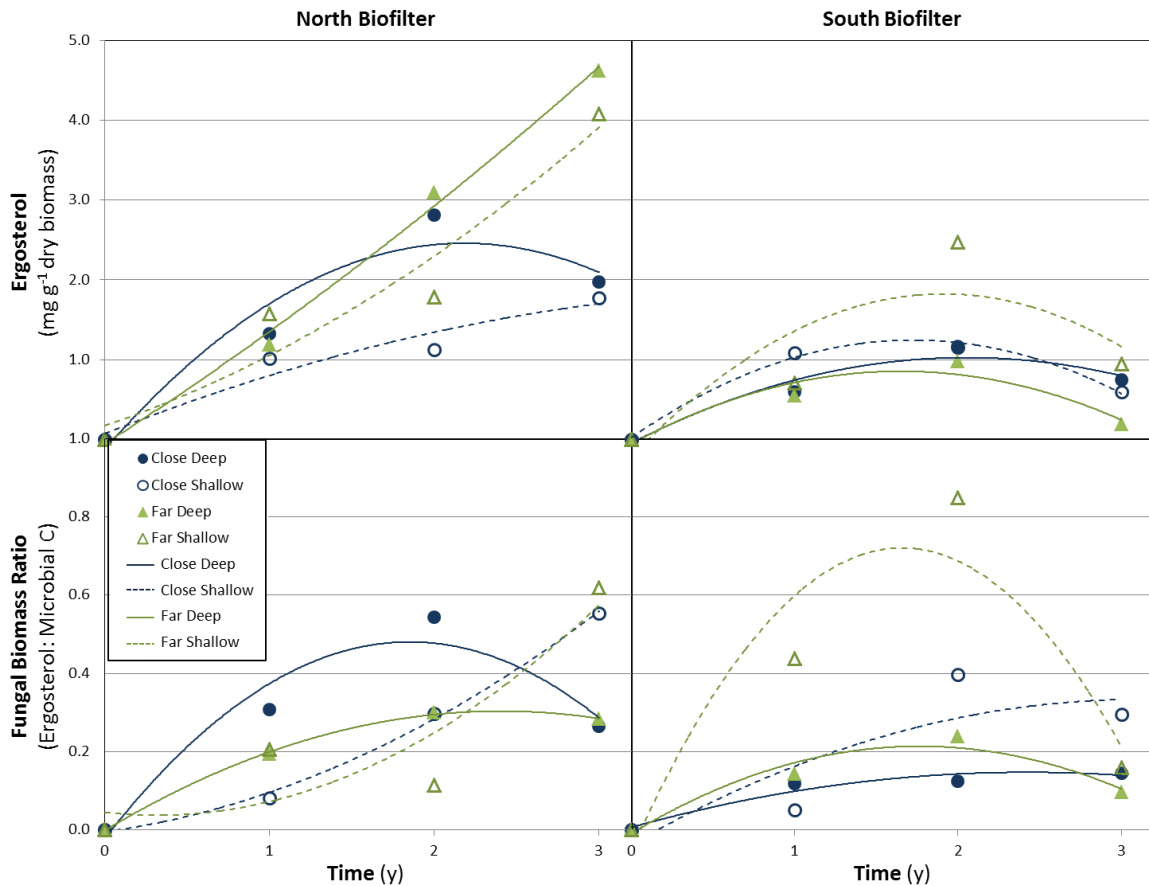


Figure 4.3 Average ergosterol and fungal biomass ratios over time in the north and south biofilters.

Average coefficients of variation were minimal for biomass measures, with a small increase in microbial C and ergosterol variability calculated with increased sampling (Figure 4.4). The deviation of this variability was greatest when comparisons were made across chips and locations. There was less variability between subsamples with comparisons across a biofilter having the smallest deviations.

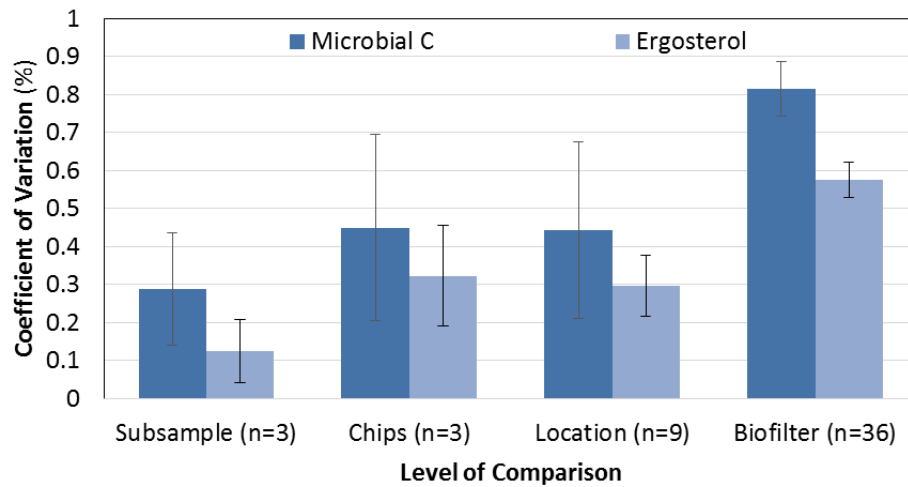


Figure 4.4 Coefficient of variation of microbial C and ergosterol biomass at the final 3 year harvest date. Levels of comparison include subsamples of the same biomass pool (subsample), biomass pools of separate chips from the same bait (chips), chips for an entire sample location (location), and all the sampled chips of a biofilter (biofilter).

4.4.3. Fungal communities in a livestock emission biofilter

Most major fungal taxa were represented in the > 350 fungal OTUs identified in the sequenced biofilter materials. Generally species richness decreased over time (Figure 4.5). When the top 50 most abundant OTUs were focused on, 91.5% could be assigned a phylum and class level designation (Figure 4.6). The potential biofilter inoculum, *time0* media and *manure*, were dominated by fungi in the phylum Basidiomycota. Tremellomycetes, which represented 61% and 91% of the OTUs for *time0* and *manure* samples, respectively, were particularly dominant. The second most abundant taxa in these samples were yeasts in the phylum Ascomycota and class Saccharomycetes. Saccharomycetes were not detected in *Yr1* or *Yr3* samples and Tremellomycetes were reduced, representing only 15% and 10% of the OTUs in *Yr1* *shallow* and *deep* samples, respectively, and only 2% or less of *Yr3* samples. The mushroom-forming

Agaricomycetes were more prevalent in *Yr1* samples, making up 28% and 22% of the shallow and deep location, respectively. Basidiomycota were generally less dominant in *Yr1* samples, however, with Zygomycota making up 31% of the *shallow* community and 41% of the *deep* community represented by the phylum Ascomycota and class Leotiomycetes. Approximately 20% of the *Yr1* OTUs were unidentifiable. By year 3, the phylum Ascomycota was clearly dominant, particularly the class Leotiomycetes which represented 91% and 77% of the *Yr3 shallow* and *deep* OTUs, respectively. Dothideomycetes represented another 20% of the *Yr3 deep* OTUs.

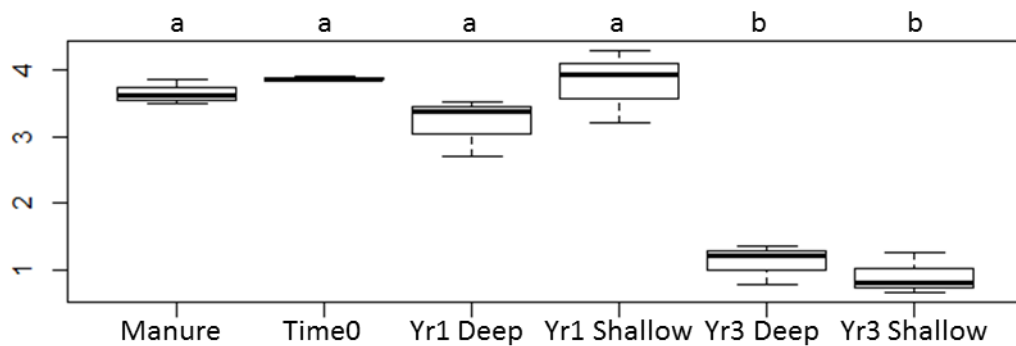


Figure 4.5 Shannon alpha diversity metrics for biofilter sample communities. Similar letters note measures that are not significantly different (n=3).

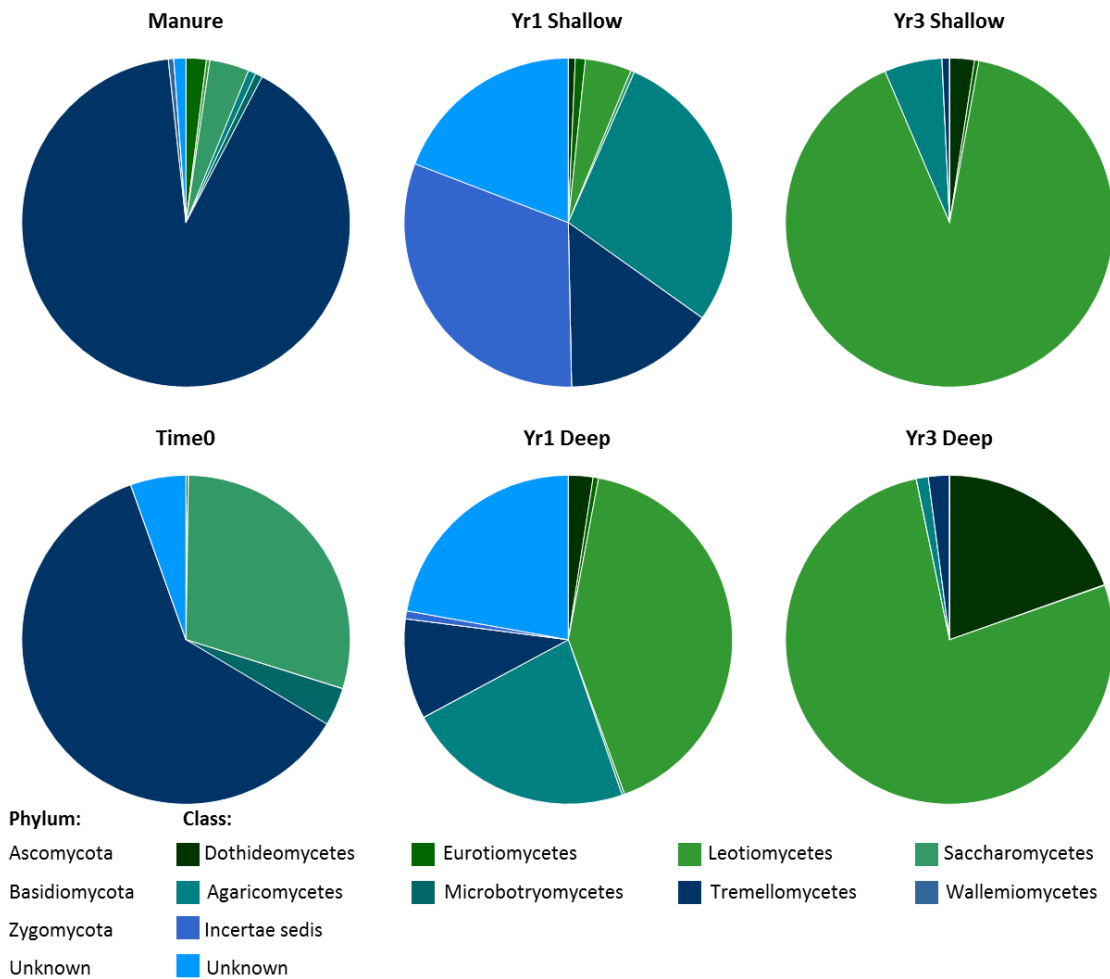


Figure 4.6 Phylum and class level fungal community structure by sample of the 50 most abundant OTUs.

Temporal shifts in fungal guilds were also observed (Figure 4.7), however, guild associations could only be made for a very small portion of the OTUs due to our limited understanding of fungal diversity. For the *manure*, *time0*, *Yr1 shallow*, *Yr1 deep*, *Yr3 shallow* and *Yr3 deep* samples, approximately 84%, 98%, 71%, 75%, 91% and 79% of the OTUs, respectively, could not be assigned a guild. Of the identifiable guilds, saprotrophs dominated. While animal-associated and unknown saprotroph guilds were

common with initial biofilter materials, wood and unknown saprotrophs were most represented in year 1 and 3 samples.

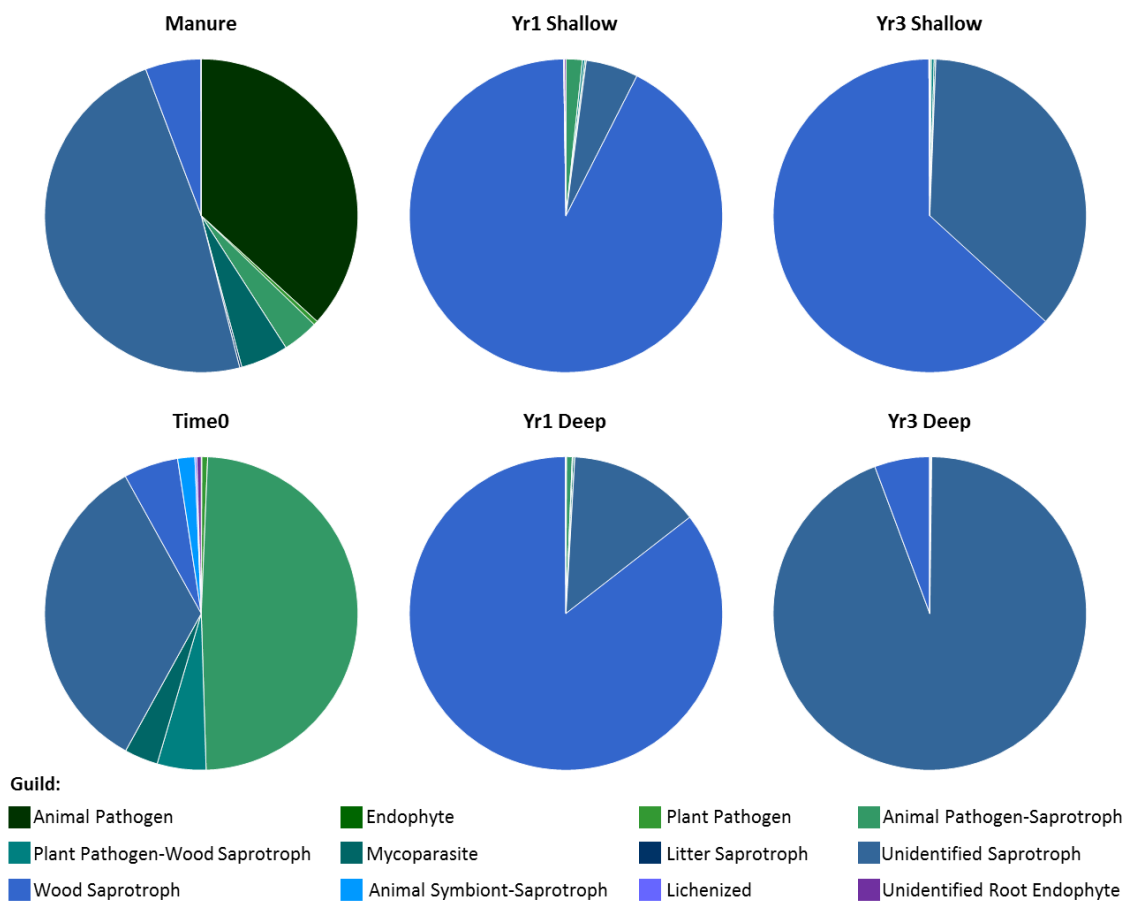


Figure 4.7 Identifiable guilds of the biofilter fungal communities.

Replicate samples from the same biofilter material show close community similarity and their respective distances from their centroid were not found to be statistically distinct. Some differences were found between sample, however, as well as a clear influence of initial communities on later, climax communities (Figure 4.8). *Time0* and *manure* sample communities were unique, indicated by their separation on the NMDS plot and verified by the pairwise permutation ($p=0.009$). *Yr1* sample communities

deviated from initial communities, but their equidistance from initial samples indicated a shared influence of these potential inoculum sources on *Yr1* samples, though *Yr1 shallow* and *time0* communities were significantly different based on pairwise permutation tests ($p=0.018$). By year 3, spatial differences in the fungal communities could not be resolved with noteworthy community overlap ($p=0.553$). While *Yr3 shallow* and *deep* communities had significantly diverged from the *Yr1 shallow* communities ($p= 0.038$ and 0.015 , respectively), there was no significant difference from *Yr1 deep* or initial microbial communities. The time vector shows support for a shift from initial fungal communities toward a year 3 climax community.

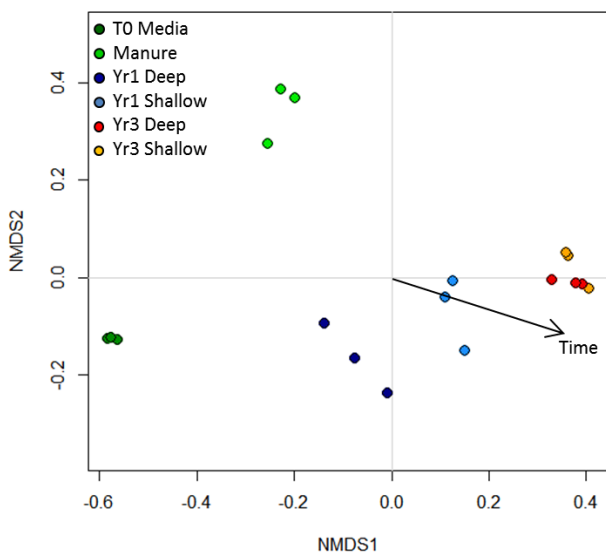


Figure 4.8 Nonmetric multidimensional scaling (NMDS) ordination of sample biofilter community data showing the influence of the vector time.

Over 20% of the initial *time0* media and manure communities were either outcompeted or could not establish in the biofilter after 1 year (Figure 4.9). By year 3 less than 4% of the initial communities were still present. While communities associated with *time0* may have been more slowly depleted, averaging slightly higher similarities at year

1 than manure, they were nearly eliminated by year 3. In contrast, ~2% of the manure community persisted at year 3.

While a significant percentage of these initial communities were lost or could not establish by years 1 and 3, some of the dominant taxa in initial samples were also abundant in later samples (Table 4.1). Manure communities were particularly influential as their dominant taxa *Trichosporon*, a genus not found in *time0* media, was an abundant taxa in all *Yr1* and *Yr3* samples. *Time0* media was less influential, but its dominant taxa *Guehomyces pullulans* was also found in *Yr1* shallow communities. Other abundant taxa in the *Yr1* and *Yr3* biofilms were present in *manure* and *time0* media but in low numbers. The dominant taxa, Helotiales and *Trametes spp.*, were present in both *manure* and *time0* media at low abundance, while the abundant taxa *Preussia spp.* was detected only in *time0* media and at very low abundance.

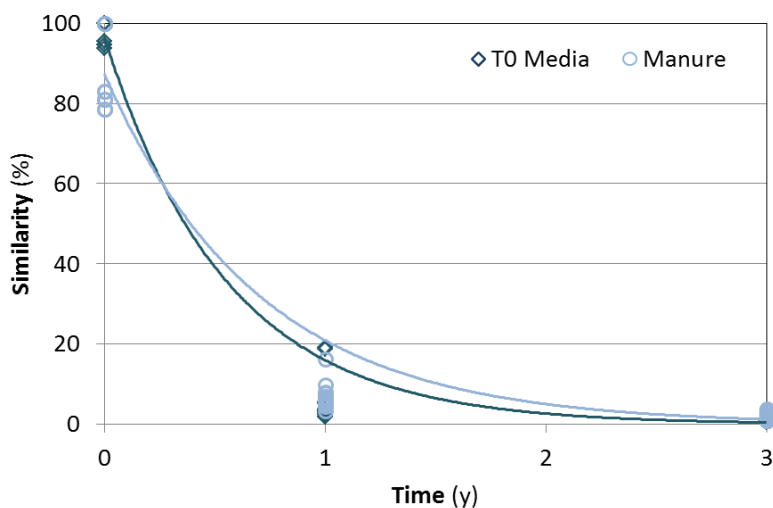


Figure 4.9 Similarity based on Bray-Curtis of year 1 and 3 communities to the initial communities of either *time0* media or the manure.

Table 4.1 The 5 dominant fungal OTUs in each sample and their percent abundance.

Rank	Manure	Time 0 Media	Yr1Deep	Yr1Shallow	Yr3Deep	Yr3Shallow
	spp %	spp %	spp %	spp %	spp %	spp %
1	<i>Trichosporon asteroides</i> 29.12	<i>Guehomyces pullulans</i> 26.99	<i>Helotiales sp</i> 39.55	Unidentified 29.43	<i>Helotiales sp</i> 76.48	<i>Helotiales sp</i> 89.07
2	<i>Trichosporon montevideense</i> 25.39	<i>Cystofilobasidium infirrominiatum</i> 26.52	<i>Trametes sp</i> 20.37	<i>Trametes sp</i> 25.36	<i>Preussia sp</i> 18.30	<i>Trametes sp</i> 5.45
3	<i>Trichosporon scarabaeorum</i> 10.69	<i>Candida mycetangii</i> 17.51	Unidentified 18.13	Unidentified 13.11	<i>Trichosporon moniliiform</i> 2.06	<i>Preussia flanaganii</i> 2.06
4	<i>Trichosporon asahii</i> 5.77	Unidentified 3.31	<i>Trichosporon moniliiform</i> 7.76	<i>Guehomyces pullulans</i> 7.27	<i>Preussia flanaganii</i> 1.15	<i>Trichosporon moniliiform</i> 0.72
5	<i>Trichosporon jirovecii</i> 5.50	<i>Candida norvegica</i> 3.18	<i>Preussia sp</i> 2.19	<i>Trichosporon moniliiform</i> 5.14	<i>Trametes sp</i> 1.11	<i>Leotiomyces sp</i> 0.52

4.5. Discussion

4.5.1. Microbial dynamics and variability in a full-scale biofilters

Both biofilters showed similar moisture, mass loss and microbial trends. Moisture content was in the range considered acceptable for effective odor mitigation (Chen & Hoff, 2009), though the north biofilter media was somewhat dry. The more optimal moisture content of the south biofilter media may explain the higher mass losses measured for this system. Similarly, when locations within a biofilter were compared, decay rates were higher in both systems close to the barn where sunlight and wind may have caused less intermittent drying. While not tightly correlated, fungal biomass was in some cases higher in these drier biofilter locations, such as the *far* location of the north biofilter. The fungal biomass ratio was also elevated in the *shallow* locations of both biofilters at year 3, biofilter locations most exposed to solar and wind drying. Finding

fungal dominance in drier and more exposed biofilter media is not surprising as fungi are known to tolerate desiccation stress better than bacteria (Kennes & Veiga, 2004).

High levels of chip to chip variability were detected for all abiotic and biotic measures. Spatial and temporal variability was significant for moisture content and media mass loss (*i.e.* decay), both conditions that affect microbial growth and consequences of their decay. While the pooling of 10 chips was sufficient for capturing media moisture and decay variability, the use of additional replicates improved the resolution of moisture content variability. Inadequate moisture content is the primary cause of biofilter performance loss (Chen & Hoff, 2009) and development of moisture sensors that can tolerate the variable and often harsh biofilter environment has slow and challenging (Yang et al., 2013). This work clearly demonstrates this variability and, in lieu of robust sensing equipment, it identifies the significant sampling efforts required to monitor media wetness when using the accurate, but labor intensive, gravimetric approach.

There was also spatial and temporal variability with microbial measures, though of smaller magnitude than was found with abiotic measures. This suggests the dominant microbial community was more homogeneous than the media conditions, possibly the result of its adaptation to the biofilter environment and tolerance to a range of abiotic conditions. Though less variable, the pooling of at least 10 chips was still necessary to account for the full variability of microbial growth in biofilters. Collectively, these findings suggest that large replicate numbers are needed to detect significant abiotic and biotic changes in the highly heterogeneous biofilter environment.

4.5.2. Successional patterns of fungi in a biofilter

Clear shifts in biofilter fungal communities occur over time with some of the dominant climax community taxa originating from the *manure* and *time0* media. The fungal communities of *manure* were dominated by *Trichosporon spp.*, a group of fungi recognized as skin endophytes with mild pathogenicity, but that are more often associated with saprobic activities (Carregaro et al., 2010; Colombo et al., 2011). The persistence of these fungi in biofilters could be the result of this ability to degrade animal cells deposited from the barn and manure storage exhaust. Perhaps *Trichosporon spp.* may then affect the abundance of other animal saprotrophs or even pathogen populations present on livestock dander and play a role in bioaerosol control. The abundance of these taxa in the dominant year 3 communities, our limited knowledge of their saprobic capacity in biofilters, and the potential for these animal saprobes to improve the biosecurity capacity of a biofilter all justify further study.

Originating from *time0* media, *Preussia spp.* was another fungus with dominance in the climax communities of the north biofilter. *Preussia spp.* are known endophytes, extremophiles (States & Christensen, 2001), and are recognized to be coprophilous (Guarro et al., 1997). These fungi are not typically found in decaying birch wood in the forest (Rajala et al., 2010) suggesting their small endophyte population is typically outcompeted. Evidently, however, in biofilters their affinities for animal excrement and tolerances to harsh abiotic conditions lead to their proliferation. There is little known about these fungi with no work investigating their responses to livestock emission or

capacities to oxidize them. Like *Trichosporon spp.*, this knowledge gap and the abundance of *Preussia spp.* in the biofilter warrants such work.

Other dominant taxa of the dominant biofilm community that developed were found in both *manure* and *time0* media, but in low abundance. These fungi included the Helotiales and *Trametes spp.* which are common in environmental samples of soils and forests. The Helotiales are the largest and most diverse grouping in the Leotiomycetes, and are largely recognized as saprobes (Wang et al., 2006). *Trametes spp.* are primarily wood decay fungi often found in decaying birch in the field (Rajala et al., 2010). The saprobic capacities of *Trametes spp.* are well characterized due to their ability to oxidize lignin (Hatakka, 1994), their potential industrial capacity (Archibald et al., 1997), as well as their breakdown of recalcitrant anthropogenic pollutants (Baldrian, 2003; Pointing, 2001). While Helotiales and *Trametes* fungi are likely involved in the decay of biofilter media, saprobic fungi, and specifically white rot fungi like *Trametes*, have demonstrated potential in the biofiltration of some industrial pollutants (Kennes & Veiga, 2004). The role of these fungi in the biofiltration of livestock emissions has not been thoroughly investigated (Ralebitso-Senior et al., 2012), though the likelihood for their influence and their presence encourages a more detailed look at their capacities in livestock emission biofilters.

4.6. Conclusions

Significant microbial and abiotic variability was found even between nearby biofilm baits. Sampling pooling requirements were made based on this extensive

variability. Using a sequencing approach, a succession of fungal taxa and guilds over 3 years of full-scale biofilter operation was noted. Both manure and time0 media were found to be significant sources of inoculum for the dominant fungal community that established. The influence of low abundant species on later communities was particularly interesting. Dominant taxa were primarily saprobic ascomycetous molds, and included animal-associated, coprophilous, extremophile, and wood decay fungi. Together these research efforts improve our understanding of microbial and abiotic system variability, and particularly highlight fungal taxa and successional patterns dynamics. These efforts can help target subsequent studies of biofilter microbiota and identify fungi with potentially important roles in biofilter performance and community stability worthy of future study.

5. LINKING MEDIA DECAY WITH TRAITS TO BETTER PREDICT BIOFILTER LONGEVITY

5.1. Summary

Biofilters can effectively treat a variety of emissions, but uncertain costs and longevity limit their adoption. To compare longevity of common media types and improve predictability for biofilter end-users, litter bags were used to test the effects of media type, nitrogen (N) enrichment and livestock production emissions on decay in a full-scale biofilter over a 27 mo. period. Generally, ‘by-product’ media (mulch, corn cobs) decayed faster than hardwood media, with softwood decay the slowest. Characterization work showed early stage decay was best predicted by nutrient content, while carbon fractions and nutrient content best predicted media longevity. N amendments and N-rich barn emissions enhanced decay relative to controls. By identifying decay rates and rate predictors specific for biofilter media, we provide biofilter engineers and farmers with a quantitative way to improve media selection based on the trade-offs between media cost and replacement frequency.

5.2. Introduction

Packed-bed bioreactors using organic media (e.g. wood mulch) are promising control technologies for treating aqueous (Schipper et al., 2010) and gaseous (Chen & Hoff, 2009) pollution. For gas-phase biofilters, removal efficiencies can exceed 90% for odor, ammonia (Chen et al., 2009), and petroleum based volatiles (Prenafeta-Boldú et al., 2012a), and range from 20 to 85% for the greenhouse gas methane (Veillette et al., 2012). In aqueous-phase bioreactors, removal efficiencies for nitrate can range from 50 to 100%

depending on loading (Robertson, 2010). Both these bioreactor systems utilize microbial growths on the solid media (biofilms) to degrade pollutants from contaminated effluents. Harnessing biofilms for waste mitigation offers several advantages, including 1) pollutant breakdown to non-hazardous products, 2) natural acclimation (adaptation) to the effluent, and 3) simultaneous treatment of many pollutants over a range of concentrations, all for a relatively low cost (Cabrol & Malhautier, 2011).

In the case of gas-phase biofilters for agricultural systems, construction and operational costs are completely within a farm budget (Delhomenie & Heitz, 2005) and design flexibility enables end-users to customize and self-construct biofilters for their specific operational needs (Schmidt et al., 2004). Though well-suited for farms, building a biofilter does not guarantee barn and manure storage emissions are efficiently controlled as loading rates, abiotic conditions and microbial communities all affect performance (Chen & Hoff, 2009). While biofilters must be managed for optimal performance, minimally managed biofilters can still be effective as biofilms can tolerate and adapt to shutdown periods, shock loading (Cabrol & Malhautier, 2011), low nutrients, pH stress, dry conditions and novel emissions (Kennes & Veiga, 2004). What will, however, ultimately result in irreversible performance loss is media degradation, compaction, and the resulting blockage of airflow (Chen & Hoff, 2009). This physical, not biological, failure of biofilters is only corrected through media refreshment or replacement, an unpredictable cost of biofilter maintenance and a potential barrier to wider adoption of the mitigation technology.

Observational evidence suggests that the typical useful life of wood-based media, the most common media used in the United States, can reach 5 years (Chen & Hoff, 2009; Schmidt et al., 2004). This will vary, however, due to media characteristics, environmental conditions, and the resident microbial community. While longer-lived, engineered media types are increasingly being used to target more regulated, non-agricultural effluents (Prenafeta-Boldú et al., 2008), their higher costs have limited adoption by U.S. livestock producers. For farmers in the U.S., biofilter usage is largely voluntary and cost is a significant impediment to more widespread use of these control technologies. Although usage of wood-based media for U.S. livestock production biofilters will likely continue, usage of agricultural by-products (e.g. corn cobs), which may be produced on farm or regionally at low cost (Ramirez-Lopez et al., 2003), is likely to expand. The useful life for biofilter media types has not yet been quantified, however, despite the utility of such data for discerning media longevity and replacement costs. Litter bags, used to study decay in natural systems, are well-developed and suitable for such research, though they have not yet been applied to engineered biofilter systems.

Our objective was to determine the longevity of biofilter media types relative to their traits in order to assess biofilter media service life. To do this, we utilized litter bags and characterized media traits to measure and predict biofilter media decay rates, adopting the approach commonly used to study decay in natural systems (Prescott, 2010). For a biogeochemist, the N rich ammonia emissions from livestock production create a unique engineered system in which to test the influence of N loading on decomposition, a

topic of current interest in natural systems (Knorr et al., 2005). By correlating these rates with media traits, including a targeted assessment of the effect of N enrichment, we hope to enable biofilter engineers and farmers to better assess media costs and replacement frequency tradeoffs. By improving service life predictions and cost analyses through direct use or incorporation into decision making tools, these data might facilitate expanded usage of biofilters on farms and for other uncontrolled effluents.

5.3. Methods

5.3.1 Biofilter media, litter bags, and field site

The biofilter media tested included locally sourced softwoods (cedar, eastern red, *Juniperus virginiana*; **pine**, eastern white, *Pinus strobus*; **SYP**, southern yellow pine, *Pinus* spp.), hardwoods (**ash**, white, *Fraxinus americana*; **aspen**, quaking, *Populus tremuloides*; **birch**, paper, *Betula papyrifera*; **maple**, sugar, *Acer saccharum*; **oak**, northern red, *Quercus rubra*), a forestry by-product (**mulch**), and an agricultural by-product (**cob**, maize, *Zea mays*). Sapwood tissues and by-products were processed using a disk chipper and then sieved, selecting chips in the 1-2 cm fraction (Appendix 5.1 a-d). Litter bags containing media (n=40 per type) were prepared using 20 cm² pieces of nylon window screen (~1 mm openings) folded in half and heat-sealed on the edges. A soldering iron was used to melt a hole in the corner of each bag, and a numbered aluminum tag was affixed with a nylon cable tie. Bags were tared, 30 g of conditioned media (65% RH, 20°C, until mass stabilized, ~2 wk.) was added, the top of the litter bag was sealed, and the total weight was recorded (Appendix 5.1 e).

Litter bags were deployed in March 2012 in the northwest, up-flow, flat-bed, Birch woodchip biofilter at the University of Minnesota West Central Research and Outreach Center swine nursery barn in Morris, MN (detailed in Janni et al. 2014). To test the effects of emissions on biofilter media decay, half of the litter bags were buried in the biofilter bed treating barn emissions from a regularly running exhaust fan ('treatment' location). The other half of the litter bags were buried in a partitioned area of the biofilter where the exhaust fan was shut off and emissions flow was restricted by plastic sheeting across the plenum ('control' location) (Appendix 5.1 f-h). Comparisons of average moisture content and inlet gas concentrations of the 2 biofilter locations are summarized in Appendix 5.2.

At 4 collection points (3, 6, 15 and 27 mo.), 5 replicate bags of each media type were collected from the treatment and control locations. Upon collection, adhering material was removed, the wet field weights were recorded, and bags were re-conditioned (65% RH, 20°C, until mass stabilized, ~2 wk.). Weight loss was calculated from the difference of the initial and post-harvest conditioned weights. Using the single, first-order exponential model of decay the decay rate constants were determined as:

$$k = \frac{\ln(M_0/M_t)}{t} \times 100 \quad (5.1)$$

where M_0 = mass of sample at time = 0 (g), M_t = mass of sample at time = t (g), t = length of decay time (y), and k = decay rate constant (y^{-1}). Constants were determined for the initial sample harvest (0-3 mo. loss), for year 1 (3-15 mo. loss, June 2012-2013 loss), year 2 (15 - 27 mo. loss, June 2013-2014) and over the entire experiment (0-27 mo. loss).

5.3.2. Media characterization

Size fractions and media bulk density were measured by the methods of Janni et al. (2014). Dry weight was calculated from the conditioned weight knowing wood conditioned at 65% RH and 20°C has an equilibrium moisture content of 12.0% (Forest Products Laboratory, 2010) and used to determine percent moisture content. Media was air dried, milled to pass 40 mesh and media chemical analyses following the methods of Schilling et al. (2015a) were conducted. To summarize, ash content was determined gravimetrically after 24 h at 600°C. Extractives content was determined on a dry weight basis following 24 h Soxhlet extraction in 90% ethanol. Extractives-free powder was then hydrolyzed in 72% H₂SO₄. Solubilized saccharides were measured using high-performance liquid chromatography while acid-soluble lignin was measured by light absorption at 320 nm for Cob and 240 nm for woody substrates. The insoluble lignin was measured gravimetrically. Wood acidity (pH) was determined in a 1 mg wood powder per 0.01 mL of 5 mM CaCl₂ solution. Dilute alkali solubility (DAS) was also determined as an assessment of rot type (Schilling et al., 2015b). Additionally, total C and N were measured by dry combustion gas chromatography (GC) analysis on a Costech Analytical ECS 4010 equipped with a TCD detector (Costech Analytical Technologies, Inc., Valencia, CA, USA) at the Nebraska Ecosystem Analytical Laboratory. Other inorganics were measured by Inductively Coupled Argon Plasma Optical Emission Spectrometry (ICP-OES) on an Optima 3000 ICP Spectrometer (Perkin Elmer, Waltham, MA, USA) at

the University of Minnesota Research Analytical Laboratory. Three replicates were run for each media type for each analysis. Initial characteristics are shown in **Table 5.1**.

5.3.3. Nitrogen treatment tests

Nitrogen is an important plant trait which can be used to predict and control decay in natural systems (Knorr et al., 2005), and its significant emission from livestock production, primarily in the form of ammonia, will enrich biofilter media. To test the influence of N content on biofilter media longevity, SYP and birch chips were vacuum infiltrated with an aqueous solution of organic N. Casein hydrolysate was the organic N used as its composition is similar to the protein and amino N that typifies the N forms found in wood (Nordin et al., 2001). Chips were also treated with water as a control. Target N concentrations were 0.2% (control), 0.50%, 0.75% (to match N levels in mulch), and 1.25% (to exceed these levels). Chips were rinsed post treatment and a leach test was conducted on N-treated media, similar to the methods of Hobbie et al. (2014). Three replicate samples of each media at each treatment level were used to measure total N (after N treatment and leaching) according to the Dumas method, using a LECO FP-528 Nitrogen Analyzer (LECO Corp., St. Joseph, MI, USA) at the University of Minnesota Research Analytical Laboratory (Appendix 5.3). Treated chips were conditioned and 20 litter bags for each media type at each treatment level were made, as before. Ten litter bags were deployed in the treatment and the control location of the biofilter in June 2013. Litter bags were harvested in June 2014 and decay rate constants were determined.

Table 5.1 Mean and (standard deviation) of initial physiochemical traits of tested biofilter media (n=3 per analysis).

Media Type	Spp.	Bulk Density g cm ⁻³	pH	Ash %	Extract %	Glucose %	Hemicell. %	Lignin %	C %	Ca ppm	K ppm	Mg ppm	N %	P ppm	C:N	Lig:N
Softwoods	Cedar	0.17 (0.00)	3.8 (0.0)	0.00 (0.00)	3.0 (0.3)	39.6 (0.5)	15.7 (0.5)	29.0 (1.1)	51.7 (0.1)	717.3 (2.0)	121.5 (9.3)	74.8 (0.3)	0.3 (0.0)	30.6 (0.1)	177.9 (19.9)	99.4 (7.8)
	Pine	0.15 (0.01)	4.1 (0.1)	0.00 (0.00)	4.9 (0.3)	40.5 (0.3)	21.7 (0.1)	31.9 (0.3)	51.5 (0.1)	640.1 (8.4)	184.9 (5.3)	103.5 (0.7)	0.2 (0.0)	17.8 (0.6)	256.8 (66.6)	158.9 (40.0)
	SYP	0.15 (0.01)	3.6 (0.1)	0.04 (0.05)	2.9 (0.2)	48.4 (0.5)	20.8 (0.5)	20.6 (0.7)	49.7 (0.1)	270.9 (2.4)	63.3 (7.1)	40.0 (0.4)	0.1 (0.0)	22.8 (1.6)	364.9 (51.2)	150.5 (17.1)
Hardwoods	Ash	0.19 (0.01)	4.6 (0.0)	0.03 (0.06)	4.5 (0.2)	45.6 (0.2)	19.8 (0.3)	22.5 (1.4)	49.0 (0.1)	438.3 (11.3)	1535 (28.9)	148.3 (5.8)	0.2 (0.0)	180.8 (4.5)	203.3 (12.2)	93.1 (1.1)
	Aspen	0.13 (0.01)	4.2 (0.0)	0.26 (0.12)	1.9 (0.5)	49.2 (0.6)	30.1 (3.2)	20.5 (1.7)	48.5 (0.1)	1105 (4.5)	107.1 (9.7)	88.9 (0.5)	0.2 (0.1)	38.0 (3.0)	234.2 (39.3)	98.4 (9.5)
	Birch	0.17 (0.01)	4.2 (0.0)	0.00 (0.00)	2.0 (0.5)	44.0 (0.7)	25.4 (0.3)	19.0 (1.3)	48.7 (0.1)	613.4 (3.6)	138.8 (3.8)	151.1 (0.8)	0.2 (0.0)	56.3 (0.6)	225.6 (18.0)	87.6 (1.3)
Maple		0.17 (0.01)	4.5 (0.0)	0.25 (0.15)	2.0 (0.2)	52.0 (0.7)	18.3 (0.6)	22.0 (0.3)	48.6 (0.1)	1130 (13.5)	330.0 (10.6)	128.8 (1.3)	0.2 (0.0)	73.5 (0.9)	216.7 (21.8)	98.0 (9.0)
	Oak	0.20 (0.01)	3.5 (0.1)	0.20 (0.06)	6.3 (0.4)	43.0 (1.0)	23.5 (2.5)	22.8 (0.5)	49.1 (0.1)	358.6 (4.6)	784.5 (14.6)	8.4 (0.3)	0.3 (0.0)	9.7 (0.2)	196.7 (19.0)	91.2 (7.3)
Byproducts	Mulch	0.13 (0.01)	6.1 (0.1)	3.05 (0.17)	2.2 (0.3)	35.6 (0.6)	17.4 (1.2)	26.7 (1.1)	48.0 (0.2)	13557 (402)	3248. (31.4)	1015 (20.1)	0.8 (0.1)	795.3 (10.4)	61.6 (3.8)	34.3 (1.0)
	Cob	0.15 (0.01)	4.4 (0.0)	0.26 (0.16)	5.3 (0.3)	38.9 (0.4)	39.9 (0.3)	18.9 (0.3)	47.2 (0.2)	202.1 (3.3)	5094 (55.9)	325.7 (5.1)	0.7 (0.2)	927.3 (19.7)	64.1 (1.7)	25.7 (1.0)

5.3.4. Statistics

To meet heteroscedasticity and normality assumptions (assessed visually and tested by Shapiro-Wilk), Log10-transformations were applied to the trait variables extractives, glucose, Fe, K, Mg, Mn, Na, P, and C:N, and reciprocal-transformations were applied to pH, lignin, total hemicellulose, Al, C, Ca, and N. Ash, xylose, galactose, arabinose, mannose, B, Cd, Ni, Zn were not used in the analyses as they were collinear with other predictors or would not fit a normal distribution. No transformations were required for mass loss, density, lignin:N, or moisture content.

Differences in media type characteristics, media type mass losses, and N treatment mass losses were compared by ANOVA with differences in means were tested by Tukey HSD. Control and treatment differences were compared by T-test. To identify predictors of media decay for each litter bag harvest, media traits and media mass loss for each time and biofilter location were correlated as is commonly done for biogeochemistry studies (Freschet et al., 2012). To further resolve drivers of decay, a multiple regressions approach was also used. For this, variables strongly correlated to mass loss (> 0.5 and $< -0.5 R^2$) were used as predictive variables in initial full models, and variables with the least significance (highest p value) were excluded one at a time from the model until a simplified model with all variable p values < 0.05 was generated. The simplified models were then compared by F-test to identify the simplest model that was statistically relevant (Motulsky & Ransnas, 1987). The statistical software program R version 3.1.3 (GNU Project) was used for all analyses.

5.4. Results

5.4.1. Decay rates of various biofilter media

For both the treatment and control biofilter locations, the by-product media decayed the fastest while the softwood media decayed the slowest (Figure 5.1 & Figure 5.2). Unlike other media, by-products lost significant mass shortly after litter bag deployment. In the first 3 mo., the average mass losses in the treatment and control biofilter locations were 31.4% and 28.7% for the mulch, respectively, and 20.1% and 11.2% for the cob, respectively. No other media lost more than 10% of its mass in the first 3 mo. (Figure 5.1 & Figure 5.2), though ash did have elevated first year k values in the control area (Table 5.2).

Average decay rates for all media types accelerated in year 2 (Table 5.2). Generally these year 2 decay rates were greater than the k values calculated for the same media using the 27 mo. losses. A notable exception was the mulch, which was the only media to have a greater 27 mo. decay rate constant. With this slowing of mulch decay in year 2, the final remaining mass percentage of mulch was not significantly different from most of the hardwoods.

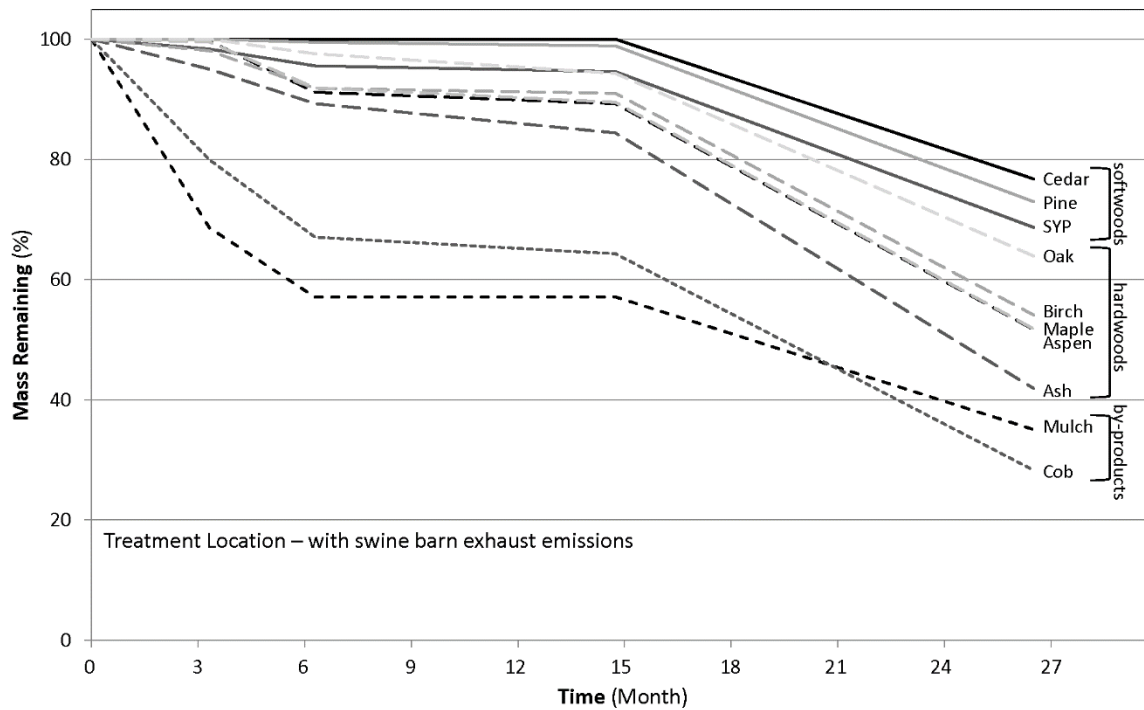


Figure 5.1 Mass loss of biofilter media incubated in the treatment location (n=5).

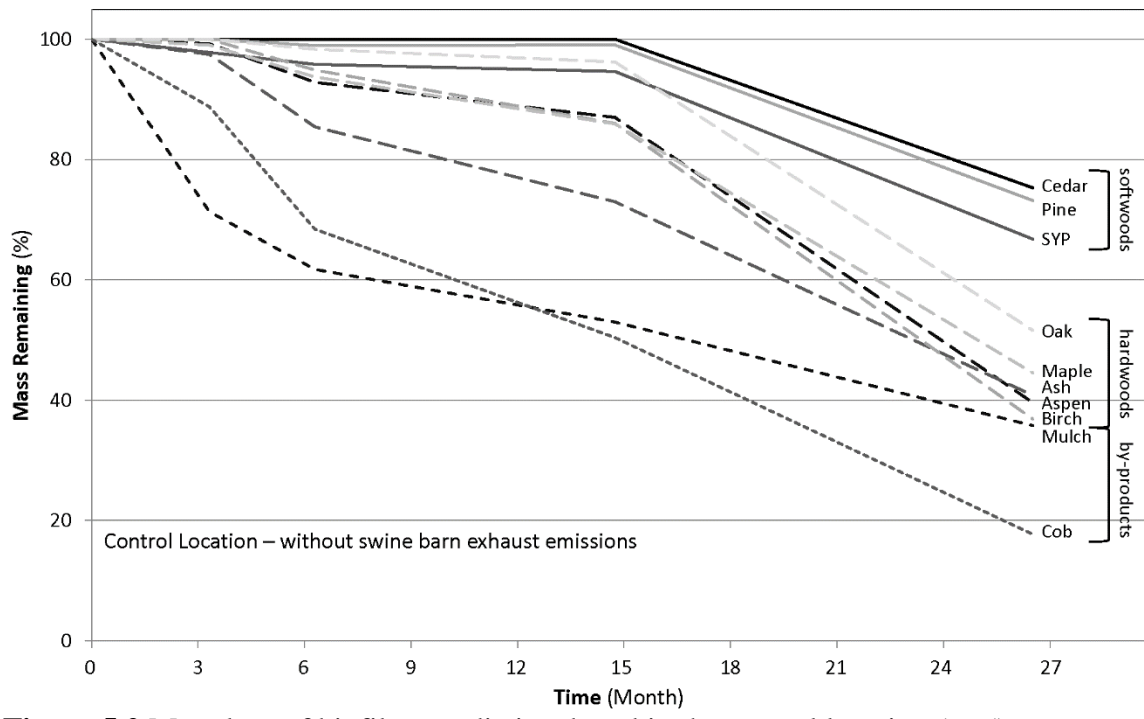


Figure 5.2 Mass loss of biofilter media incubated in the control location (n=5).

Table 5.2 Means and (standard deviations) of decay rate constants (yr^{-1}) for the first 3 mo. ($k_{3\text{mo}}$), for losses from June 2012-June 2013 ($k_{\text{year 1}}$), for losses from June 2013-2014 ($k_{\text{year 2}}$), and for the full 27mo. of decay ($k_{27\text{mo}}$) for both the treatment and control biofilter locations (n=5).

Location	Media Type	Spp.	$k_{3\text{mo}}$ yr^{-1}	SD yr^{-1}	$k_{\text{year 1}}$ yr^{-1}	SD yr^{-1}	$k_{\text{year 2}}$ yr^{-1}	SD yr^{-1}	$k_{27\text{mo}}$ yr^{-1}	SD yr^{-1}
Control	Softwoods	Cedar	-0.074	0.004	0.007	0.008	0.292	0.006	0.126	0.005
		Pine	-0.059	0.019	0.026	0.007	0.303	0.013	0.139	0.005
		SYP	0.088	0.012	0.034	0.005	0.342	0.006	0.180	0.004
	Hardwoods	Ash	0.044	0.197	0.306	0.064	0.591	0.164	0.405	0.084
		Aspen	0.006	0.075	0.140	0.030	0.791	0.111	0.414	0.047
		Birch	-0.068	0.033	0.170	0.058	0.859	0.242	0.450	0.086
		Maple	0.032	0.044	0.146	0.053	0.660	0.141	0.364	0.068
	Byproducts	Oak	-0.058	0.033	0.054	0.006	0.632	0.051	0.294	0.023
		Mulch	1.356	0.189	0.277	0.046	0.428	0.468	0.478	0.157
		Cob	0.486	0.316	0.579	0.207	1.044	0.226	0.775	0.079
Treatment	Softwoods	Cedar	-0.089	0.013	0.008	0.016	0.283	0.038	0.118	0.009
		Pine	-0.044	0.019	0.022	0.003	0.293	0.028	0.140	0.009
		SYP	0.065	0.008	0.039	0.009	0.319	0.015	0.167	0.008
	Hardwoods	Ash	0.205	0.074	0.118	0.015	0.700	0.126	0.390	0.058
		Aspen	0.015	0.039	0.110	0.010	0.554	0.170	0.298	0.074
		Birch	0.078	0.045	0.075	0.026	0.519	0.068	0.274	0.034
		Maple	0.021	0.117	0.105	0.038	0.555	0.093	0.294	0.043
	Byproducts	Oak	-0.048	0.017	0.071	0.035	0.387	0.048	0.199	0.006
		Mulch	1.509	0.160	0.178	0.086	0.503	0.561	0.504	0.232
		Cob	0.898	0.141	0.217	0.068	1.142	0.289	0.722	0.127

5.4.2. Predictors of biofilter media longevity

Media traits were useful predictors of media longevity, particularly C fractions and nutrient content. In the treatment location the top 5 predictors of 27 mo. decay were P ($R^2 = 0.886$), C ($R^2 = -0.863$), K ($R^2 = 0.785$), lignin:N ($R^2 = -0.772$) and pH ($R^2 = -0.742$), while C ($R^2 = -0.930$), lignin:N ($R^2 = -0.726$), P ($R^2 = 0.707$), lignin ($R^2 = -0.642$) and K ($R^2 = 0.627$) ranked highest for the control location (Appendix 5.4). Nutrient content was also a key predictor of mid- and early-decay, where decay for both biofilter locations at 3, 6 and 15 mo. was best correlated with P ($R^2 > 0.802$) followed by other nutrient predictors (e.g. N, P, K, Mg, pH).

The multiple trait model approach also identified C fractions and nutrient variables as best predictors of long-term decay and nutrient variables as best predictors of early decay. For 27 mo. mass loss, the best predictor for both biofilter locations was C, followed by Mg and K for the treatment and C:N and hemicellulose for the control (Table 5.3). Both of these regressions could predict over 95% of the 27 mo. media mass loss. Over 83% of the mass loss in the treatment and 88% of the mass loss in the control could be explained by C and N metrics alone (Table 5.3). For 3 mo. mass loss, the best predictor for both locations was pH, followed by other metrics of media quality (e.g. N, C:N, C) (Table 5.3). These regressions could explain over 96% and 88% of 3 mo. mass loss in the treatment and control locations, respectively.

Table 5.3 Significant simplified models for predicting biofilter media weight loss for early (3 mo.) and long-term (27 mo.) decay for each biofilter location (control & treatment) noting the intercept, coefficient values, degrees of freedom (df) and the coefficients of determination (R^2). Long-term models using only C and N as predictors are also included.

Dependent Variable	Intercept	Predictor Variables *							df	R^2
		(in order of significance from left to right)								
Mass Loss		Value of Coefficient								
3 mo. Control	4.9490	pH ⁻¹ -1.3310	Al ⁻¹ -0.2140	N ⁻¹ -0.0002					26	0.8833
3 mo. Treatment	1.9988	pH ⁻¹ -1.2330	log ₁₀ Fe 0.0466	Dens -0.8301	N ⁻¹ -0.0062	log ₁₀ CN 0.0121	log ₁₀ Na 0.0132	C ⁻¹ -3.0643	22	0.9636
27 mo. Control	5.3767	C ⁻¹ -9.3875	log ₁₀ CN -0.0004	Hemi ⁻¹ -0.0340					26	0.9547
27 mo. Treatment	3.5246	C ⁻¹ -7.0797	log ₁₀ Mg 0.1002	log ₁₀ K 0.0828					26	0.9526
27 mo. Control	6.0960	C ⁻¹ -11.2000	N ⁻¹ -0.0002						27	0.8787
27 mo. Treatment	5.0910	C ⁻¹ -9.1240	N ⁻¹ -0.0003						27	0.8352

* p values for all models was < 0.001

5.4.3. Effect of N loading on decay of biofilter media

Increasing the N content of birch and SYP significantly enhanced decay of these media in both the treatment and control biofilter locations. With the birch media, increasing the N content approximately 1% resulted in a 26.4% and 17.3% increase in mass loss for the treatment and control locations, respectively (Figure 5.3). Even a modest N increase to ~0.5% enhanced media mass loss significantly by 16.1% and 12.6% for the treatment and control locations, respectively. The k values associated with N-treated birch media were significantly higher than controls and reached values larger than those calculated for by-product media (Table 5.2 & Table 5.4).

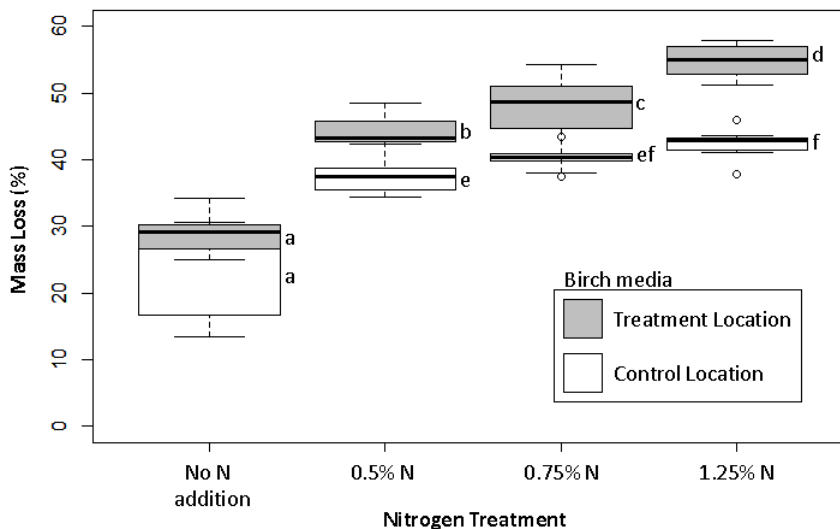


Figure 5.3 Mass loss of N-amended birch media incubated in the treatment and control locations of the biofilter for 12 mo. (n=10). Different letters note means that are significantly different ($\alpha=0.05$).

Similar, though smaller N effects were evident for the N-treated SYP media (Figure 5.4). With this media, increasing the N content to the 1.25% N target resulted in a 6.8% and 11.1% increase in mass loss for the treatment and control locations, respectively. At lower N treatments, increased decay was also observed. The k values

associated with N-treated SYP media were significantly higher than the controls and reached values as large as those for hardwood media (Table 5.2 & Table 5.4).

Table 5.4 Means and standard deviations of decay rate constants (yr^{-1}) for the N treated birch and SYP media for both the treatment ($k_{\text{Treatment}}$) and the control (k_{Control}) biofilter locations.

Spp	N	$k_{\text{Treatment}}$		k_{Control}	
		yr^{-1}		yr^{-1}	
Birch	Control	0.336	0.029	0.292	0.092
	0.5	0.591	0.042	0.473	0.043
	0.75	0.672	0.122	0.517	0.028
	1.25	0.796	0.053	0.552	0.038
SYP	Control	0.283	0.013	0.053	0.007
	0.5	0.342	0.022	0.125	0.018
	0.75	0.352	0.022	0.138	0.019
	1.25	0.378	0.032	0.177	0.021

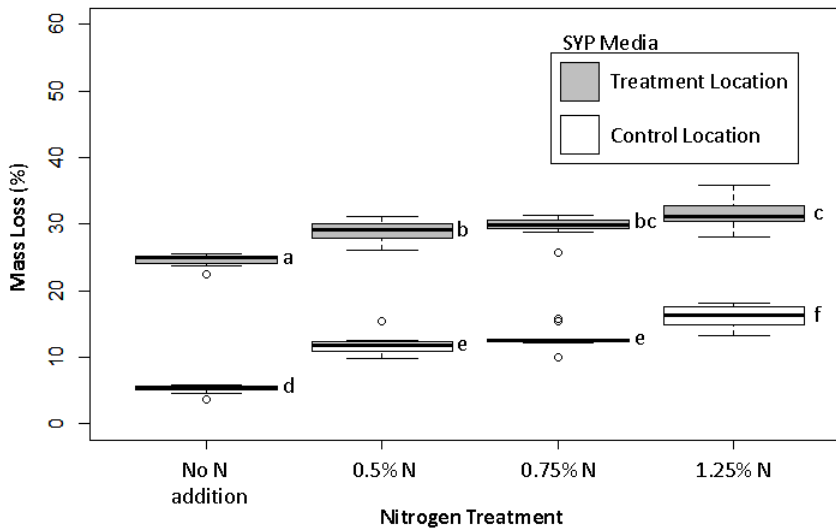


Figure 5.4 Mass loss of N-amended SYP media incubated in the treatment and control locations of the biofilter for 12 mo. ($n=10$). Different letters note means that are significantly different ($\alpha = 0.05$).

5.4.4. Influence of livestock production emissions on decay rates

The control location of the biofilter had significantly lower livestock emission concentrations than the treatment location. Methane, ammonia and hydrogen sulfide concentrations were more than 3, 6, and 31 times lower in the control location, respectively (Appendix 5.2). No significant differences were seen with carbon dioxide, nitrous oxide or sulfur dioxide. The treatment location was found to be slightly drier than the control location when moisture content data was pooled for all sample collections, though levels for both locations were normal for biofilter operation (Chen & Hoff, 2009).

Differences in decay between the treatment and control biofilter locations were varied and time dependent for mixed media types, but stimulation of decay by emissions was evident in the N treatment experiment. With the mixed media types, treatment losses were slightly larger than control losses for the first collections of litter bags (Figure 5.1, Figure 5.2 & Appendix 5.5). These differences were only significant at 3 mo. for birch and cob media and at 6 mo. for birch and mulch media. In later collections this pattern shifted, with slightly less decay measured for the treatment versus the control location. These differences were only significant at 15 mo. for ash and cob media and at 27 mo. for aspen, birch and oak media. No significant difference was measured between treatment and control locations for any time collection when softwood or hardwood media losses were collectively compared (Appendix 5.5).

In the N treatment experiment, both birch and SYP media decayed more rapidly in the presence of emissions regardless of their N content. These differences were

significant in all cases except for the untreated birch control. To explore the effect of emissions on untreated media, the no N birch and SYP weight losses were compared to losses of birch and SYP media from the mixed media litter bag experiment (Appendix 5.6). When located in the control location the average mass losses of the no N media were more similar to year 1 losses, but when located in the treatment they were more similar to the larger year 2 losses. There were also combined effects of N treatment and emissions. In the control location, the N treated birch and SYP media average mass losses approached the losses observed for year 2 litter bags and for birch there was no significant difference between the mass loss of the 1.25% N treatment and the average mass losses for year 2. In the treatment location, the combined effect of emissions and N resulted in N treated birch and SYP average mass losses to exceed year 2 losses. This was significant for birch and SYP at N treatments of 0.5% and above.

5.5. Discussion

5.5.1. Media decay patterns were distinct

Using the litter bag approach, we were successful in comparing the decay patterns of various biofilter media under full-scale operational conditions. Our results show that softwood media were most durable, while the by-product materials decayed fastest during the 27 mo. trial. This was not surprising as these patterns are typical of woody litter in natural systems. The meta-analysis by Weedon et al. (2009) covering all forested continents, for example, showed softwood k values routinely smaller than their hardwood counterparts. Despite this similarity in relative decay rates among media types, decay was

unanimously faster in our engineered environment. Observed k values were roughly an order of magnitude greater than average k values for comparable fine and coarse woody debris in natural systems (Pietsch et al., 2014; Russell et al., 2014; Weedon et al., 2009). Decay rate constants for by-product biofilter media were also larger than woody mulches decayed in natural environments (Valenzuela-Solano & Crohn, 2006) and corn cobs decayed in agricultural fields (Wienhold et al., 2011). In fact, when k values are compared, woody biofilter media degraded as quickly as mulches in natural environments while by-product biofilter media degraded as quickly as some foliar litters (Pietsch et al., 2014).

Decay rates are likely higher in a biofilter than in a natural system because of the unique environment of the packed bed and its enrichment in ammonia-N. A biofilter is an engineered system designed and managed for optimal microbial activity and performance (Cabrol & Malhautier, 2011). Biofilter media is selected to both promote air flow and to stimulate diverse microbial biofilms, with water content and sometimes pH actively managed to support these growths. The tempered effluents with diverse emissions further stimulates these microbial growths (Cabrol & Malhautier, 2011), and ammonia-N enrichment of the C-rich woody substrates can decrease C:N and enhance media breakdown by biofilter microbes.

Direct comparisons of decay rates between environments (i.e. biofilter and natural) can vary, however, by media size and by differences in the decay rate calculation method (Harmon et al., 2000). Regarding media size, it is reasonable to assume that our

chipped media may be small and of a higher surface area to volume ratio than woody debris of a forest, and this difference could contribute to elevated decay rates of biofilter media. Our biofilter media k values still often exceeded published k values for smaller twigs and fine woody debris (Fasth et al., 2011) suggesting size differences may not explain the differences in rates. For the calculation method, we assumed negative exponential decomposition. While this is the most commonly used approach, studies of short duration can result in inflated k values due to the changes in decay rates over time (Cornwell & Weedon, 2014; Harmon et al., 2000). Though our study was relatively short in duration (Russell et al., 2014), 27 mo. nears the half-life of most biofilter media (Chen & Hoff, 2009) and the weight losses we report for biofilter media at 27 mo. approximate weight losses reported after 5 years of decay in natural systems. It is also unlikely that our media has reached an asymptote of decay, as outlined by Harmon et al. (2000), or that decay would stall for several years. It seems reasonable therefore that biofilter media decays more rapidly and that calculation of higher k values is not an artifact of study length.

When biofilter media k values were calculated for different fractions of the decay period, clear differences between initial, year 1 and year 2 rates were observed. Unlike natural and urban systems where the rate of decay progressively diminishes for most tree litters (Cornwell & Weedon, 2014; Hobbie et al., 2014), the decay rate for most biofilter media seemed to increase over time. Only mulch, cob and to some degree ash showed the expected rapid phase of early decay, but even with these media, their k values for year 2

exceeded or were not significantly different than initial rates. An initial lag time in decay for some wood types has been attributed to slow colonization by decomposing organisms (Harmon et al., 2000). It is recognized in forest systems that there are transitions from an endemic decay community in wood to more dominant decay organisms, and that the rate of this shift is dependent on the organisms involved, litter conditions and the environment (Hiscox et al., 2015). Temporal changes in biofilter communities are likely governed by similar principles (Cabrol & Malhautier, 2011) and though this work did not explore biofilter microbial communities, perhaps the selective pressure of the unique biofilter environment slowed the initial colonization of media by robust decay organisms, but then stimulated their growth following colonization.

5.5.2. Media quality predicted decay

Though the patterns of decay showed some deviation from natural systems, the predictors of decay for biofilter media were familiar. Our correlations showed decay rates increased with nutrient levels (N, P, K, Ca, and Mg), and decreased with recalcitrant fractions (C and lignin). These variables, which were highly effective at predicting biofilter media decay, are regular components of models developed for decay predictions in natural systems (Prescott, 2010). Similar to the work of others like Prescott (2010), which has identified lignin:N as the key predictor of long-term decay, our work found recalcitrant fractions (C and lignin), nutrients, and their ratio (i.e. lignin:N) were highly predictive of biofilter media longevity.

As decay was initiating, recalcitrant fractions were less important and nutrient content was the key predictor. As decay progressed, the role of C and lignin emerged as a better predictor. A similar shift in predictors of early- and long-term decay is typical in natural systems (Prescott et al., 2004). It is interesting to note that while P was the tightly correlated to early biofilter mass loss, it was not a significant variable in the regressions, seemingly replaced by pH. While pH does correlate with P (Appendix 5.4), and may be indicative of base cation content, its role in decay can vary depending on the substrates tested (Freschet et al., 2012; Schilling et al., 2015a). Nitrogen was another prominent nutrient predictor, in early decay as N, and over longer decay periods as C:N. Though the significant models included additional quality variables, simple regressions using only C and N could effectively predict media mass loss.

It is important to note that other predictors of decay that were not measured here, such as microbial community functional indexes, may also have predictive capacity. Different microbial communities are known to degrade certain plant tissues and types (Veen et al., 2015) and DAS values in this study do suggest different rot types for different media types (Appendix 5.7). Discerning the microbial community and more importantly its role is a difficult task (Cabrol & Malhautier, 2011), however, and would be beyond the capabilities of most biofilter end-users. The adequate predictors of C and N, on the other hand, are familiar to most livestock producers and laboratory services are already in place for their analyses. These services and our models provide end-users with

a means to choose between two outwardly similar mixed media (i.e. mulches) and identify the one likely to provide the best longevity.

5.5.3. N enrichment altered decay rates

With N a predictor of decay for both early and late stages, it is without surprise that by increasing the N content of soft- and hardwood chips, decay significantly increased. Our findings also provide some evidence that livestock emissions rich in N can alter decay rates. Though varied effects of biofilter location were observed for the mixed media types, the decay of SYP and birch litter bags with and without N treatment was significantly higher in the treatment location. The stimulatory effect of media N concentrations on birch media appeared more significant with the emissions enrichment, while the effect was smaller for the lower quality SYP media despite higher N retention in the media. Nitrogen stimulation of decay is known to depend on litter quality, with a stronger stimulation for high quality (i.e. low lignin, high-nutrient) litters (Knorr et al., 2005). Our characterization work showed birch media to be somewhat higher quality than SYP media (**Table 5.1**) explaining, in part, the variable effect. Although birch had a larger response to the N treatment, SYP had a larger response to enrichment from the effluent, regardless of N content. It is likely that the interactions of litter quality, N form and decay communities all collectively impact biofilter media decay rates. Here we provide some evidence for these processes and highlight the potential of the biofilter system to further explore these dynamics.

5.5.4. Recommendations for biofilter end-users

Although biofilters offer a low cost pollution control technology compared to other mitigation options for farm emissions (Delhomenie & Heitz, 2005), costs can still be $> \$1,000 \text{ m}^{-3}$ (van Lith et al., 1997) with sizing dependent on effluent size and emissions flow rates (Schmidt et al., 2004). Media may not be as significant a construction cost as ducting and labor, but costs can still be significant, ranging from \$0 to $\$25 \text{ m}^{-3}$ for by-products, $\$20$ to $\$40 \text{ m}^{-3}$ for woodchips (based on regional quotes), and $\$100$ to $\$300 \text{ m}^{-3}$ for engineered media (van Lith et al., 1997). While many biofilter media types have been shown effective at mitigating livestock production emissions, including various soft- and hardwoods (Akdeniz et al., 2011; Janni et al., 2014), wood mulch is most commonly used (Chen & Hoff, 2009). Agricultural by-products have promise as a future media type and might be readily available, low-cost and functional media types (Ramirez-Lopez et al., 2003), but our work suggests they might also require more frequent replacement. With additional quantification of media decay rates, however, media longevity and cost tradeoffs can be properly assessed.

To provide an example of applying our data, we can set a reasonable lifespan for a mulch biofilter at 3 y, and use the calculated decay rate constant of 0.504 and the exponential decay model to find 22.1% of the mass remains at the time the media is exhausted. Using this level of decay as a threshold, we can estimate softwood media to last 10.7 y, hardwood media to last 5.2 y, and cob media to last 2.1 y. If we apply these values to an example swine barn biofilter system, (30,000 cfm ventilation rate, 5 s empty

bed contact time, required media volume of 70 m³ based on biofilter design guidelines of Schmidt et al., 2004), we can then compare costs. Estimating media costs (\$35 m⁻³ softwood, \$30 m⁻³ hardwood, \$25 m⁻³ mulch, \$15 m⁻³ cobs) and delivery charge (set at \$250, but will vary from on-farm vs. off-farm), the replacement costs would be \$2,700, \$2,350, \$2,000 and \$1,300 for softwood, hardwood, mulch, and cob media, respectively. If, however, we divide by longevity in order to factor replacement frequency, the annual costs shift to \$252, \$452, \$667, and \$619 for softwoods, hardwood, mulch, and cob media, respectively. This would effectively make the most expensive media to replace (softwood chips) the best overall value. When considering biofilters for multiple barns these differences could be more dramatic. In any case this must be placed in context with varying delivery charges, performance attributes, media costs and availability, but the example demonstrates the potential to integrate these decay data to support end-user decision-making tools (e.g. Feedlot Air Emissions Treatment Cost Calculator; (Lazarus, 2013)) and potentially hasten adoption of this promising technology.

5.6. Conclusions

Decay rates of widely-used biofilter media types were assessed and the biochemical drivers of biofilter media decay were identified. Like natural systems, softwood media decayed more slowly than hardwood media, with mulch and cob materials degrading the fastest. Media quality, particularly N content was highly predictive of media longevity, and both increased media N and the presence of emissions sped media decay rates. As exemplified, the decision making of biofilter engineers and

farmers is enabled by this assessment of media decay rates and quantitative estimates of media longevity. We hope this data can be incorporated into decision making tools to clarify actual operational costs, improve selection of media, and ultimately facilitate the increased usage of biofilters for livestock production emissions.

6. POTENTIAL ROLE OF BIOFILTER FUNGI IN CH₄ CAPTURE

6.1. Summary

Livestock production accounts for a third of total U.S. anthropogenic methane (CH₄) emissions. Mitigating these greenhouse gas (GHG) emissions is central to efforts aimed at curbing near-term climate change, but low-cost, practical technologies are needed to reduce fugitive CH₄ from farms. Biofilters have mitigation potential, but current designs for odor are limited in their ability to capture CH₄. Fungi have been shown to improve capture of hard to target gases in other biofilter applications, and were investigated here for their ability to capture CH₄. Using a lab-scale biofilter, several fungal species were shown to improve CH₄ capture compared to a bacterial system and sterile control. A subsequent experiment with *Pleurotus ostreatus* found capture to increase with increasing levels of fungal biomass. A chromatographic isotherm also showed that fungal materials were capable of sorbing CH₄ with greater sorption capacity possible by increasing fungal biomass. These results, demonstrate the ability of fungi to capture CH₄ and warrant their investigation as a way to improve the CH₄ mitigation capacity of livestock emission biofilters.

6.2. Introduction

Livestock production is the largest global source of anthropogenic CH₄ (Steinfeld et al., 2006). In the U.S., animal farms and their wastes are also the primary source, responsible for a third of CH₄ releases with upward trends since 1990 (US-EPA, 2015a). Recent reports in Nature (Montzka et al., 2011), Science (Shindell et al., 2012), by the

United Nations (UNEP & WMO, 2011), the U.S. State Department (U.S. Department of State, 2010), and the White House (White House, 2014) all highlight the importance of mitigating agricultural CH₄ emissions. These documents target CH₄ for its relatively short atmospheric life (~10 y) and potency (~25× the warming potential of CO₂), making its reduction an effective strategy for mitigating near-term climate change. With this growing awareness and political interest, livestock production facilities in the U.S. and elsewhere will likely see increased regulation of their GHG emissions (Pratt et al., 2013). This creates an urgent need for cost-effective mitigation solutions which are practical for usage on farms.

Biofiltration is a viable option for reducing CH₄ from livestock operations, used already for farm odor (Chen & Hoff, 2009), and for CH₄ from landfills (Menard et al., 2012), petroleum systems (Venugopal et al., 2004) and coal mines (Limbri et al., 2014). Utilizing diverse microbial biofilms to capture and degrade pollutants, biofilters can effectively treat effluents with mixed and low-concentration gases (Chen & Hoff, 2009), including CH₄ levels too dilute to recover for energy generation (Limbri et al., 2014; Menard et al., 2012; Venugopal et al., 2004). This makes biofilters uniquely suitable for treating fugitive farm CH₄ that cannot be reduced by improved animal diet or controlled by manure digestion/biogas systems.

The main challenge limiting the biofiltration of CH₄ emitted from livestock facilities is capture. While CH₄ is successfully biofiltered from long-residence, passive-flow landfills and effluents, typical barn and manure storage exhausts are mechanically

emitted at high-velocity. Short residence times sufficient for capturing soluble odors (i.e. NH_3 , H_2S) (Chen & Hoff, 2009) are too short for capturing hydrophobic CH_4 (Melse & Van der Werf, 2005; Nikiema & Heitz, 2009). As large-volume biofilters are not cost-effective for use on farms (Melse & Van der Werf, 2005; Montes et al., 2013; Nikiema & Heitz, 2009; Streese & Stegmann, 2005), or the use of specialized liquid phase sorbents (Estrada et al., 2014; Kennelly et al., 2014; Ramirez et al., 2012), other CH_4 capture improvements must be developed.

Capture inefficiencies in landfill and mine biofilters have been improved by optimizing aerobic CH_4 -oxidizing bacterial communities (methanotrophs) (Gebert et al., 2004; Kallistova et al., 2007; Lee et al., 2009; Murrell & Radajewski, 2000; Yoon et al., 2009; Yuan et al., 2009), based on their responses to media conditions (Nikiema et al., 2005; Rose et al., 2012), CH_4 , and other pollutants (Kim et al., 2013; Menard et al., 2014; Ni et al., 2012). However, the biofilm community and ecological feedbacks that dictate methanotroph performance in livestock emission biofilters have been little studied. It is known that unlike passive-flow biofilters, where methanotrophs colonize thin bands between counter-gradients of O_2 and CH_4 , methanotroph communities in forced air biofilters are dispersed by unidirectional flows of O_2 , CH_4 (Gebert et al., 2004; Yuan et al., 2009) and other volatiles (Ni et al., 2012). This dispersal alters the ratio of type I/II methanotrophs (separated by ultrastructure and methane monooxygenase (MMO) differences (Chen et al., 2007)), which impacts CH_4 oxidation. It is also known that NH_3 and H_2S can suppress MMO and CH_4 biofiltration (Caceres et al., 2014; Veillette et al.,

2011), and may need to be pre-filtered. What is not understood, however, is how microbial communities other than methanotrophs may impact CH₄ capture.

Microbial populations can enhance biofilter capture of select emissions. Though not yet harnessed for CH₄ or farm applications, fungal dominant biofilters have been shown to improve capture of various industrial emitted hydrophobic gases (Cox et al., 1997; Estevez et al., 2005b; Jorio et al., 2009; Kennes & Veiga, 2004; Prenafeta-Boldú et al., 2012a; Rene et al., 2012; Spigno et al., 2003; van Groenestijn, 2001). The ability of fungi to improve capture of these gases relates in part to their unique filamentous growths (hyphae), which increase the effective surface area of the biofilter media. Secreted hydrophobic proteins (hydrophobins) coat this fungal hyphae, lowering surface tension at the aqueous-gas interphase of the biofilm, and enabling the hyphae to extend into the air stream (Wosten, 2001; Wosten et al., 1999). When cultivated in the presence of hydrophobic VOCs, fungal biomass increases in hydrophobicity as well as surface area, further increasing gas capture potential (Vergara-Fernandez et al., 2006). Not only this response but the hydrophobin sheath of the fungal hyphae itself may be involved in the sorption of hydrophobic gases. If these characteristics of biofilter fungi can be harnessed to enhance capture of CH₄ from livestock facilities, biofilters may be developed at low-cost to meet the anticipated GHG mitigation needs of farmers. Using a lab-scale biofilter and a chromatographic (flow-through) isotherm, this ability of fungal biomass to improve CH₄ capture was investigated.

6.3. Methods

6.3.1. Lab-scale biofilter

To investigate the influence of fungi on CH₄ capture under typical biofilter operational conditions, a lab-scale biofilter system was constructed (Figure 6.1). This system consisted of 16 - triplicate, aluminum columns (0.33 m × 0.12 m ID) fitted tightly with aluminum pipe caps and connected in series with 13 mm ID tubing that fit inlet and outlet fittings on the caps. An aluminum ring (12 cm OD, 7 cm ID, 2 mm thick) was installed in the bottom of each column to prevent bypass flow and to position the media support screen. The columns were designed to be large enough for realistic bulk media, but small enough for replication and autoclaving. Assembling columns in triplicate enabled staging of different microbial treatments.

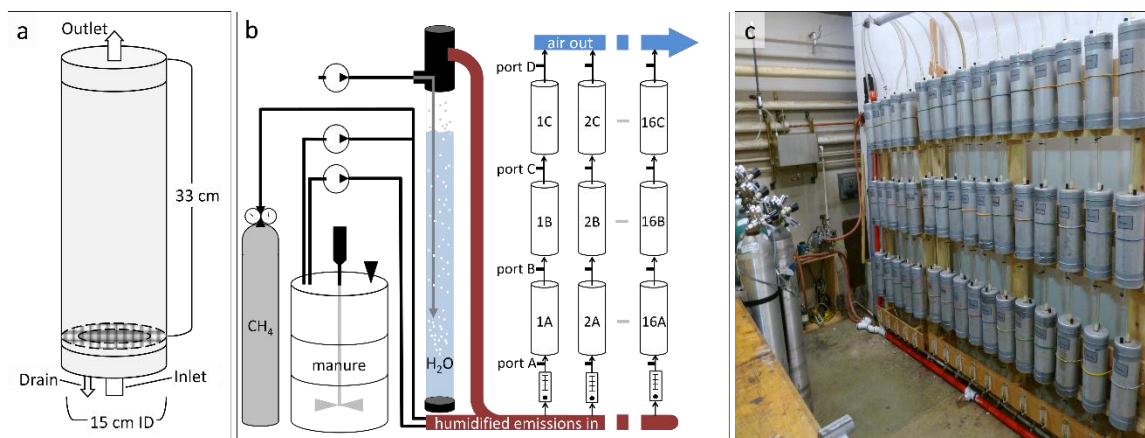


Figure 6.1 Schematics of **a)** the single biofilter column, **b)** the lab-scale biofilter assembly, and **c)** a photograph of the installed system.

The biofilter columns were fed emissions from either the headspace of a 200 L anaerobic swine manure storage or from cylinder gas. Vacuum pumps moved these emissions and a humidified air stream into a mixing chamber packed with glass wool

then into the inlet manifold. This mixing, along with flow meters, which regulated flow to achieve a 25 s EBCT (calculated by the methods of Schmidt et al. (2004)), ensured consistent effluent emissions were delivered to all columns (Appendix 6.1). Exhaust emissions were plumbed into a fume hood. A peristaltic pump was used to aseptically add 100 mL of sterile water to each column daily to maintain ~ 50% moisture content. To assess treatment performance, inlet and outlet CH₄ emissions were measured using an INNOVA Model 1412, LumaSense Technologies multi-gas monitor (Ballerup, Denmark) and calibration cylinder gas was used to set measurement correction factors.

6.3.2. Screening the potential of fungi to improve CH₄ biofiltration.

The first experiment compared 3 fungal inocula against a bacterial consortium and a sterile control. For this, all triplicate columns were packed with either, 1) *Pleurotus ostreatus* (Grey DoveTM, Field & Forest Products, Peshtigo, WI, USA), 2) *Phanerochaete chrysosporium* (#24725, American Type Culture Collection, Manassas, VA, USA), 3) *Dichostereum effuscatum* (field isolate), 4) a bacterial consortium (mix of field isolates), or 5) sterile chips (n=3). All selected fungi utilize the white rot decay mechanism which has demonstrated utility in other bioremediation systems (Pointing, 2001). Specifically, *P.ostreatus* was also selected because its spawn is widely available, *P. chrysosporium* was also selected because it has unique thermophilic and asexual spore production capabilities that make it well-suited for growth in mulch, and *D. effuscatum* was also selected because it dominated a large area of a full-scale biofilter treating swine emissions.

The fungal culture, *D. effuscatum*., was directly isolated from heavily colonized biofilter media (SE biofilter, Morris, MN; see Janni et al. (2014)) using a Basidiomycete selective agar (Appendix 6.2), with its identity verified using molecular methods. In brief, DNA was extracted from pure culture fungal hyphae using the Extract-N-Amp™ Plant PCR Kit (Sigma-Aldrich, St. Louis, MO, USA) with reagent volumes scaled down 10-fold. ITS-1 and ITS-4 primers were used to amplify fungal DNA. DNA template was Sanger sequenced at the University of Minnesota Genomics Center (Saint Paul, MN, USA) and the sequence was compared to the Basic Local Alignment Search Tool (BLAST) database (National Center for Biotechnology Information, Bethesda, MD, USA). The isolate shared 99% sequence similarity with other *D. effuscatum* submissions.

The bacterial consortium was a mix of bacterial cultures isolated from biofilter media (SE and NE biofilters, Morris, MN; see Janni et al. (2014)) purified from fungi using BBL™ Trypticase™ Soy Agar (Beck, Dickinson & Co., Sparks, MD, USA) amended with cycloheximide (50 µg mL⁻¹, Sigma-Aldrich, St. Louis, MO, USA). The isolates that comprised the bacterial consortium were not identified to species, but the presence of methanotrophs in the consortium was confirmed by PCR using methanotroph specific primer sets (data not shown).

To prepare the treatments, birch (*Betula papyrifera*) wood chips (0.5-2.5 cm) were soaked 24 h in tap water, drained, packed into autoclavable polypropylene culture bags (#UG-080519-A, Unicorn Bags, Plano, TX, USA), and sterilized (110 kPa, 121°C, 2 h, twice, 24 h apart). Cooled bags were inoculated with cultures, sealed and incubated 4

wk. Colonized media was homogenized and aseptically packed into sterilized biofilter columns and the columns were plumbed to the inlet and outlet manifolds. The anaerobic manure storage headspace was used as the emission source with target CH₄ emissions between 25 and 75 ppm; emissions averaged 39.2 ± 21.9 . The experiment was run for 7 wk. (1-4 wk., normal emissions; wk. 5 - simulated shutdown period; wk. 6 and 7 - normal emissions) at room temperature (~22°C).

6.3.3. Effect of fungal biomass on CH₄ biofiltration.

The second experiment tested the effects of fungal inoculum ratios on CH₄ capture, using *Pleurotus ostreatus* (Grey Dove™). Four treatments were tested, 1) all 3 biofilter stages were packed with sterilized media, 2) the top stage was packed with *P. ostreatus*, the bottom 2 stages were sterilized media, 3) the top 2 stages were packed with *P. ostreatus*, the bottom stage with sterile chips, and 4) all 3 stages were packed with *P. ostreatus* (n=4). Inocula were prepared as above. Purified CH₄ was diluted with air to achieve an inlet gas concentrations of ~100 ppm, which averaged 105.2 ± 9.6 ppm. The experiment was run for 4 wk. at room temperature (~22°C).

6.3.4. Chromatographic isotherm - Sorption of CH₄ by fungal materials

To test the influence of microbial materials on CH₄ sorption, a flow-through chromatographic isotherm approach was used (**Figure 6.2**), similar to the experimental set-up used by Goss (1992) to study vapor partitioning in soils. The isotherm test column consisted of a 10 cm × 1.6 cm ID stainless steel tube capped at both ends with 2 mm thick, 0.5 μm pore stainless steel fritted metal disks. Stainless steel compression fittings

secured the disks in place, enabled quick exchanges of test media and were fitted with denatured capillary gas chromatography (GC) columns (0.320 mm × 60 cm, Agilent Technologies, Santa Clara, CA, USA).

In an up-flow orientation, the test column was plumbed to the injection port and FID detector in the oven of a Shimadzu GC (2010 Plus, Shimadzu Corp., Kyoto, Japan). An inert carrier gas was used (He), and CH₄ injections (10 μL, 100 ppm) were made with a gas-tight syringe fitted with a Chaney adapter (Hamilton Co., Reno, NV, USA). Tests were run under dry conditions, the GC oven was maintained near ambient (25°C), and the carrier gas flow rate was set to achieve a 25 s EBCT. Ultrapure sand (40-100 mesh), muffle furnace to remove any residual organics, was used as inert control media, while fungal materials were homogenized with sand in various ratios for the treatments. Fungal spores were used for their uniformity, and like fungal hyphae, are known to have hydrophobic surface properties (Sulc et al., 2009; Tucker & Talbot, 2001). Spores representing both major fungal phyla (Basidiomycota and Ascomycota) were tested. Homogenization of spores and fungal materials was done gravimetrically and visualized using scanning electron microscopy (SEM). For SEM, sand/spore samples were mounted onto an SEM stub, sputter coated, and imaged on a Hitachi S3500N Variable Pressure SEM (Hitachi Ltd., Chiyoda, Tokyo, Japan) at the University of Minnesota Imaging Center.

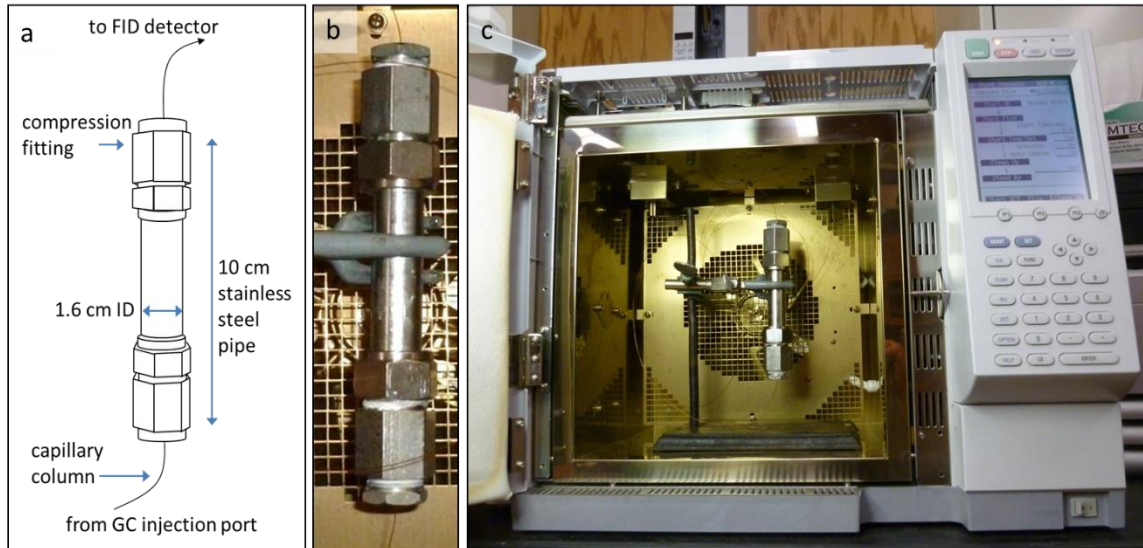


Figure 6.2 a) Schematic of the isotherm column, and a photo of b) the column, and c) the column installed into the GC.

Unlike batch isotherm studies, the flow-through design of this system better models actual biofilter dynamics. Furthermore, by retrofitting a GC, abiotic conditions were tightly controllable, and the detection was real-time and highly sensitive. Under isothermic conditions, the observed CH_4 retention is a measure of its sorption patterns. By comparing sorption patterns of a treatment to the sorption patterns of the control, the ability of fungal materials to sorb CH_4 can be tested (i.e. smaller peak areas with treatments compared to controls suggest CH_4 is sorbed to the fungal material being tested).

6.3.5. Statistical analyses

All statistical analyses were conducted with R 3.1.3 (GNU Project). For the lab-scale biofilter tests, normality was verified by Shapiro-Wilk testing, and ANOVA tests were used to compare differences in CH_4 capture for each time point independently. For isotherm tests, due to outlier points, normal distribution was not verified by a Shapiro-

Wilk test, and therefore, Kruskal-Wallis was used to test for differences in mean peak areas. Tukey HSD was used post-hoc for all tests to explore differences in CH₄ capture and peak area means. The alpha level was set to 0.05 for all analyses.

6.4. Results

6.4.1. Ability of fungal biofilters to mitigate CH₄

Greater capture of CH₄ was achieved by fungal inoculated columns than by the bacterial or sterile control treatments, which closely tracked one another (**Figure 6.3**). *Pleurotus ostreatus* was the top performing fungal treatment capable of capturing > 50 ppm CH₄ early in the experiment. Performances of the fungal treatments were typically higher early in the experiment, though significant CH₄ (~30 ppm) was captured by both *P. ostreatus* and *P. chrysosporium* at the end of 7 wk.

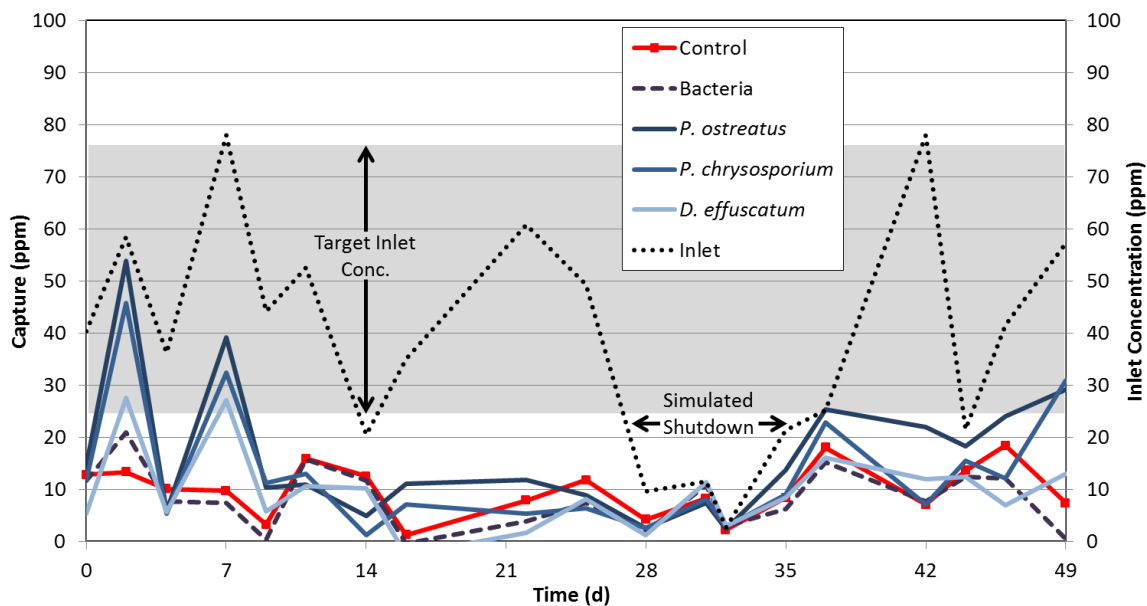


Figure 6.3 Capture of manure storage CH₄ by biofilter columns with various microbial inocula.

The ability of fungal treatments to capture CH₄ was greatest when anaerobic manure storage CH₄ emissions peaked and following the shutdown period (Figure 6.3). When performances of the various treatments were compared during these peak emission events, *P. ostreatus* and often the other fungal treatments had the greatest ability to capture CH₄ (Table 6.1). Only at a few time points was the ability to capture CH₄ shared with the bacterial treatment or sterile control.

Table 6.1 Statistical differences in CH₄ capture of microbial treatments during peak emissions.

Time (d)	Shock Amplitude (ppm)	Inlet Conc. (ppm)	Treatment				
			<i>P. ostreatus</i>	<i>P. chrysosporium</i>	<i>D. effuscatum</i>	Bacteria	Control
2	18.12	58.39	a	ab	bc	c	c
14	41.77	78.00	a	a	ab	b	b
16	14.47	34.99	a	ab	c	bc	bc
22	40.31	60.83	a	bc	b	bc	ac
35	18.68	21.4	a	ab	b	b	b
37	22.54	25.26	a	ab	bc	c	ac
42	75.22	77.94	a	bc	ab	b	b
46	19.94	41.45	a	bc	b	ac	bc
49	36.36	70.79	a	a	ab	c	bc

6.4.2. Increased *P. ostreatus* biomass improved CH₄ biofiltration.

Generally, with increased fungal biomass (inclusion of more fungal inoculated stages) CH₄ capture increased (Figure 6.4). While capture for sterile chips stayed below 6 ppm and averaged 3.3 ± 2.0 ppm, capture when all 3 stages were inoculated with *P. ostreatus* reached 22.5 ppm initially and averaged 13.0 ± 2.9 ppm. Greater CH₄ capture by the 3 stage fungal systems than by sterile controls was significant in 8 of the 14 time points. Most of these were with the earlier time points (Figure 6.5). When fewer fungal stages were used, CH₄ capture declined, with capture by the 2 stage *P. ostreatus* system averaging 10.2 ± 2.2 ppm and the 1 stage *P. ostreatus* system averaging 9.0 ± 2.1 ppm.

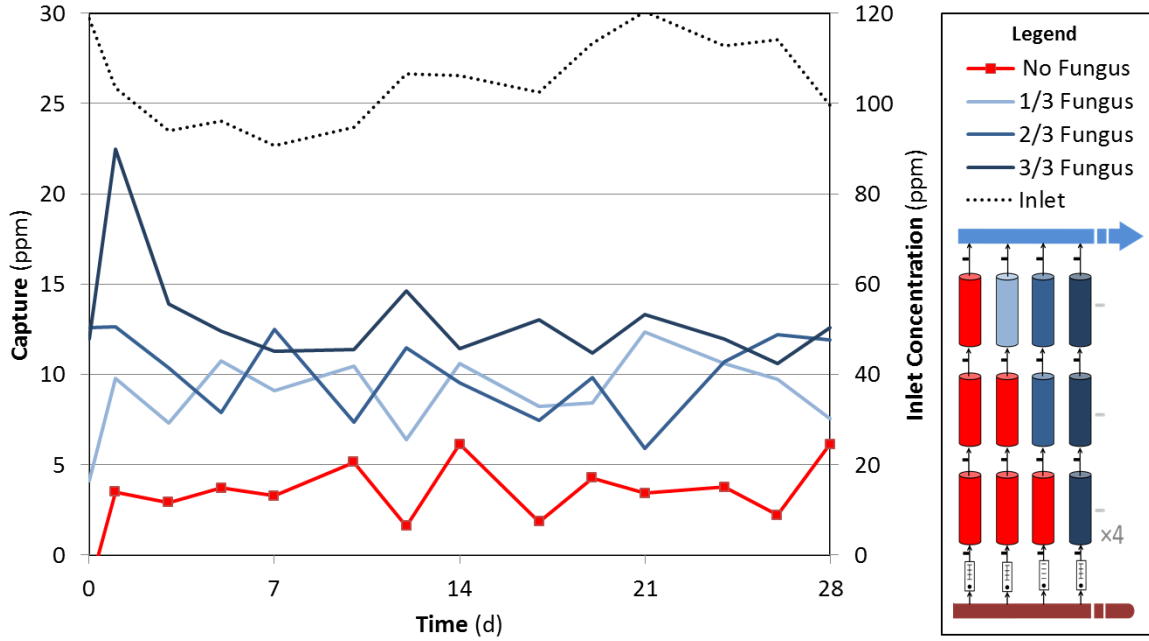


Figure 6.4 CH₄ capture by lab-scale biofilter columns packed with increasing amounts of *P. ostreatus* fungal biomass.

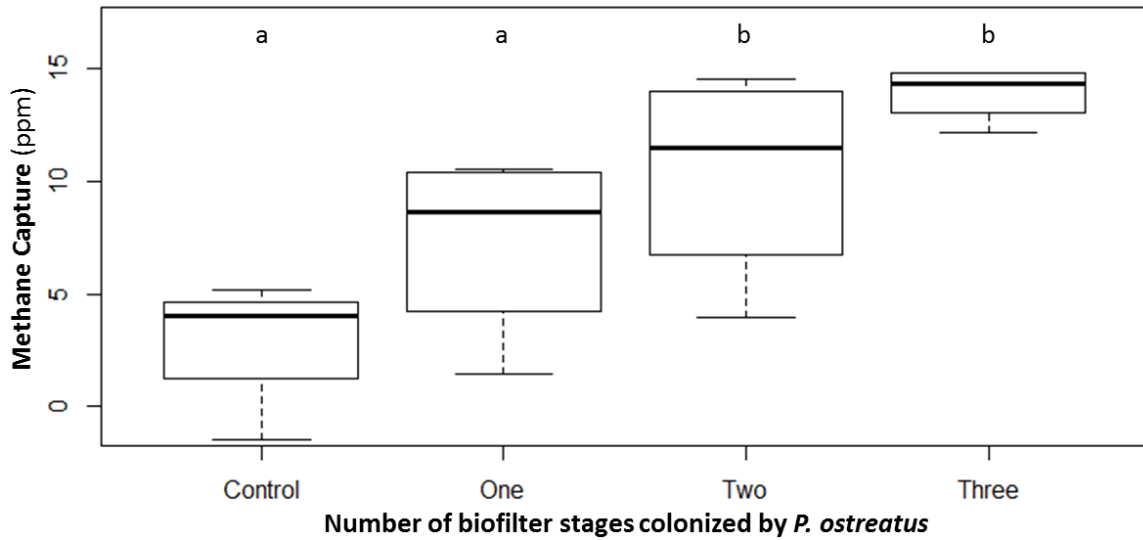


Figure 6.5 Boxplot of CH₄ capture by *P. ostreatus* at day 3 (n=4). Different letters note statistically different means ($\alpha=0.05$).

6.4.3. Fungal sorption of CH₄ in a chromatographic isotherm

To look at spore surface dynamics and homogenization with sand particles, SEM was used. SEM images of test sorbent material mixtures verified even coating of sand with spores (**Figure 6.6**) and results suggest fungal materials were capable of sorbing CH₄. When the inert sand control chromatographs were compared to chromatographs from a test sorbent, significant sorption of CH₄ was observed (**Figure 6.7**). Evident by the consistent peak area of the treatments (*i.e.* the area did not increase with subsequent injections(Appendix 6.3)); the sorption sites appear to be un-saturated even when small fungal levels were present. The lack of significant peak tailing suggests the fungal sorption of CH₄ is long-lasting or irreversible.

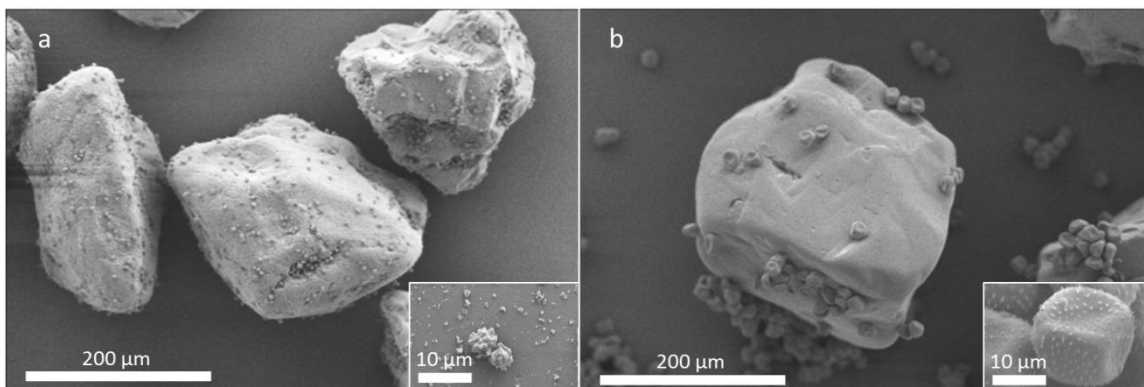


Figure 6.6 SEM images of sand mixed with **a**) ascomycete and **b**) basidiomycete fungal spores. Insert photos show the spores at higher magnification.

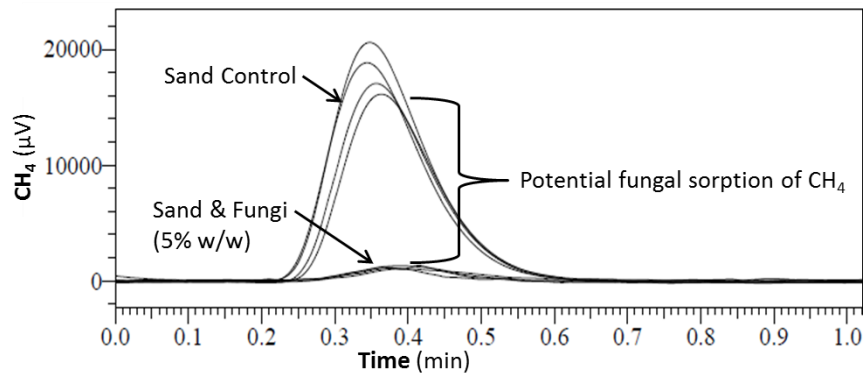


Figure 6.7 Overlay of chromatographic outputs of a sand control and a sand/basidiospore test sorbent.

Fungal materials from both major phyla (Ascomycota & Basidiomycota) showed an ability to sorb CH₄ (**Figure 6.8**). Increasing the proportion of fungal material relative to the inert sand increased the ability of the isotherm column to sorb injected CH₄ (*i.e.* peak area was negatively correlated to the fungal ratio). This pattern was not significant for the ascomycete material for the ratios tested, but the ascomycete material tested apparently sorbed more of the spiked CH₄ than the basidiomycete materials.

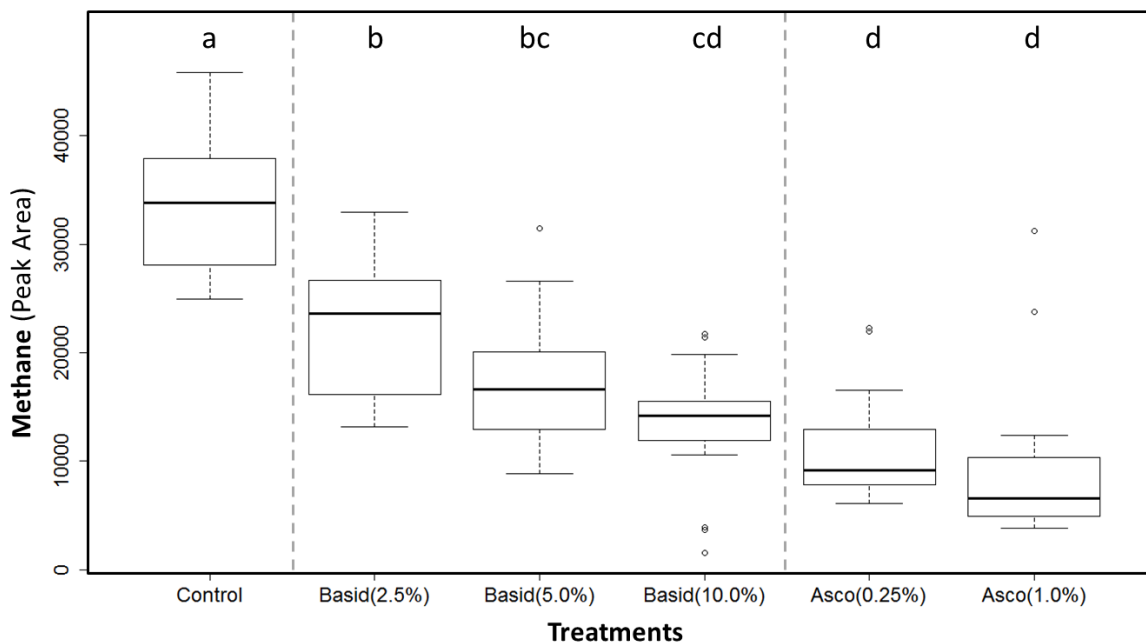


Figure 6.8 Peak area of control and test sorbents for various levels (w/w) of basidiomycete (Basid) or ascomycete (Asco) fungal materials (n=20). Different letters denote significantly different mean values ($\alpha=0.5$)

6.5. Discussion

6.5.1. Fungi improved CH₄ biofiltration at lab-scale

Fungal biofilms showed an enhanced ability to capture CH₄ compared to the bacterial biofilm. *Pleurotus ostreatus* was the top performing fungal treatment in the initial experimental screen with CH₄ capture sometimes nearing inlet concentrations. In the second experiment, CH₄ sorption was increased by adding biofilter stages colonized by *P. ostreatus*. This suggests fungi, like *Pleurotus*, have biosorbent capacities and may offer a low-cost means to improve CH₄ mitigation by biofilters designed currently for odor.

Pleurotus ostreatus is the second most cultivated fungal species globally, with spawn widely available for biotechnology applications. This fungus is fast growing, able to colonize a range of woody and agricultural residue substrates, sterilized or not (Sanchez, 2010), and can compete well in mulch and soil environments though wood is its natural substrate (Baldrian, 2008). The ability to grow fast on assorted, non-sterile substrates in concert with the capacities of *Pleurotus* ligninolytic enzymes to degrade organopollutants has led to extensive investigation and use of this fungus in bioremediation systems (Cohen et al., 2002). Inorganic pollutants can also be treated by white rot fungi, and *Pleurotus* has a demonstrated ability to absorb and accumulate heavy metals (Baldrian, 2003), an ability likely related to their regulation of metal dependent ligninolytic enzymes. This metal sorption capacity of white rot fungi has been utilized to remove Ni(II), Cu(II), Zn(II), and Cr(IV) from solutions (Javaid et al., 2011). Functional groups of hyphal sheath proteins and carbohydrates have been identified as sites of this biosorption in *P. ostreatus*. Along with the ability to generate high surface area hyphal growths, which can reach $51.16 \text{ m}^2 \text{ g}^{-1}$ (Hu et al., 2014), *P. ostreatus* shows extensive sorption capacity. Furthermore, the ability to reuse these hyphal growths as biosorbent has been demonstrated (Javaid et al., 2011) with up to 90% of the metal sorption capacity shown to be reversible when a dilute acid eluent was used (Hu et al., 2014).

In our lab-scale biofilter trials, the performance of fungal columns was best early in the experiment or following an increase in inlet emissions. The lack of sustained performance suggests that CH_4 sorption sites became saturated and that no oxidation by

fungi occurred. While metal sorption is known to be reversible (Hu et al., 2014), it required an eluent, not used here, to hasten the process. Slow desorption of CH₄ may be preferred in a biofilter setting anyway, permitting time for methanotrophic bacteria to oxidize the gas. The ability of fungal treatments to capture CH₄ effectively during early peak emissions and following a shut-down period is also advantageous, steadying inlet perturbations to stabilize CH₄ levels reaching methanotrophs. The ability of a biofilter to capture stochastic spikes in emissions which are typical of full-scale emissions patterns would ensure the systems was adequately robust for CH₄ mitigation on farms

6.5.2. Fungi can sorb CH₄

The chromatographic isotherm studies also showed the ability of fungal materials to sorb CH₄. Like the lab-scale system, increasing fungal biomass (here by increasing ascomycete and basidiomycete spore masses) improved CH₄ capture. The use of ‘inactive’ resting spores supports the notion that this is not an active biodegradation process, but a biosorption process. Like hyphae, spores are known to possess hydrophobic protein sheaths (Sulc et al., 2009; Tucker & Talbot, 2001). Utilized by spores for attachment to plant hosts, these hydrophobin layers also appear capable of capturing a poorly-soluble GHG. The more significant capture of CH₄ by the ascospores can be explained in part by the smaller spore size and higher surface area to volume ratio of the ascospores. Assessed visually here, Brunauer–Emmett–Teller (BET) testing would be required to more quantitatively assess the differences in spore surface area to normalize isotherm responses.

As with the lab-scale biofilter trials, there was little evidence in the chromatograms for rapid reversibility of CH₄ sorption. Reversibility would have been observed in the peak overlay which found no significant peak tailing or shift in detection time. There was also no indication that the CH₄ sorption capacity of the spore materials had been reached based on over 30 minutes of repeated CH₄ injections (Appendix 6.3). If reversibility was evident, peak area would have slowly increased to the area of sand only controls. Further work will thus be needed to identify the sorption capacity of these materials. Additionally follow-up trials will be needed to investigate active fungal hyphae and test the effects of field relevant moisture on CH₄ sorption.

6.5.3. Interactions of fungi and methanotrophs

Fungi and bacteria closely compete and cooperate in natural substrates (Baldrian, 2008) and must often act jointly in biofilters for optimal mitigation to occur (Prenafeta-Boldú et al., 2012a). Just as CH₄ generation is typically a combined bacterial and fungal effort (Beckmann et al., 2011), it is likely that capture and oxidation of CH₄ is also a community dynamic. Currently, we have a limited knowledge of the interactions between fungi and methanotrophs or their co-localization. While the fungal degradation of secondary turnover C from methanotrophs does not always occur, fungal growth is stimulated by CH₄-rich landfill gas similarly to methanotrophs (Watzinger et al., 2008). Based on this demonstration of CH₄ capture by fungi, perhaps fungi play an active, upstream role in the CH₄ biofiltration and gain some unresolved benefit from

methanotrophs. Answering these questions will be central to our understanding of CH₄ biofilter ecology and the role of fungi in CH₄ capture.

6.6. Conclusions

To our knowledge, this is the first work demonstrating the ability of fungi to sorb the greenhouse gas CH₄. Despite the preliminary nature of the work, and undoubted need for more testing, these findings suggest microbes other than CH₄ oxidizing methanotrophs may govern rate limits that affect the ability of biofilters to mitigate CH₄. If fungi can improve CH₄ capture in a biofilter, thus facilitating subsequent oxidation, it is possible that by selecting for specific fungi or microbial communities in a biofilter a potent GHG can be mitigated simultaneously to odorous livestock production emissions.

7. CONCLUSIONS

The aim of this research was to develop methodologies to study the microbial communities, specifically fungal, in livestock emission biofilters, characterizing their dynamics, consequences, and role in methane biofiltration. By developing and using a novel bait approach, biofilter abiotic and biotic dynamics were measured and their spatial and temporal shifts and methodological and environmental variability were assessed. Fungi were found to be desiccation tolerant potentially enabled by their filamentous growth form. Using a sequencing approach, fungal community taxa, guilds and succession were defined with dominant taxa worthy of future study identified. The durability of media to decay was tested with longevity estimates made based on measured decay rates. Drivers of media decay were also identified, with nutrient content, N and emissions all increasing decay rates. By parameterizing decay rates identifying drivers of decay, biofilter end-users are better equipped to select media types and anticipate replacement costs. The ability of fungi to capture CH₄ and the potential for a biological control of biofilter capture rate limits was also demonstrated using lab-scale and isotherm approaches. Collectively these research efforts can direct future studies of biofilter microbial dynamics, support the design and management decisions of end-users, and highlight the unique potential of fungi in biofiltration systems. If the role of fungi can be better resolved and harnessed, significant improvements in biofilter operation may be achievable and the protection of air quality and sustainability of livestock systems improved. This work establishes a foundation to pursue this important work.

8. BIBLIOGRAPHY

- Akdeniz, N., Janni, K.A., Hetchler, B.P. 2014. Mitigation of multiple air emissions from swine buildings using corn cob biofilters. in: *American Society of Agricultural and Biological Engineering Annual Meeting*. Montreal, Quebec Canada, July 13 – July 16, 2014.
- Akdeniz, N., Janni, K.A., Salnikov, I.A. 2011. Biofilter performance of pine nuggets and lava rock as media. *Bioresource Technology*, 102(8), 4974-4980.
- APHA, American Public Health Association. 2003. Precautionary moratorium on new animal feeding operations. *Advocacy & Policy*, Policy No. 20037, <http://www.apha.org/advocacy/policy/policysearch/default.htm?id=1243> (19 March 2013).
- Archibald, F.S., Bourbonnais, R., Jurasek, L., Paice, M.G., Reid, I.D. 1997. Kraft pulp bleaching and delignification by *Trametes versicolor*. *Journal of Biotechnology*, 53(2-3), 215-236.
- Arriaga, S., Revah, S. 2005. Improving hexane removal by enhancing fungal development in a microbial consortium biofilter. *Biotechnology and Bioengineering*, 90(1), 107-115.
- Baldrian, P. 2003. Interactions of heavy metals with white-rot fungi. *Enzyme and Microbial Technology*, 32(1), 78-91.
- Baldrian, P. 2008. Wood-inhabiting ligninolytic basidiomycetes in soils: Ecology and constraints for applicability in bioremediation. *Fungal Ecology*, 1, 4-12.
- Beckmann, S., Kruger, M., Engelen, B., Gorbushina, A.A., Cypionka, H. 2011. Role of Bacteria, Archaea and Fungi involved in Methane Release in Abandoned Coal Mines. *Geomicrobiology Journal*, 28(4), 347-358.
- Briones, A., Raskin, L. 2003. Diversity and dynamics of microbial communities in engineered environments and their implications for process stability. *Current Opinion in Biotechnology*, 14(3), 270-276.
- Cabrol, L., Malhautier, L. 2011. Integrating microbial ecology in bioprocess understanding: the case of gas biofiltration. *Applied Microbiology and Biotechnology*, 90(3), 837-849.
- Cabrol, L., Malhautier, L., Poly, F., Lepeuple, A.S., Fanlo, J.L. 2010. Assessing the bias linked to DNA recovery from biofiltration woodchips for microbial community investigation by fingerprinting. *Applied Microbiology and Biotechnology*, 85(3), 779-790.
- Cabrol, L., Malhautier, L., Poly, F., Lepeuple, A.S., Fanlo, J.L. 2012a. Bacterial dynamics in steady-state biofilters: beyond functional stability. *FEMS Microbiology Ecology*, 79(1), 260-271.
- Cabrol, L., Malhautier, L., Poly, F., Lepeuple, A.S., Fanlo, J.L. 2009. Shock loading in biofilters: impact on biodegradation activity distribution and resilience capacity. *Water Science and Technology*, 59(7), 1307-1314.

- Cabrol, L., Malhautier, L., Poly, F., Roux, X.L., Lepeuple, A.-S., Fanlo, J.-L. 2012b. Resistance and resilience of removal efficiency and bacterial community structure of gas biofilters exposed to repeated shock loads. *Bioresource Technology*, 123(0), 548-557.
- Caceres, M., Gentina, J.C., Aroca, G. 2014. Oxidation of methane by *Methylobacterium album* and *Methylocystis* sp in the presence of H₂S and NH₃. *Biotechnology Letters*, 36(1), 69-74.
- Cairney, J.W.G. 1992. Translocation of solutes in ectomycorrhizal and saprotrophic rhizomorphs. *Mycological Research*, 96(2), 135-141.
- Capper, J.L., Cady, R.A., Bauman, D.E. 2009. The environmental impact of dairy production: 1944 compared with 2007. *Journal of Animal Science*, 87, 2160-2167.
- Cardenas-Gonzalez, B., Ergas, S.J., Switzenbaum, M.S., Phillibert, N. 1999. Evaluation of full-scale biofilter media performance. *Environmental Progress*, 18(3), 205-211.
- Carregaro, F.B., Spanamberg, A., Sanches, E.M.C., Argenta, J.S., Pereira, D.I.B., Zanette, R., Santurio, J.M., de Barcellos, D., Ferreiro, L. 2010. Fungal microbiota isolated from healthy pig skin. *Acta Scientiae Veterinariae*, 38(2), 147-153.
- CDC. 2004. Toxicological Profile for Ammonia, United States Department of Health and Human Services, Public Health Service, Agency for Toxic Substances and Disease Registry, Center for Disease Control.
- CDC. 2006. Toxicological Profile for Hydrogen Sulfide, United States Department of Health and Human Services, Public Health Service, Agency for Toxic Substances and Disease Registry, Center for Disease Control.
- Chen, L., Hoff, S. 2009. Mitigating odors from agricultural facilities: A review of literature concerning biofilters. *Applied Engineering in Agriculture*, 25(5), 751-766.
- Chen, L., Hoff, S., Lingshuang, C., Koziel, J., Zelle, B. 2009. Evaluation of Wood Chip-Based Biofilters to Reduce Odor, Hydrogen Sulfide, and Ammonia from Swine Barn Ventilation Air. *Journal of the Air & Waste Management Association (1995)*, 59(5), 520-530.
- Chen, L., Hoff, S.J., Cai, L., Koziel, J.A. 2008a. Odor reduction during biofiltration as affected by air flow rate and media moisture content. *ASABE Annual International Meeting*, St. Joseph, MI.
- Chen, L., Hoff, S.J., Koziel, J.A., Cai, L., Zelle, B., Sun, G. 2008b. Performance evaluation of a wood-chip based biofilter using solid-phase microextraction and gas chromatography-mass spectroscopy-olfactometry. *Bioresource Technology*, 99(16), 7767-7780.
- Chen, Y., Dumont, M.G., Cebron, A., Murrell, J.C. 2007. Identification of active methanotrophs in a landfill cover soil through detection of expression of 16S rRNA and functional genes. *Environmental Microbiology*, 9(11), 2855-2869.

- Chung, Y.C. 2007. Evaluation of gas removal and bacterial community diversity in a biofilter developed to treat composting exhaust gases. *Journal of Hazardous Materials*, 144(1-2), 377-385.
- Cohen, R., Persky, L., Hadar, Y. 2002. Biotechnological applications and potential of wood-degrading mushrooms of the genus *Pleurotus*. *Applied Microbiology and Biotechnology*, 58(5), 582-594.
- Cole, D., Todd, L., Wing, S. 2000. Concentrated Swine Feeding Operations and Public Health: A Review of Occupational and Community Health Effects. *Environmental Health Perspectives*, 108(8), 685-699.
- Colombo, A.L., Padovan, A.C.B., Chaves, G.M. 2011. Current Knowledge of *Trichosporon* spp. and Trichosporonosis. *Clinical Microbiology Reviews*, 24(4), 682-+.
- Cornwell, W.K., Weedon, J.T. 2014. Decomposition trajectories of diverse litter types: a model selection analysis. *Methods in Ecology and Evolution*, 5(2), 173-182.
- Cox, H.H.J., Moerman, R.E., vanBaalen, S., vanHeiningen, W.N.M., Doddema, H.J., Harder, W. 1997. Performance of a styrene-degrading biofilter containing the yeast *Exophiala jeanselmei*. *Biotechnology and Bioengineering*, 53(3), 259-266.
- Deines, P., Sekar, R., Husband, P.S., Boxall, J.B., Osborn, A.M., Biggs, C.A. 2010. A new coupon design for simultaneous analysis of in situ microbial biofilm formation and community structure in drinking water distribution systems. *Applied Microbiology and Biotechnology*, 87(2), 749-756.
- Delhomenie, M.C., Heitz, M. 2005. Biofiltration of air: A review. *Critical Reviews in Biotechnology*, 25(1-2), 53-72.
- Deshusses, M.A. 1997. Biological waste air treatment in biofilters. *Current Opinion in Biotechnology*, 8(3), 335-339.
- Devinny, J.S., Deshusses, M.A., Webster, T.S. 1999. *Biofiltration for air pollution control*. Lewis Publishers, Boca Raton, FL.
- Devinny, J.S., Ramesh, J. 2005. A phenomenological review of biofilter models. *Chemical Engineering Journal*, 113(2-3), 187-196.
- Ding, Y., Das, K.C., Whitman, W.B., Kastner, J.R. 2006. Enhanced biofiltration of hydrogen sulfide in the presence of methanol and resultant bacterial diversity. *Transactions of the Asabe*, 49(6), 2051-2059.
- Ding, Y., Wu, W.X., Han, Z.Y., Chen, Y.X. 2008. Correlation of reactor performance and bacterial community composition during the removal of trimethylamine in three-stage biofilters. *Biochemical Engineering Journal*, 38(2), 248-258.
- Donham, K.J., Wing, S., Osterberg, D., Flora, J.L., Hodne, C., Thu, K.M., Thorne, P.S. 2006. Community health and socioeconomic issues surrounding concentrated animal feeding operations. *Environmental Health Perspectives*, 115(2), 317-320.
- Edwards, S., Massey, R. 2011. Animal feeding operations and residential value: Summary of literature. *University of Missouri Extension*, MP748.

- Elias, A., Barona, A., Gallastegi, G., Rojo, N., Gurtubay, L., Ibarra-Berastegi, G. 2010. Preliminary Acclimation Strategies for Successful Startup in Conventional Biofilters. *Journal of the Air & Waste Management Association*, 60(8), 959-967.
- Estevez, E., Veiga, M.C., Kennes, C. 2005a. Biodegradation of toluene by the new fungal isolates *Paecilomyces variotii* and *Erophiala oligosperma*. *Journal of Industrial Microbiology & Biotechnology*, 32(1), 33-37.
- Estevez, E., Veiga, M.C., Kennes, C. 2005b. Biofiltration of waste gases with the fungi *Exophiala oligosperma* and *Paecilomyces variotii*. *Applied Microbiology and Biotechnology*, 67(4), 563-568.
- Estrada, J.M., Lebrero, R., Quijano, G., Perez, R., Figueroa-Gonzalez, I., Garcia-Encina, P.A., Munoz, R. 2014. Methane abatement in a gas-recycling biotrickling filter: Evaluating innovative operational strategies to overcome mass transfer limitations. *Chemical Engineering Journal*, 253, 385-393.
- Falk, M.W., Song, K.G., Matiasek, M.G., Wuertz, S. 2009. Microbial community dynamics in replicate membrane bioreactors - Natural reproducible fluctuations. *Water Research*, 43(3), 842-852.
- Fath, B.G., Harmon, M.E., Sexton, J., White, P. 2011. Decomposition of fine woody debris in a deciduous forest in North Carolina. *Journal of the Torrey Botanical Society*, 138(2), 192-206.
- Fierer, N., Grandy, A.S., Six, J., Paul, E.A. 2009. Searching for unifying principles in soil ecology. *Soil Biology & Biochemistry*, 41, 2249-2256.
- Fierer, N., Jackson, J.A., Vilgalys, R., Jackson, R.B. 2005. Assessment of soil microbial community structure by use of taxon-specific quantitative PCR assays. *Applied and Environmental Microbiology*, 71(7), 4117-4120.
- Forest Products Laboratory. 2010. *Wood handbook - Wood as an engineering material. General Technical Report FPL-GTR-190*. U.S. Department of Agriculture, Forest Service, Forest Products Laboratory, Madison, WI.
- Franklin, R.B., Mills, A.L. 2006. Structural and functional responses of a sewage microbial community to dilution-induced reductions in diversity. *Microbial Ecology*, 52(2), 280-288.
- Freschet, G.T., Weedon, J.T., Aerts, R., van Hal, J.R., Cornelissen, J.H.C. 2012. Interspecific differences in wood decay rates: insights from a new short-term method to study long-term wood decomposition. *Journal of Ecology*, 100(1), 161-170.
- Friedrich, U., Van Langenhove, H., Altendorf, K., Lipski, A. 2003. Microbial community and physicochemical analysis of an industrial waste gas biofilter and design of 16S rRNA-targeting oligonucleotide probes. *Environmental Microbiology*, 5(3), 183-201.
- Gebert, J., Grongroft, A., Schlöter, M., Gättinger, A. 2004. Community structure in a methanotroph by phospholipid fatty acid biofilter as revealed analysis. *Fems Microbiology Letters*, 240(1), 61-68.
- Goldstein, N. 1999. Longer Life for Biofilters. *BioCycle*, 40(7), 62.

- Goss, K.-U. 1992. Effects of temperature and relative humidity on the sorption of organic vapors on quartz sand. *Environ. Sci. Technol.*, 26, 2287-2294.
- Guarino, M., Jacobson, L.D., Janni, K.A. 2007. Dust reduction from oil-based feed additives. *Applied Engineering in Agriculture*, 23(3), 329-332.
- Guarro, J., AlSaadoon, A.H., Abdullah, S.K. 1997. Two new coprophilous species of *Preussia* (Ascomycota) from Iraq. *Nova Hedwigia*, 64(1-2), 177-183.
- Guo, X., Zhan, Y.L., Chen, C.M., Zhao, L.J., Guo, S.H. 2014. The influence of microbial synergistic and antagonistic effects on the performance of refinery wastewater microbial fuel cells. *Journal of Power Sources*, 251, 229-236.
- Hall-Stoodley, L., Costerton, J.W., Stoodley, P. 2004. Bacterial biofilms: From the natural environment to infectious diseases. *Nature Reviews Microbiology*, 2(2), 95-108.
- Hamon, L., Andres, Y., Dumont, E. 2012. Aerial pollutants in swine buildings: A review of their characterization and methods to reduce them. *Environmental Science & Technology*, 46(22), 12287-12301.
- Harmon, M.E., Krankina, O.N., Sexton, J. 2000. Decomposition vectors: a new approach to estimating woody detritus decomposition dynamics. *Canadian Journal of Forest Research-Revue Canadienne De Recherche Forestiere*, 30(1), 76-84.
- Hatakka, A. 1994. Lignin-modifying enzymes from selected white-rot fungi - Production and role in lignin degradation. *Fems Microbiology Reviews*, 13(2-3), 125-135.
- Hayes, A.C., Zhang, Y.F., Liss, S.N., Allen, D.G. 2010. Linking performance to microbiology in biofilters treating dimethyl sulphide in the presence and absence of methanol. *Applied Microbiology and Biotechnology*, 85(4), 1151-1166.
- Hayes, E.T., Leek, A.B.G., Curran, T.P., Dodd, V.A., Carton, O.T., Beattie, V.E., O'Doherty, J.V. 2004. The influence of diet crude protein level on odour and ammonia emissions from finishing pig houses. *Bioresource Technology*, 91(3), 309-315.
- Hiscox, J., Savoury, M., Vaughan, I.P., Muller, C.T., Boddy, L. 2015. Antagonistic fungal interactions influence carbon dioxide evolution from decomposing wood. *Fungal Ecology*, 14, 24-32.
- Ho, K.L., Chung, Y.C., Lin, Y.H., Tseng, C.P. 2008. Microbial populations analysis and field application of biofilter for the removal of volatile-sulfur compounds from swine wastewater treatment system. *Journal of Hazardous Materials*, 152(2), 580-588.
- Hobbie, S., Baker, L., Buyarski, C., Nidzgorski, D., Finlay, J. 2014. Decomposition of tree leaf litter on pavement: implications for urban water quality. *Urban Ecosystems*, 17(2), 369-385.
- Holland, R.E., Carson, T.L., Donham, K.J. 2002. Iowa Concentrated Animal Feeding Operations Air Quality Study - Final Report - Iowa State University and The University of Iowa Study Group. Chapter 6.2. Animal Health Effects.

- Hristov, A.N., Hanigan, M., Cole, A., Todd, R., McAllister, T.A., Ndegwa, P.M., Rotz, A. 2011. Review: Ammonia emissions from dairy farms and beef feedlots. *Canadian Journal of Animal Science*, 91(1), 1-35.
- Hu, X.J., Yan, L.L., Gu, H.D., Zang, T.T., Jin, Y., Qu, J.J. 2014. Biosorption mechanism of Zn²⁺ from aqueous solution by spent substrates of *Pleurotus ostreatus*. *Korean Journal of Chemical Engineering*, 31(11), 1911-1918.
- Ilea, R.C. 2009. Intensive Livestock Farming: Global Trends, Increased Environmental Concerns, and Ethical Solutions. *Journal of Agricultural & Environmental Ethics*, 22(2), 153-167.
- IPCC. 2007. Climate Change 2007: The physical science basis. Contribution of working group I to the fourth assessment report of the intergovernmental panel on climate change. Chapter 2, changes in atmospheric constituents and in radiative forcing. *Intergovernmental Panel on Climate Change*.
- Isakson, H.R., Ecker, M.D. 2008. An analysis of the impact of swine CAFOs on the value of nearby houses. *Agricultural Economics*, 39(3), 365-372.
- Jacobson, L.D., Auvermann, B.W., Massey, R., Mitloehner, F.M., Sutton, A.L., Xin, H. 2011. Air Issues Associated with Animal Agriculture: A North American Perspective. *CAST Issue Paper*, 47.
- Jacobson, L.D., Heber, A.J., Hoff, S.J., Zhang, Y., Beasley, D.B., Koziel, J.A., Hetchler, B.J. 2006. Aerial pollutants emissions from confined animal buildings. *Proceedings of the Workshop on Agricultural Air Quality: State of the Science*, June 5-8. pp. 775-784.
- Jacobson, L.D., Hetchler, B.P., Johnson, V.J., Nicolai, R.E., Schmidt, D.R., Goodrich, P.R., Heber, A.J., Ni, J.Q., Lim, T.T., Tao, P.C., Hoff, S.J., Bundy, D.S., Huebner, M.A., Zelle, B.C., Zhang, Y., McClure, J., Roberts, M., Koziel, J.A., Baek, B.H., Balota, A., Pinhirme, J.P., Sweeten, J.M., Beasley, D.B., Baughman, G.R., Manilla, R. 2004. Preliminary NH₃, H₂S, and PM₁₀ Data from Pig and Poultry Buildings from Six-State Project. *ASAE Paper 044156*.
- Jagmann, N., Philipp, B. 2014. Design of synthetic microbial communities for biotechnological production processes. *Journal of Biotechnology*, 184, 209-218.
- Janni, K.A., Jacobson, L.D., Hetchler, B.P., Oliver, J.P., Johnston, L.J. 2014. Semi-continuous air sampling versus 24-hour bag samples to evaluate biofilters on a swine nursery in warm weather. *Transactions of the ASABE*, 57(5), 1501-1515.
- Jasalavich, C.A., Ostrofsky, A., Jellison, J. 2000. Detection and Identification of Decay Fungi in Spruce Wood by Restriction Fragment Length Polymorphism Analysis of Amplified Genes Encoding rRNA. *Appl. Environ. Microbiol.*, 66(11), 4725-4734.
- Javaid, A., Bajwa, R., Shafique, U., Anwar, J. 2011. Removal of heavy metals by adsorption on *Pleurotus ostreatus*. *Biomass & Bioenergy*, 35(5), 1675-1682.
- Jenkinson, D.S., Powlson, D.S. 1976. The effects of biocidal treatments on metabolism in soil - V. A method for measuring soil biomass. *Soil Biology & Biochemistry*, 8(3), 209-213.

- Joergensen, R.G., Wichern, F. 2008. Quantitative assessment of the fungal contribution to microbial tissue in soil. *Soil Biology and Biochemistry*, 40(12), 2977-2991.
- Jorio, H., Jin, Y.M., Elmrini, H., Nikiema, J., Brzezinski, R., Heitz, M. 2009. Treatment of VOCs in biofilters inoculated with fungi and microbial consortium. *Environmental Technology*, 30(5), 477-485.
- Juhler, S., Revsbech, N.P., Schramm, A., Herrmann, M., Ottosen, L.D.M., Nielsen, L.P. 2009. Distribution and rate of microbial processes in an ammonia-loaded air filter biofilm. *Applied and Environmental Microbiology*, 75(11), 3705-3713.
- Kallistova, A.Y., Kevbrina, M.V., Nekrasova, V.K., Shnyrev, N.A., Einola, J.K.M., Kulomaa, M.S., Rintala, J.A., Nozhevnikova, A.N. 2007. Enumeration of methanotrophic bacteria in the cover soil of an aged municipal landfill. *Microbial Ecology*, 54(4), 637-645.
- Kennelly, C., Gerrity, S., Collins, G., Clifford, E. 2014. Liquid phase optimisation in a horizontal flow biofilm reactor (HFBR) technology for the removal of methane at low temperatures. *Chemical Engineering Journal*, 242, 144-154.
- Kennes, C., Veiga, M.C. 2004. Fungal biocatalysts in the biofiltration of VOC-polluted air. *Journal of Biotechnology*, 113(1-3), 305-319.
- Kim, T.G., Lee, E.H., Cho, K.S. 2013. Effects of nonmethane volatile organic compounds on microbial community of methanotrophic biofilter. *Applied Microbiology and Biotechnology*, 97(14), 6549-6559.
- Klimes, A., Dobinson, K.F. 2006. A hydrophobin gene, VDH1, is involved in microsclerotial development and spore viability in the plant pathogen *Verticillium dahliae*. *Fungal Genetics and Biology*, 43(4), 283-294.
- Knorr, M., Frey, S.D., Curtis, P.S. 2005. Nitrogen additions and litter decomposition: A meta-analysis. *Ecology*, 86(12), 3252-3257.
- Kristiansen, A., Lindholm, S., Feilberg, A., Nielsen, P.H., Neufeld, J.D., Nielsen, J.L. 2011a. Butyric Acid- and Dimethyl Disulfide-Assimilating Microorganisms in a Biofilter Treating Air Emissions from a Livestock Facility. *Applied and Environmental Microbiology*, 77(24), 8595-8604.
- Kristiansen, A., Pedersen, K.H., Nielsen, P.H., Nielsen, L.P., Nielsen, J.L., Schramm, A. 2011b. Bacterial community structure of a full-scale biofilter treating pig house exhaust air. *Systematic and Applied Microbiology*, 34(5), 344-352.
- Lazarus, W. 2013. Feedlot Air Emissions Treatment Cost Calculator, University of Minnesota Extension Service. <http://wlazarus.cfans.umn.edu/william-f-lazarus-water-air-quality/>.
- Lee, S.-W., Im, J., DiSpirito, A., Bodrossy, L., Barcelona, M., Semrau, J. 2009. Effect of nutrient and selective inhibitor amendments on methane oxidation, nitrous oxide production, and key gene presence and expression in landfill cover soils: characterization of the role of methanotrophs, nitrifiers, and denitrifiers. *Applied Microbiology and Biotechnology*, 85(2), 389-403.

- Liang, Y., Xin, H., Li, H., Gates, R.S., Wheeler, E.F., Casey, K.D. 2006. Effects of measurement intervals on estimation of ammonia emissions from layer houses. *Transactions of the ASABE*, 49(1), 183-186.
- Limbri, H., Gunawan, C., Thomas, T., Smith, A., Scott, J., Rosche, B. 2014. Coal-Packed Methane Biofilter for Mitigation of Green House Gas Emissions from Coal Mine Ventilation Air. *Plos One*, 9(4).
- Linder, M.B. 2009. Hydrophobins: Proteins that self assemble at interfaces. *Current Opinion in Colloid & Interface Science*, 14(5), 356-363.
- Liu, Z., Powers, W., Mukhtar, S. 2014. A review of practices and technologies for odor control in swine production facilities. *Applied Engineering in Agriculture*, 30(3), 477-492.
- Lo, Y.C.M., Koziel, J.A., Cai, L.S., Hoff, S.J., Jenks, W.S., Xin, H.W. 2008. Simultaneous chemical and sensory characterization of volatile organic compounds and semi-volatile organic compounds emitted from swine manure using solid phase microextraction and multidimensional gas chromatography-mass spectrometry-olfactometry. *Journal of Environmental Quality*, 37(2), 521-534.
- Madigan, M.T., Martinko, J.M., Dunlap, P.V., Clark, D.P. 2009. *Biology of Microorganisms, 12th Edition*. Pearson Education Inc., San Francisco.
- Mah, T.F.C., O'Toole, G.A. 2001. Mechanisms of biofilm resistance to antimicrobial agents. *Trends in Microbiology*, 9(1), 34-39.
- Maia, G.D.N., Day, G.B., Gates, R.S., Taraba, J.L. 2012a. Ammonia biofiltration and nitrous oxide generation during the start-up of gas-phase compost biofilters. *Atmospheric Environment*, 46, 659-664.
- Maia, G.D.N., Day, G.B., Gates, R.S., Taraba, J.L., Coyne, M.S. 2012b. Moisture effects on greenhouse gases generation in nitrifying gas-phase compost biofilters. *Water Research*, 46(9), 3023-3031.
- Malhautier, L., Cabrol, L., Bayle, S., Fanlo, J.-L. 2013. Identification and characterization of microbial communities in bioreactors. 1st ed. in: *Air Pollution Prevention and Control: Bioreactors and Bioenergy*, (Eds.) C. Kennes, M.C. Veiga, John Wiley & Sons. West Sussex, UK.
- Manter, D.K., Vivanco, J.M. 2007. Use of the ITS primers, ITS1F and ITS4, to characterize fungal abundance and diversity in mixed-template samples by qPCR and length heterogeneity analysis. *Journal of Microbiological Methods*, 71(1), 7-14.
- Manter, D.K., Weir, T.L., Vivanco, J.M. 2010. Negative effects of sample pooling on PCR-based estimates of soil microbial richness and community structure. *Applied and Environmental Microbiology*, 76(7), 2086-2090.
- May, S., Romberger, D.J., Poole, J.A. 2012. Respiratory Health Effects of Large Animal Farming Environments. *Journal of Toxicology and Environmental Health-Part B-Critical Reviews*, 15(8), 524-541.

- McCrary, D.F., Hobbs, P.J. 2001. Additives to reduce ammonia and odor emissions from livestock wastes: A review. *Journal of Environmental Quality*, 30(2), 345-355.
- McIlroy, S.J., Porter, K., Seviour, R.J., Tillett, D. 2009. Extracting nucleic acids from activated sludge which reflect community population diversity. *Antonie Van Leeuwenhoek International Journal of General and Molecular Microbiology*, 96(4), 593-605.
- Meda, B., Hassouna, M., Aubert, C., Robin, P., Dourmad, J.Y. 2011. Influence of rearing conditions and manure management practices on ammonia and greenhouse gas emissions from poultry houses. *Worlds Poultry Science Journal*, 67(3), 441-455.
- Melse, R.W., Van der Werf, A.W. 2005. Biofiltration for mitigation of methane emission from animal husbandry. *Environmental Science & Technology*, 39(14), 5460-5468.
- Menard, C., Ramirez, A.A., Heitz, M. 2014. Kinetics of simultaneous methane and toluene biofiltration in an inert packed bed. *Journal of Chemical Technology and Biotechnology*, 89(4), 597-602.
- Menard, C., Ramirez, A.A., Nikiema, J., Heitz, M. 2012. Biofiltration of methane and trace gases from landfills: A review. *Environmental Reviews*, 20(1), 40-53.
- Montes, F., Meinen, R., Dell, C., Rotz, A., Hristov, A.N., Oh, J., Waghorn, G., Gerber, P.J., Henderson, B., Makkar, H.P.S., Dijkstra, J. 2013. Special Topics - Mitigation of methane and nitrous oxide emissions from animal operations: II. A review of manure management mitigation options. *Journal of Animal Science*, 91(11), 5070-5094.
- Montzka, S.A., Dlugokencky, E.J., Butler, J.H. 2011. Non-CO₂ greenhouse gases and climate change. *Nature*, 476(7358), 43-50.
- Motulsky, H.J., Ransnas, L.A. 1987. Fitting curves to data using nonlinear-regression - A practical and nonmathematical review. *FASEB Journal*, 1(5), 365-374.
- Mudliar, S., Giri, B., Padoley, K., Satpute, D., Dixit, R., Bhatt, P., Pandey, R., Juwarkar, A., Vaidya, A. 2010. Bioreactors for treatment of VOCs and odour - A review. *Journal of Environmental Management*, 91, 1039-1054.
- Murrell, J.C., Radajewski, S. 2000. Cultivation-independent techniques for studying methanotroph ecology. *Research in Microbiology*, 151(10), 807-814.
- NAS. 2003. *AIR EMISSIONS From Animal Feeding Operations Current Knowledge, Future Needs*. National Academies Press, Washington, DC.
- Needelman, B.A., Wander, M.M., Shi, G.S. 2001. Organic carbon extraction efficiency in chloroform fumigated and non-fumigated soils. *Soil Science Society of America Journal*, 65(6), 1731-1733.
- Newell, S.Y., Arsuffi, T.L., Fallon, R.D. 1988. Fundamental procedures for the determining of ergosterol content of decaying plant-material by liquid-chromatography. *Applied and Environmental Microbiology*, 54(7), 1876-1879.
- Nguyen, N.H., Smith, D., Peay, K., Kennedy, P. 2015. Parsing ecological signal from noise in next generation amplicon sequencing. *New Phytologist*, 205(4), 1389-1393.

- Ni, J.Q., Robarge, W.P., Xiao, C.H., Heber, A.J. 2012. Volatile organic compounds at swine facilities: A critical review. *Chemosphere*, 89(7), 769-788.
- Nicolai, R., Lefers, R. 2006. Biofilters used to reduce emissions from livestock housing - A literature review. *Workshop on Agricultural Air Quality*, Washington, DC. pp. 952-1014.
- Nicolai, R.E., Clanton, C.J., Janni, K.A., Malzer, G.L. 2006. Ammonia removal during biofiltration as affected by inlet air temperature and media moisture content. *Transactions of the ASABE*, 49(4), 1125-1138.
- Nicolai, R.E., Janni, K.A., Schmidt, D. 2008. Biofiltration - Mitigation odor and gas emissions from animal operations. *Proceedings of the National Conference on Mitigating Air emissions from Animal Feeding Operations*, Des Moines, Iowa.
- Nikiema, J., Bibeau, L., Lavoie, J., Brzezinski, R., Vigneux, J., Heitz, M. 2005. Biofiltration of methane: An experimental study. *Chemical Engineering Journal*, 113(2-3), 111-117.
- Nikiema, J., Heitz, M. 2009. The influence of the gas flow rate during methane biofiltration on an inorganic packing material. *Canadian Journal of Chemical Engineering*, 87(1), 136-142.
- Nordin, A., Uggla, C., Nasholm, T. 2001. Nitrogen forms in bark, wood and foliage of nitrogen-fertilized *Pinus sylvestris*. *Tree Physiology*, 21(1), 59-64.
- NYS-DOH. 2004. The facts about ammonia. https://www.health.ny.gov/environmental/emergency/chemical_terrorism/ammonia_tech.htm.
- Nyvad, B., Crielaard, W., Mira, A., Takahashi, N., Beighton, D. 2013. Dental caries from a molecular microbiological perspective. *Caries Research*, 47(2), 89-102.
- O'Connor, A.M., Auvermann, B., Bickett-Weddle, D., Kirkhorn, S., Sargeant, J.M., Ramirez, A., Von Essen, S.G. 2010. The Association between Proximity to Animal Feeding Operations and Community Health: A Systematic Review. *Plos One*, 5(3).
- Osborne, C.A., Zwart, A.B., Broadhurst, L.M., Young, A.G., Richardson, A.E. 2011. The influence of sampling strategies and spatial variation on the detected soil bacterial communities under three different land-use types. *FEMS Microbiology Ecology*, 78(1), 70-79.
- Peay, K.G. 2014. Back to the future: natural history and the way forward in modern fungal ecology. *Fungal Ecology*, 12(0), 4-9.
- Pietsch, K.A., Ogle, K., Cornelissen, J.H.C., Cornwell, W.K., Bönisch, G., Craine, J.M., Jackson, B.G., Kattge, J., Peltzer, D.A., Penuelas, J., Reich, P.B., Wardle, D.A., Weedon, J.T., Wright, I.J., Zanne, A.E., Wirth, C. 2014. Global relationship of wood and leaf litter decomposability: the role of functional traits within and across plant organs. *Global Ecology and Biogeography*, 23(9), 1046-1057.
- Pointing, S.B. 2001. Feasibility of bioremediation by white-rot fungi. *Applied Microbiology and Biotechnology*, 57(1-2), 20-33.

- Posmanik, R., Gross, A., Nejidat, A. 2014. Effect of high ammonia loads emitted from poultry-manure digestion on nitrification activity and nitrifier-community structure in a compost biofilter. *Ecological Engineering*, 62, 140-147.
- Pratt, C., Deslippe, J., Tate, K.R. 2013. Testing a Biofilter Cover Design to Mitigate Dairy Effluent Pond Methane Emissions. *Environmental Science & Technology*, 47(1), 526-532.
- Prenafeta-Boldú, F.X., Guivernau, M., Gallastegui, G., Viñas, M., de Hoog, G.S., Elías, A. 2012a. Fungal/bacterial interactions during the biodegradation of TEX hydrocarbons (toluene, ethylbenzene and p-xylene) in gas biofilters operated under xerophilic conditions. *FEMS Microbiology Ecology*, 80(3), 722-734.
- Prenafeta-Boldú, F.X., Illa, J., van Groenestijn, J.W., Flotats, X. 2008. Influence of synthetic packing materials on the gas dispersion and biodegradation kinetics in fungal air biofilters. *Applied Microbiology and Biotechnology*, 79(2), 319-327.
- Prenafeta-Boldú, F.X., Ortega, O., Arimany, M., Canalias, F. 2012b. Assessment of process limiting factors during the biofiltration of odorous VOCs in a full-scale composting plant. *Compost Science & Utilization*, 20(2), 73-78.
- Prescott, C.E. 2010. Litter decomposition: what controls it and how can we alter it to sequester more carbon in forest soils? *Biogeochemistry*, 101(1-3), 133-149.
- Prescott, C.E., Vesterdal, L., Preston, C.M., Simard, S.W. 2004. Influence of initial chemistry on decomposition of foliar litter in contrasting forest types in British Columbia. *Canadian Journal of Forest Research*, 34(8), 1714-1729.
- Rajala, T., Peltoniemi, M., Pennanen, T., Makipaa, R. 2010. Relationship between wood-inhabiting fungi determined by molecular analysis (denaturing gradient gel electrophoresis) and quality of decaying logs. *Canadian Journal of Forest Research-Revue Canadienne De Recherche Forestiere*, 40(12), 2384-2397.
- Ralebitso-Senior, T.K., Senior, E., Di Felice, R., Jarvis, K. 2012. Waste gas biofiltration: Advances and limitations of current approaches in microbiology. *Environmental Science & Technology*, 46(16), 8542-8573.
- Ramirez-Lopez, E., Hernandez, J.C., Dendooven, L., Rangel, P., Thalasso, F. 2003. Characterization of five agricultural by-products as potential biofilter carriers. *Bioresource Technology*, 88(3), 259-263.
- Ramirez, A.A., Garcia-Aguilar, B.P., Jones, J.P., Heitz, M. 2012. Improvement of methane biofiltration by the addition of non-ionic surfactants to biofilters packed with inert materials. *Process Biochemistry*, 47(1), 76-82.
- Rene, E.R., Mohammad, B.T., Veiga, M.C., Kennes, C. 2012. Biodegradation of BTEX in a fungal biofilter: Influence of operational parameters, effect of shock-loads and substrate stratification. *Bioresource Technology*, 116, 204-213.
- Rene, E.R., Veiga, M.C., Kennes, C. 2013. Biofilters. 1st edn. ed. in: *Air Pollution Prevention and Control: Bioreactors and Bioenergy*, (Eds.) C. Kennes, M.C. Veiga, John Wiley & Sons. West Sussex, UK.

- Ritz, C.W., Fairchild, B.D., Lacy, M.P. 2004. Implications of ammonia production and emissions from commercial poultry facilities: A review. *Journal of Applied Poultry Research*, 13, 684-692.
- Robertson, W.D. 2010. Nitrate removal rates in woodchip media of varying age. *Ecological Engineering*, 36(11), 1581-1587.
- Rose, J.L., Mahler, C.F., Izzo, R.L.D. 2012. Comparison of the methane oxidation rate in four media. *Revista Brasileira De Ciencia Do Solo*, 36(3), 803-812.
- Ross, D.J. 1989. Estimation of soil microbial-C by a fumigation-extraction procedure - influence of soil-moisture content. *Soil Biology & Biochemistry*, 21(6), 767-772.
- Russell, M., Woodall, C., Fraver, S., D'Amato, A., Domke, G., Skog, K. 2014. Residence times and decay rates of downed woody debris biomass/carbon in Eastern US forests. *Ecosystems*, 17(5), 765-777.
- Sakano, Y., Kerkhof, L. 1998. Assessment of changes in microbial community structure during operation of an ammonia biofilter with molecular tools. *Applied and Environmental Microbiology*, 64(12), 4877-4882.
- Sanchez, C. 2010. Cultivation of *Pleurotus ostreatus* and other edible mushrooms. *Applied Microbiology and Biotechnology*, 85(5), 1321-1337.
- Satter, L.D., Klopfenstein, T.J., Erickson, G.E. 2002. The role of nutrition in reducing nutrient output from ruminants. *Journal of Animal Science*, 80(2), E143-E156.
- Schiffman, S.S., Bennett, J.L., Raymer, J.H. 2001. Quantification of odors and odorants from swine operations in North Carolina. *Agricultural and Forest Meteorology*, 108(3), 213-240.
- Schilling, J.S., Ayres, A., Kaffenberger, J.T., Powers, J.S. 2015a. Initial white rot type dominance of wood decomposition and its functional consequences in a regenerating tropical dry forest. *Soil Biology and Biochemistry*, 88(0), 58-68.
- Schilling, J.S., Duncan, S.M., Presley, G.N., Filley, T.R., Jurgens, J.A., Blanchette, R.A. 2013. Colocalizing incipient reactions in wood degraded by the brown rot fungus *Postia placenta*. *International Biodeterioration & Biodegradation*, 83(0), 56-62.
- Schilling, J.S., Kaffenberger, J.T., Liew, F.J., Song, Z. 2015b. Signature wood modifications reveal decomposer community history. *PLoS ONE*, 10(3), e0120679.
- Schipper, L.A., Robertson, W.D., Gold, A.J., Jaynes, D.B., Cameron, S.C. 2010. Denitrifying bioreactors—An approach for reducing nitrate loads to receiving waters. *Ecological Engineering*, 36(11), 1532-1543.
- Schmidt, D., Jacobson, L.D., Nicolai, R.E. 2004. Biofilter design information. University of Minnesota Extension Service, Biosystems and Agricultural Engineering Update (BAEU) 18, St. Paul, Minnesota.
- Semrau, J.D., DiSpirito, A.A., Yoon, S. 2010. Methanotrophs and copper. *Fems Microbiology Reviews*, 34(4), 496-531.
- Seth, E.C., Taga, M.E. 2014. Nutrient cross-feeding in the microbial world. *Frontiers in Microbiology*, 5.

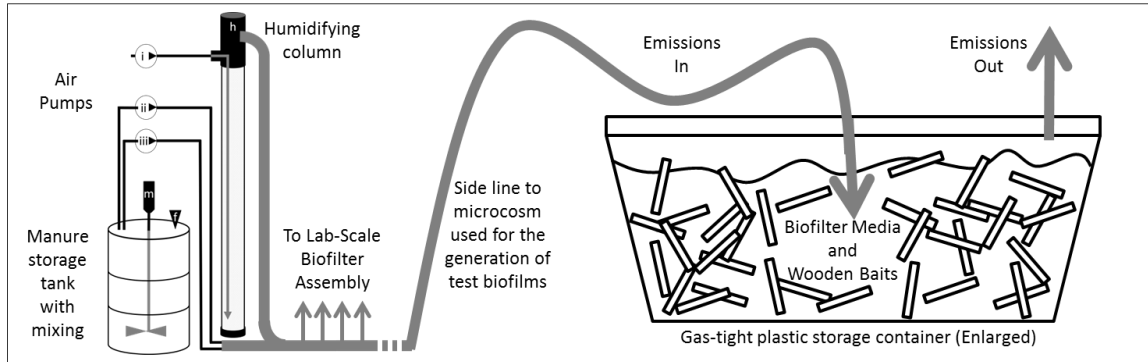
- Shindell, D., Kuylenstierna, J.C.I., Vignati, E., van Dingenen, R., Amann, M., Klimont, Z., Anenberg, S.C., Muller, N., Janssens-Maenhout, G., Raes, F., Schwartz, J., Faluvegi, G., Pozzoli, L., Kupiainen, K., Höglund-Isaksson, L., Emberson, L., Streets, D., Ramanathan, V., Hicks, K., Oanh, N.T.K., Milly, G., Williams, M., Demkine, V., Fowler, D. 2012. Simultaneously Mitigating Near-Term Climate Change and Improving Human Health and Food Security. *Science*, 335(6065), 183-189.
- Sipma, J., Osuna, M.B., Emanuelsson, M.A.E., Castro, P.M.L. 2010. Biotreatment of industrial wastewaters under transient-state conditions: Process stability with fluctuations of organic load, substrates, toxicants, and environmental parameters. *Critical Reviews in Environmental Science and Technology*, 40(2), 147-197.
- Song, Z., Vail, A., Sadowsky, M.J., Schilling, J.S. 2014. Quantitative PCR for measuring biomass of decomposer fungi in planta. *Fungal Ecology*, 7(0), 39-46.
- Spigno, G., Pagella, C., Fumi, M.D., Molteni, R., De Faveri, D.M. 2003. VOCs removal from waste gases: gas-phase bioreactor for the abatement of hexane by *Aspergillus niger*. *Chemical Engineering Science*, 58(3-6), 739-746.
- States, J.S., Christensen, M. 2001. Fungi associated with biological soil crusts in desert grasslands of Utah and Wyoming. *Mycologia*, 93(3), 432-439.
- Steele, J.A., Ozis, F., Fuhrman, J.A., Devinny, J.S. 2005. Structure of microbial communities in ethanol biofilters. *Chemical Engineering Journal*, 113(2-3), 135-143.
- Steinfeld, H., Gerber, P., Wassenaar, T., Castel, V., Rosales, M., Haan, C.d. 2006. *Livestock's long shadow: Environmental issues and options*. Food and Agriculture Organization of the United Nations, FAO, Rome, Italy.
- Streese, J., Stegmann, R. 2005. Potentials and limitations of biofilters for methane oxidation. *10th International Waste Management and Landfill Symposium*, October 5-9, 2005, Santa Margherita di Pula, Sardinia. CISA.
- Strickland, M.S., Rousk, J. 2010. Considering fungal:bacterial dominance in soils - Methods, controls, and ecosystem implications. *Soil Biology & Biochemistry*, 42(9), 1385-1395.
- Sulc, M., Peslova, K., Zabka, M., Hajduch, M., Havlicek, V. 2009. Biomarkers of *Aspergillus* spores: Strain typing and protein identification. *International Journal of Mass Spectrometry*, 280(1-3), 162-168.
- Sutton, A.L., Kephart, K.B., Verstegen, M.W.A., Canh, T.T., Hobbs, P.J. 1999. Potential for reduction of odorous compounds in swine manure through diet modification. *Journal of Animal Science*, 77(2), 430-439.
- Szadkowska-Stanczyk, I., Brodka, K., Buczynska, A., Cyprowski, M., Kozajda, A., Sowiak, M. 2010. Exposure to bioaerosols among CAFO workers (swine feeding). *Medycyna Pracy*, 61(3), 257-269.
- Tank, J.L., Webster, J.R. 1998. Interaction of substrate and nutrient availability on wood biofilm processes in streams. *Ecology*, 79(6), 2168-2179.

- Trabue, S., Scoggin, K., Li, H., Burns, R., Xin, H., Hatfield, J. 2010. Speciation of volatile organic compounds from poultry production. *Atmospheric Environment*, 44(29), 3538-3546.
- Tucker, S.L., Talbot, N.J. 2001. Surface attachment and pre-penetration stage development by plant pathogenic fungi. *Annual Review of Phytopathology*, 39, 385-+.
- U.S. Department of State. 2010. U.S. Climate Action Report. *Global Publishing Services*.
- Ubeda, Y., Lopez-Jimenez, P.A., Nicolas, J., Calvet, S. 2013. Strategies to control odours in livestock facilities: a critical review. *Spanish Journal of Agricultural Research*, 11(4), 1004-1015.
- UNEP & WMO. 2011. Summary of Decision Makers of the Integrated Assessment of Black Carbon and Tropospheric Ozone. *United Nations Environmental Program & World Meteorological Organization*, Doc. UNEP/GC/26/INF/20.
- US-EPA. 2012a. 2008 National Emissions Inventory, version 2. Technical Support Document,. DRAFT, (Ed.) O.o.A.Q.P.a.S. U.S. Environmental Protection Agency, Air Quality Assessment Division, Emissions Inventory and Analysis Group, http://www.epa.gov/ttn/chief/net/2008neiv2/2008_neiv2_tsd_draft.pdf. Research Triangle Park, North Carolina.
- US-EPA. 2013. Draft Inventory of U.S. Greenhouse gas emissions and sinks: 1990-2011. *U.S. Environmental Protection Agency FRL-9784-3*.
- US-EPA. 2004. National Emission Inventory - Ammonia Emissions from Animal Husbandry Operations. http://www.epa.gov/ttnchie1/ap42/ch09/related/nh3inventorydraft_jan2004.pdf.
- US-EPA. 2015a. Overview of greenhouse gases - Methane. *United States Environmental Protection Agency*, <http://epa.gov/climatechange/ghgemissions/gases/ch4.html>.
- US-EPA. 2015b. Regulatory Definitions of Large CAFOs, Medium CAFOs, and Small CAFOs. *U.S. Environmental Protection Agency*, http://www.epa.gov/npdes/pubs/sector_table.pdf.
- US-EPA. 2012b. U.S. Greenhouse Gas Inventory Report - Inventory of U.S. Greenhouse Gas Emissions and Sinks: 1990-2010. *United States Environmental Protection Agency*.
- US-EPA. 2015c. What is a CAFO? *U.S. Environmental Protection Agency*, <http://www.epa.gov/region07/water/cafo/index.htm>.
- Valenzuela-Solano, C., Crohn, D.M. 2006. Are decomposition and N release from organic mulches determined mainly by their chemical composition? *Soil Biology & Biochemistry*, 38(2), 377-384.
- Vallero, D. 2008. *Fundamentals of Air Pollution, 4th Edition*. Academic Press, Amsterdam, NL.
- van Groenestijn, J.W., van Heiningen, W.N.M., Kraakman, N.J.R. 2001. Biofilters based on the action of fungi. *Water Science and Technology*, 44(9), 227-232.

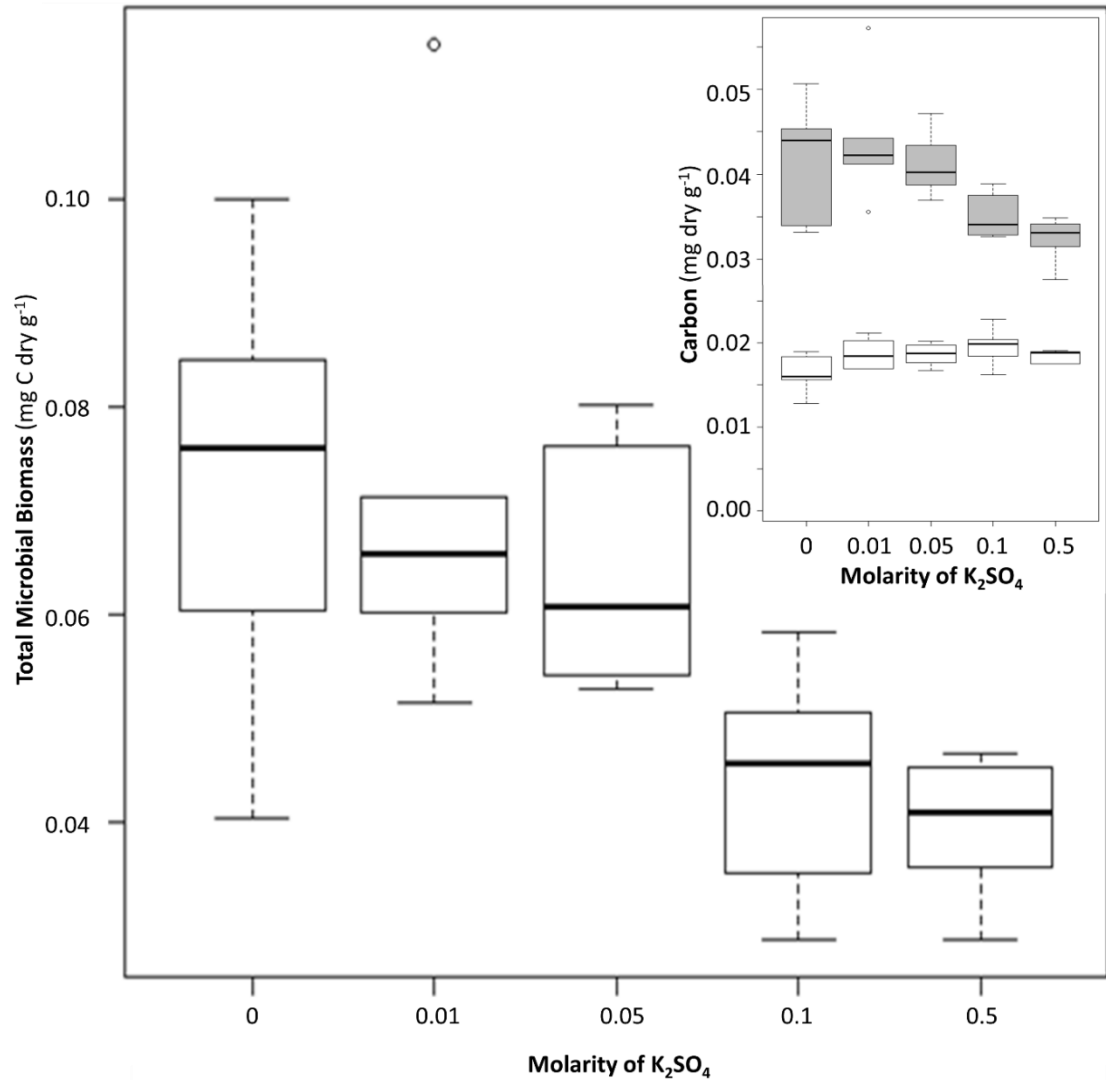
- van Lith, C., Leson, G., Michelsen, R. 1997. Evaluating design options for biofilters. *Journal of the Air & Waste Management Association*, 47(1), 37-48.
- Veen, G.F., Freschet, G.T., Ordonez, A., Wardle, D.A. 2015. Litter quality and environmental controls of home-field advantage effects on litter decomposition. *Oikos*, 124(2), 187-195.
- Veillette, M., Girard, M., Viens, P., Brzezinski, R., Heitz, M. 2012. Function and limits of biofilters for the removal of methane in exhaust gases from the pig industry. *Applied Microbiology and Biotechnology*, 94(3), 601-611.
- Veillette, M., Pascal, V., Ramirez, A., Brzezinski, R., Heitz, M. 2011. Effect of ammonium concentration on microbial population and performance of a biofilter treating air polluted with methane. *Chemical Engineering Journal*, 171, 1114-1123.
- Venugopal, S., Chandrakanthi, M., Hettiaratchi, P. 2004. Applications of methanotrophic biofilters (mbfs) in treating methane (CH₄) emissions from oil and gas industry. *Research Report of TransCanada Pipe-Lines Ltd.*
- Vergara-Fernandez, A., Hernandez, S., Revah, S. 2011. Elimination of hydrophobic volatile organic compounds in fungal biofilters: Reducing start-up time using different carbon sources. *Biotechnology and Bioengineering*, 108(4), 758-765.
- Vergara-Fernandez, A., Van Haaren, B., Revah, S. 2006. Phase partition of gaseous hexane and surface hydrophobicity of *Fusarium solani* when grown in liquid and solid media with hexanol and hexane. *Biotechnology Letters*, 28(24), 2011-2017.
- Wang, Z., Binder, M., Schoch, C.L., Johnston, P.R., Spatafora, J.W., Hibbett, D.S. 2006. Evolution of helotialean fungi (Leotiomycetes, Pezizomycotina): A nuclear rDNA phylogeny. *Molecular Phylogenetics and Evolution*, 41(2), 295-312.
- Wäsche, S., Horn, H., Hempel, D.C. 2002. Influence of growth conditions on biofilm development and mass transfer at the bulk/biofilm interface. *Water Research*, 36(19), 4775-4784.
- Watzinger, A., Stemmer, M., Pfeffer, M., Rasche, F., Reichenauer, T.G. 2008. Methanotrophic communities in a landfill cover soil as revealed by C-13 PLFAs and respiratory quinones: Impact of high methane addition and landfill leachate irrigation. *Soil Biology & Biochemistry*, 40(3), 751-762.
- Weedon, J.T., Cornwell, W.K., Cornelissen, J.H.C., Zanne, A.E., Wirth, C., Coomes, D.A. 2009. Global meta-analysis of wood decomposition rates: a role for trait variation among tree species? *Ecology Letters*, 12(1), 45-56.
- White House. 2014. Climate action plan, strategy to reduce methane emissions. (http://www.whitehouse.gov/sites/default/files/strategy_to_reduce_methane_emissions_2014-03-28_final.pdf).
- Wienhold, B.J., Varvel, G.E., Jin, V.L. 2011. Corn cob residue carbon and nutrient dynamics during decomposition. *Agronomy Journal*, 103(4), 1192-1197.
- Wilson, S.M., Howell, F., Wing, S., Sobsey, M. 2002. Environmental injustice and the Mississippi hog industry. *Environmental Health Perspectives*, 110, 195-201.

- Wing, S., Cole, D., Grant, G. 2000. Environmental injustice in North Carolina's hog industry. *Environmental Health Perspectives*, 108(3), 225-231.
- Wosten, H.A.B. 2001. Hydrophobins: Multipurpose proteins. *Annual Review of Microbiology*, 55, 625-646.
- Wosten, H.A.B., van Wetter, M.A., Lugones, L.G., van der Mei, H.C., Busscher, H.J., Wessels, J.G.H. 1999. How a fungus escapes the water to grow into the air. *Current Biology*, 9(2), 85-88.
- Xue, N.T., Wang, Q.H., Wang, J., Wang, J.H., Sun, X.H. 2013. Odorous composting gas abatement and microbial community diversity in a biotrickling filter. *International Biodeterioration & Biodegradation*, 82, 73-80.
- Xue, N.T., Wang, Q.H., Wu, C.F., Zhao, P., Xie, W.M. 2011. Elimination of NH₃ and odor from composting by biotrickling filter and preliminary exploration on molecular biology. *Water Science and Technology*, 63(4), 747-753.
- Yang, L., Wang, X., Funk, T.L., Gates, R.S., Zhang, Y. 2013. Impedance-based moisture sensor design and test for gas-phase biofilter applications. *Transactions of the ASABE*, 56(4), 1613-1621.
- Yoon, S., Carey, J., Semrau, J. 2009. Feasibility of atmospheric methane removal using methanotrophic biotrickling filters. *Applied Microbiology and Biotechnology*, 83(5), 949-956.
- Yuan, L., Abichou, T., Chanton, J., Powelson, D., De Visscher, A. 2009. Long-term numerical simulation of methane transport and oxidation in compost biofilter. *Practice Periodical of Hazardous, Toxic, and Radioactive Waste Management*, 13(3), 196-202.

9. APPENDIXES



Appendix 3.1 Schematic of microcosm used to generate test biofilms.



Appendix 3.2 Effect of extractant salinity on total microbial C. There is no significant difference between the mean microbial C measured using the recommended 0.5 M concentration and the 0.1 M test concentration despite a small impact on variability. The inset figure shows the extracted C concentrations for both the non-fumigated subsamples (white boxplots) and the chloroform fumigated subsamples (grey boxplots) used to determine microbial C.

Appendix 3.3 Average (\pm standard deviations) values of biomarkers for various sample fractions used to target biofilms.

Sample Fraction	Total Microbial C	Total Ergosterol	Total DNA
	mg	μ g	ng
Intact Whole	0.60 (\pm 0.35)	79 (\pm 84)	171 (\pm 27)
Intact Ground	1.50 (\pm 0.68)	128 (\pm 23)	1128 (\pm 729)
Biofilm	0.07 (\pm 0.03)	14 (\pm 10)	122 (\pm 87)
Wood Whole	0.46 (\pm 0.19)	149 (\pm 35)	701 (\pm 103)
Sum	0.53 (\pm 0.19)	170 (\pm 44)	1128 (\pm 729)
Biofilm	0.05 (\pm 0.05)	21 (\pm 29)	110 (\pm 75)
Wood Ground	0.74 (\pm 0.74)	163 (\pm 44)	1219 (\pm 497)
Sum	0.76 (\pm 0.75)	178 (\pm 46)	1329 (\pm 525)

Appendix 3.4 Average (\pm standard deviations) values of biomarkers and coefficients of variation for various biofilm sample sizes.

Sample Size	Total Microbial C	Total Ergosterol	Total DNA
mg	mg g ⁻¹	μ g g ⁻¹	ng g ⁻¹
10	68.9 (\pm 17.1)	206 (\pm 100)	2691 (\pm 1018)
30	62.5 (\pm 14.1)	388 (\pm 33)	3881 (\pm 1535)
50	83.0 (\pm 13.6)	445 (\pm 31)	1445 (\pm 1392)
100	88.6 (\pm 10.6)	451 (\pm 75)	2886 (\pm 2119)
150	87.4 (\pm 8.9)	513 (\pm 46)	2701 (\pm 739)
200	91.2 (\pm 9.6)	488 (\pm 29)	2026 (\pm 335)

Appendix 3.5 Average (\pm standard deviations) values of moisture content, microbial C, ergosterol and total fungal:total microbial biomass ratios for the 4 field sample locations.

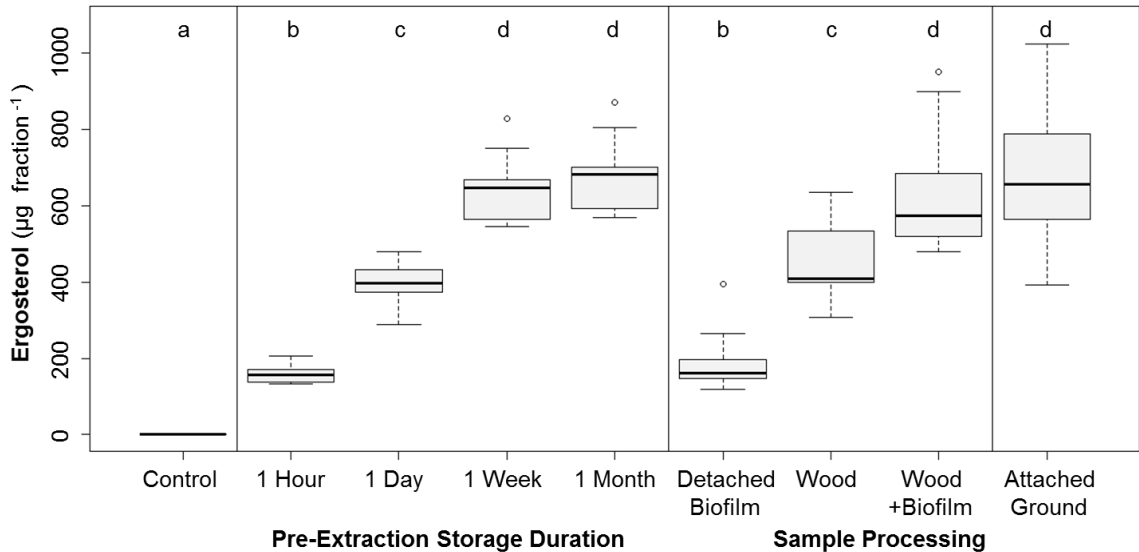
Location	Moisture Content	Chloroform Labile-C		Total Ergosterol		Total Fungal : Total Microbial Ratio	
		<u>Wood</u>	<u>Biofilm</u>	<u>Wood</u>	<u>Biofilm</u>	<u>Wood</u>	<u>Biofilm</u>
	%	mg g ⁻¹	mg g ⁻¹	mg g ⁻¹	mg g ⁻¹		
Close Deep	75.20 (\pm 0.79)	1.85 (\pm 0.38)	15.56 (\pm 2.51)	0.09 (\pm 0.04)	0.39 (\pm 0.37)	0.05 (\pm 0.02)	0.03 (\pm 0.02)
Close Shallow	73.71 (\pm 3.50)	2.25 (\pm 1.23)	11.30 (\pm 4.39)	0.11 (\pm 0.02)	0.28 (\pm 0.17)	0.06 (\pm 0.02)	0.03 (\pm 0.02)
Far Deep	69.33 (\pm 3.51)	2.32 (\pm 0.25)	27.89 (\pm 3.90)	0.09 (\pm 0.01)	1.71 (\pm 0.41)	0.04 (\pm 0.01)	0.06 (\pm 0.02)
Far Shallow	65.50 (\pm 4.65)	1.14 (\pm 0.39)	4.71 (\pm 0.63)	0.07 (\pm 0.02)	0.75 (\pm 0.32)	0.07 (\pm 0.04)	0.16 (\pm 0.06)

Appendix 3.6 Average (\pm standard deviations) Ct values of bacteria and fungi, and the fungal:bacterial Ct ratio using the largest Ct values from the run as a calibrator.

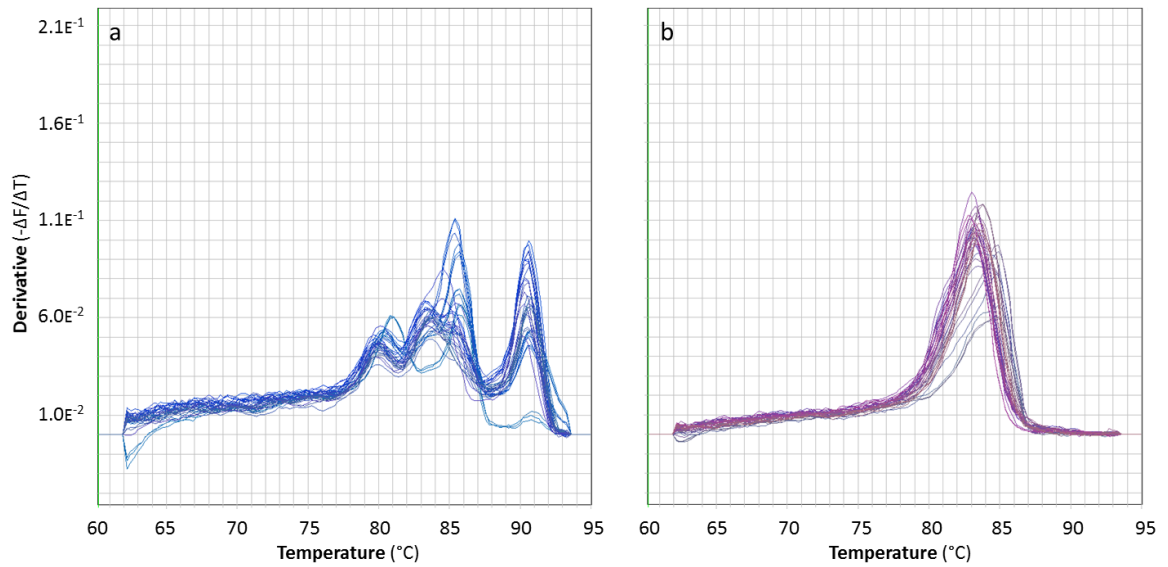
Location	Bacteria*	Fungi**	Fungal :Bacterial Ratio
	Ct _{100% eff.}	Ct _{100%eff}	Δ Ct _{Fungi} : Δ Ct _{Bacteria}
Close Deep	13.28 (\pm 1.25)	19.66 (\pm 1.74)	0.53 (\pm 0.08)
Close Shallow	11.15 (\pm 1.93)	17.75 (\pm 1.73)	0.58 (\pm 0.04)
Far Deep	14.82 (\pm 1.79)	20.31 (\pm 2.87)	0.53 (\pm 0.17)
Far Shallow	13.41 (\pm 2.94)	20.75 (\pm 4.33)	0.42 (\pm 0.26)

* Based on universal primers for bacteria (Eub 338/Eub 518)

** Based on universal primers for fungi (ITS1/ITS4)



Appendix 3.7 The effect of sample storage time on the measurement of total ergosterol as compared to the values for other sample fractions. Fourteen soil-block microcosms (AWPA 2006) each containing 6 birch chip baits were inoculated with plugs of an isolate of *Coprinellus micaceus* cultured from the biofilter being tested. *C. micaceus* was isolated into agar culture from a fruiting body, and morphological identification was confirmed by PCR amplification of the non-coding rDNA ITS region using the ITS-1 and ITS-4 primers and BLAST searching against sequences previously uploaded in the NCBI-Genbank. Soil-block microcosms contained equal portions of dried peat, vermiculite, and non-amended potting soil, plus 2 birch feeder strips (tongue depressors, 2 × 5 × 0.2 cm). Following incubation (6 mo., 22 °C, in the dark), baits were aseptically harvested and subsampled for gravimetric moisture content determination. From each set of 6 baits in the soil-block microcosms, one was ground in a Wiley® Mini-Mill to pass a 10 mesh (attached ground), one was scraped free of biofilm using a sterile single-edge razor blade (detached biofilm) leaving biofilm-free wood (wood) and the remaining four left attached. All bait and biofilm subsamples were immediately placed into 5 mL of cold methanol and stored at -20 °C. The four baits with attached biofilm were stored for various lengths of time (1 hour, 1 day, 1 week, 1 month) before extraction. Processed samples were all stored in methanol for 1 mo. before extraction; a typical storage length. Fourteen non-inoculated baits were stored in methanol 1 mo. before extraction and were used as negative controls.



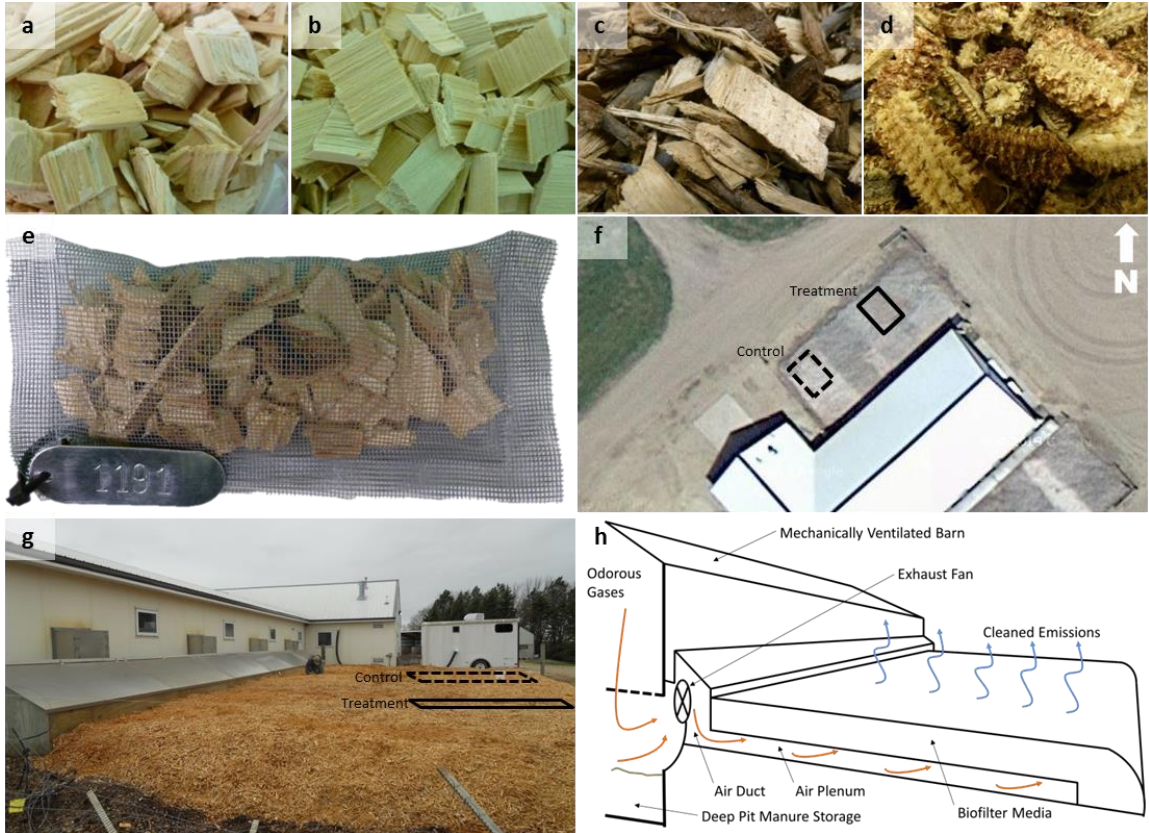
Appendix 3.8 a) Example qPCR melting curves for fungal DNA templates and **b)** prokaryotic DNA templates following DNA purification and optimization of primers and reactions.



Appendix 4.1 a) Aerial photograph of the field site (Imagery ©2015 Google, Map data ©2015 Google), b) photograph of the wooden baits, c) schematic of the biofilters, and photographs of the d) south biofilter, e) north biofilter, f) south biofilter media, g) baits in the north biofilter, and h) north biofilter media.

Appendix 4.2 Summary of ergosterol recoveries and internal standard losses for various extraction conditions.

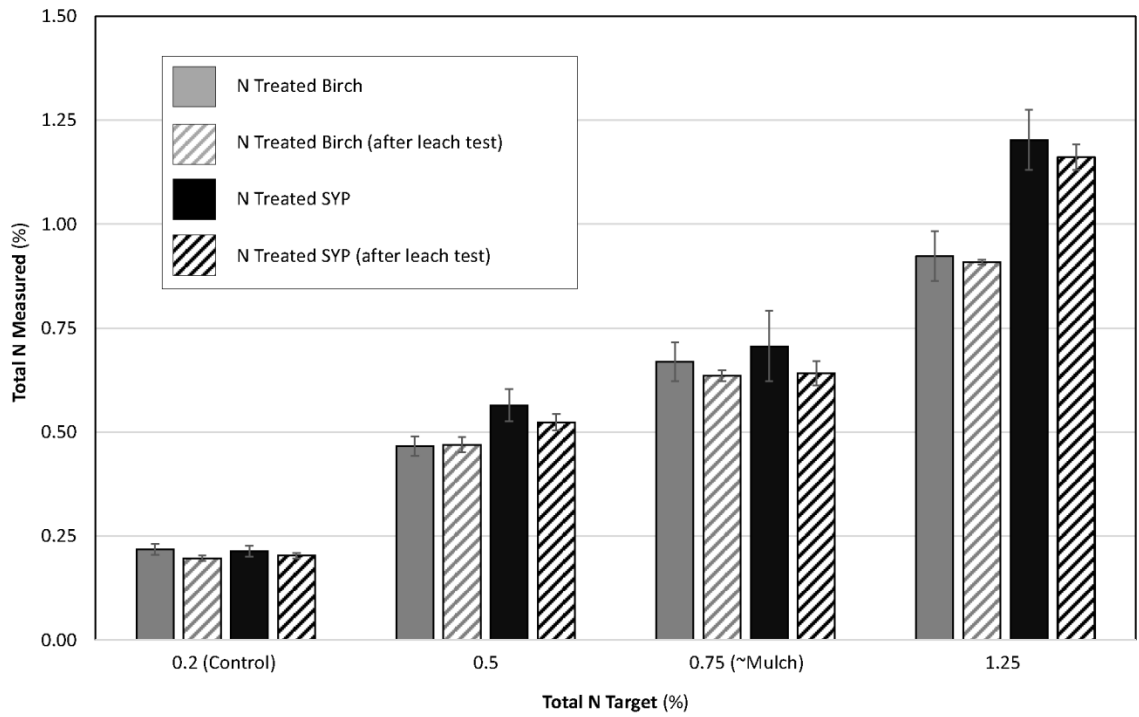
Extraction Conditions	Ergosterol	SD	Internal cholesterol standard loss	SD
Reflux time (hr)				
No. of MeOH rinses	ug g ⁻¹ dry biofilm	ug g ⁻¹ dry biofilm	%	%
No. of pentane rinses				
0.5	274.23	9.07	30.56	9.44
1				
2				
1	273.22	7.40	29.58	2.04
1				
2				
2	280.54	9.69	58.29	11.61
1				
2				
2	276.40	15.07	53.51	2.13
2				
2				
2	288.64	9.21	34.10	2.78
1				
3				
2	280.50	5.43	45.89	3.30
2				
3				



Appendix 5.1 Photos of example media types, **a**) softwood SYP, **b**) hardwood Birch, **c**) Mulch, **d**) Cobs. **e**) Photo of a litter bag. **f**) An aerial image (Imagery ©2015 Digital Globe, Map data ©2015 Google) and **g**) a photo of the field site with the boxes noting the sample locations. **h**) Schematic of the studied biofilter.

Appendix 5.2 Average media moisture content and the average inlet emissions for the treatment and control biofilter locations. Emissions were measured in the inlet air plenum for the treatment and control locations of the biofilter according to the methods outlined in Janni et al. (2014). Different letters note location means that are significantly different ($\alpha = 0.05$).

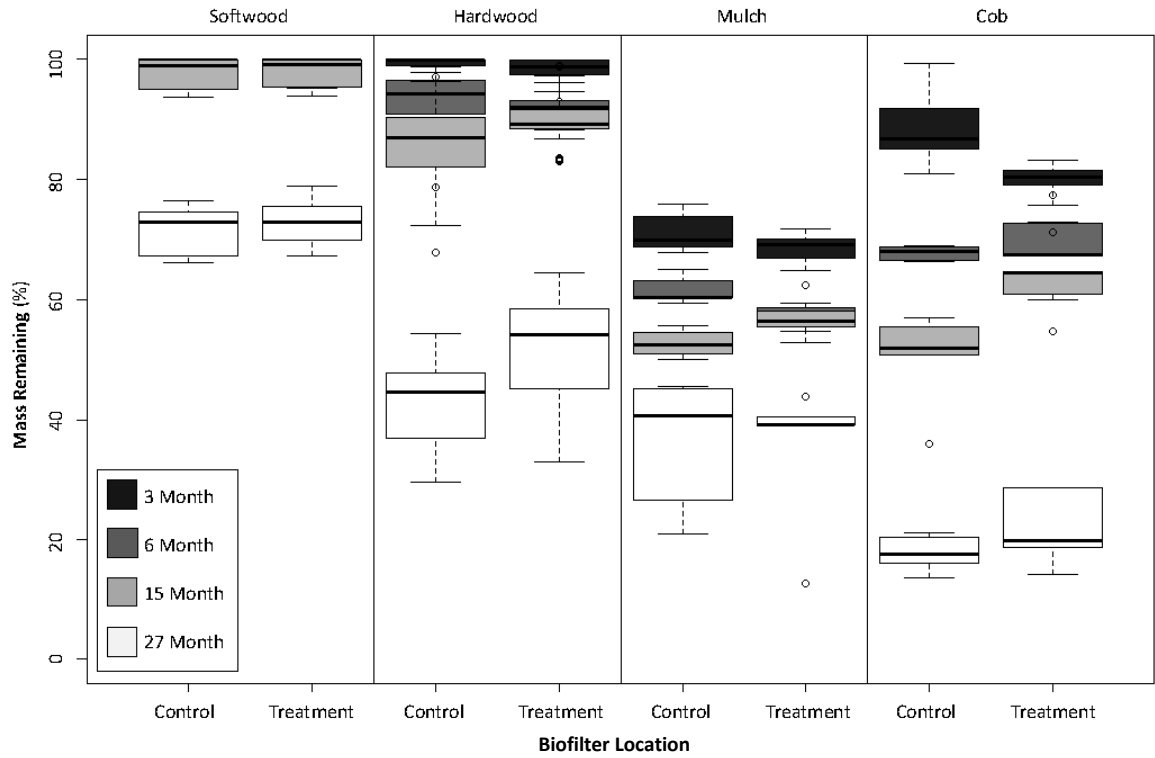
Location	Moisture Content	Ammonia	Carbon Dioxide	Nitrous Oxide	Methane	Sulfur Dioxide	Hydrogen Sulfide
	%	ppm	ppm	ppm	ppm	ppb	ppb
Treatment	51.22 a	9.22 a	958.5 a	1.02 a	79.74 a	10.47 a	274.9 a
	19.01	6.17	748.2	0.92	66.20	5.52	261.1
Control	61.62 b	1.36 b	1134 a	1.05 a	21.20 b	8.53 a	8.76 b
	11.91	0.78	958.5	1.26	66.20	6.03	10.88



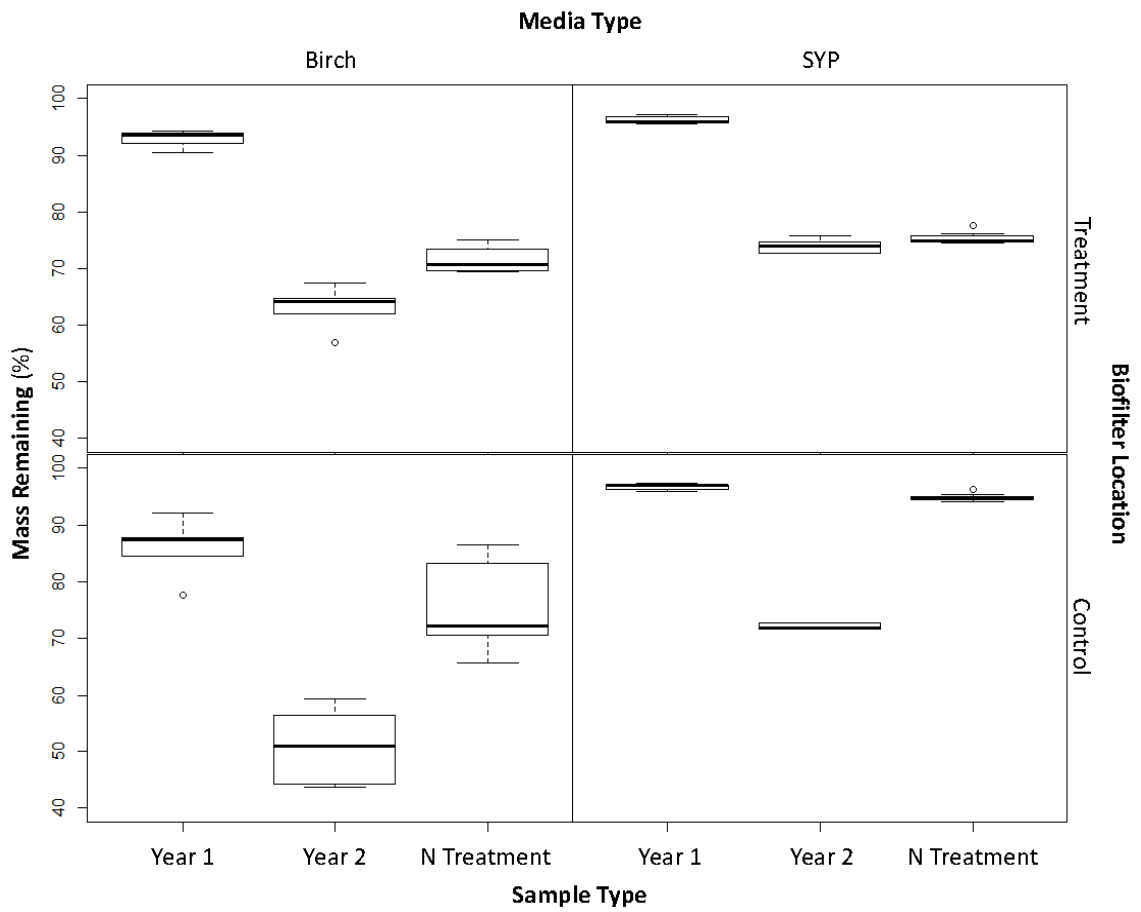
Appendix 5.3 Nitrogen content of Birch and SYP media post N treatment with casein hydrolysate and after leach testing.

Appendix 5.4 Correlations of all normalized physiochemical prediction variables.

	Dens	pH ¹	Lignin ¹	log ₁₀ Ext	Hemr ¹	Al ¹	C ¹	Ca ¹	log ₁₀ Fe	log ₁₀ K	log ₁₀ Mg	log ₁₀ Mn	N ¹	log ₁₀ Na	log ₁₀ P	log ₁₀ CN	Lignin	CMHC	CLoss	TSMC	T3Loss	CMHC	CLoss	CMHC	CLoss	TMHC	TB Loss	CMHC	CLoss	TMHC	T15Loss	CMHC	CLoss	T27MC	T27Loss	
Bulk Density	1.0000																																			
pH ¹	0.4633	1.0000																																		
Lignin ¹	0.0322	-0.1761	1.0000																																	
log ₁₀ Extractives	-0.3844	-0.4388	0.1687	1.0000																																
log ₁₀ Sucrose	0.6138	-0.1634	0.0746	0.2274	1.0000																															
Hemicellulose ¹	0.5644	-0.1167	-0.6670	0.1347	0.6982	1.0000																														
Al ¹	0.4498	0.1733	0.2261	0.1728	0.2888	0.0106	1.0000																													
C ¹	0.2356	0.8711	-0.6944	-0.2522	0.0342	0.6249	0.0662	1.0000																												
Ca ¹	0.1648	0.2981	0.6393	-0.6893	-0.1717	-0.6520	-0.1388	-0.1956	1.0000																											
log ₁₀ Fe	-0.1048	-0.3383	0.1117	-0.2788	-0.1378	-0.2780	-0.6904	-0.5683	0.2183	1.0000																										
log ₁₀ K	-0.0401	-0.5241	0.0005	-0.3656	-0.1788	-0.1701	-0.3882	-0.6026	0.2106	0.6979	1.0000																									
log ₁₀ Mg	-0.0835	-0.7051	-0.0655	0.3297	-0.2345	0.0448	-0.3453	-0.4006	-0.2458	0.1711	0.4809	1.0000																								
log ₁₀ Mn	-0.1144	-0.0688	-0.6515	0.2374	0.3259	0.7222	-0.3835	0.3703	-0.4619	-0.1716	-0.1163	0.1218	1.0000																							
N ¹	0.2180	0.4563	0.0797	0.1228	0.2971	0.0673	0.2896	0.4041	0.0550	-0.7980	-0.6735	-0.2365	1.0000																							
log ₁₀ Na	0.0650	-0.6102	0.2374	0.1162	0.6026	0.2220	-0.0656	-0.5389	-0.0611	0.3162	0.6526	0.3006	0.2471	-0.4433	1.0000																					
log ₁₀ P	-0.0288	-0.8303	0.2132	0.0848	-0.1749	-0.1375	-0.3038	-0.6709	0.0958	0.3632	0.7777	0.8966	-0.0382	-0.1498	0.6550	1.0000																				
log ₁₀ CN	0.2172	0.4817	0.0367	0.0977	0.2824	0.0806	0.2771	0.4489	0.0523	0.3827	-0.8062	-0.6767	0.2120	0.9695	-0.4632	-0.7346	1.0000																			
Lignin ¹	0.1950	0.5913	-0.3037	-0.0208	0.1206	0.2106	0.1715	0.6789	-0.0697	-0.3882	-0.7681	-0.6161	0.0638	0.9029	-0.8217	-0.7823	0.9223	1.0000																		
Control3mo	-0.6852	-0.0986	-0.2349	-0.2610	-0.6026	-0.1722	-0.3820	0.0637	0.1626	0.1048	0.4638	0.3967	0.0639	-0.2430	-0.2778	0.3093	-0.2217	-0.0744	1.0000																	
Moisture Content	-0.6338	-0.7609	-0.0705	0.0548	-0.1879	0.0368	-0.6316	-0.5164	-0.0642	0.6223	0.7056	0.7248	0.2642	-0.6895	0.5227	0.8016	-0.6888	-0.6628	0.9235	1.0000																
Mass Loss	0.0068	0.1173	-0.2511	-0.0606	-0.3078	0.0378	0.1778	0.1941	-0.2033	-0.1683	0.0184	0.0408	-0.0174	-0.1792	-0.1719	-0.0431	-0.1644	-0.0606	0.2401	-0.0426	1.0000															
Treatment3mo	-0.6435	-0.7803	-0.0382	0.0448	-0.1850	0.0011	-0.8077	-0.5638	-0.0431	0.6311	0.7616	0.2189	-0.7340	0.6194	0.6650	-0.7397	-0.7168	0.3989	0.9665	-0.0906	1.0000															
Mass Loss	-0.6437	-0.1843	-0.1184	-0.0274	-0.6880	-0.3181	-0.2240	0.2161	-0.0687	0.1718	0.4243	0.5722	-0.6558	-0.1274	0.4712	-0.6520	-0.3861	0.3744	0.9372	0.3093	0.4189	1.0000														
Moisture Content	-0.6054	-0.8085	0.1412	0.0034	-0.2631	-0.1719	-0.4174	-0.6913	0.0835	0.6015	0.8274	0.7764	-0.0499	-0.7162	0.5390	0.9380	-0.7321	-0.7487	0.3814	0.9046	-0.0008	0.9399	1.0000													
Mass Loss	-0.2933	0.0122	-0.3869	0.0096	-0.4982	-0.0019	-0.1356	0.0732	-0.4035	0.1471	0.1047	0.1634	0.0682	-0.2481	-0.2119	-0.0005	-0.2388	-0.0515	0.3088	0.1430	0.3988	0.1904	0.4108	0.1396	1.0000											
Treatment3mo	-0.6395	-0.8273	0.1487	0.1770	-0.1942	-0.1388	-0.8069	-0.7188	0.0030	0.6226	0.7761	0.0889	-0.7310	0.5904	0.9084	-0.7469	-0.7781	0.3125	0.9268	-0.0492	0.9633	0.4397	0.9361	0.1725	1.0000											
Control3mo	-0.6832	-0.4651	0.1666	-0.0719	-0.7680	-0.6376	-0.3828	-0.6092	0.2382	0.4228	0.6802	0.6976	-0.3633	-0.6317	-0.0808	0.7371	-0.6387	0.6477	0.8022	0.0926	0.4427	0.6871	0.7834	0.2486	0.6983	1.0000										
Mass Loss	-0.8938	0.7837	0.3117	0.0484	-0.2328	-0.2923	-0.3482	-0.7782	0.1676	0.5483	0.8288	0.7824	-0.1438	-0.7105	0.6372	0.9644	-0.7311	-0.7893	0.1937	0.8178	-0.1244	0.8832	0.4891	0.8434	-0.0079	0.9185	0.7819	1.0000								
Treatment3mo	-0.1759	-0.1746	-0.1239	0.1313	0.2044	-0.0069	-0.0831	-0.0383	-0.0777	0.0800	0.1687	0.2168	0.0079	-0.1454	0.0397	0.2085	-0.1407	-0.0661	0.1273	0.1744	-0.1894	0.1912	0.1812	0.2514	-0.1483	0.1722	0.2888	0.2745	1.0000							
Control3mo	-0.8985	-0.8537	0.2166	0.8907	-0.2129	-0.1874	-0.4410	-0.7435	0.0699	0.6160	0.6988	0.7762	0.0223	-0.7204	0.6714	0.9340	-0.7304	-0.7656	0.2905	0.9890	-0.0982	0.9290	0.4509	0.9744	0.0895	0.9712	0.7130	0.9591	0.2942	1.0000						
Moisture Content	-0.3398	-0.3651	0.1118	0.0729	-0.5448	-0.6527	-0.0414	-0.6581	0.2312	0.3388	0.6198	0.4124	-0.5689	-0.4388	-0.6857	0.3111	-0.3988	0.2060	0.4128	0.3988	-0.0260	0.4128	0.6109	0.8896	0.0604	0.6121	0.7770	0.6683	1.0000							
Mass Loss	-0.1111	-0.5935	0.8417	0.1822	-0.2038	-0.6091	0.0107	-0.9287	0.1848	0.4302	0.2889	0.7025	-0.4303	-0.5195	0.4417	0.7070	-0.6538	-0.7281	0.0115	0.4628	-0.0494	0.9221	0.3848	0.6757	-0.0281	0.6798	0.6131	0.7915	0.0288	0.7087	0.7711	1.0000				
Control3mo	-0.2935	-0.4128	0.1138	0.0078	-0.4029	-0.0247	-0.4857	-0.1222	0.2751	0.0778	0.2021	-0.2666	-0.4727	-0.1873	0.0593	-0.4896	-0.4577	0.4689	0.3570	0.3374	0.1658	0.3408	0.9599	0.3789	0.9396	0.5345	0.4792	-0.0818	0.4813	0.5773	0.6102	1.0000				
Moisture Content	-0.2882	-0.7412	0.4390	0.0478	-0.1834	-0.3948	-0.1922	0.8826	0.1815	0.6286	0.7651	0.6183	-0.2675	-0.6414	0.6288	0.6892	-0.6702	-0.7724	0.2184	0.7018	-0.0144	0.1458	0.4372	0.8768	-0.0544	0.8826	0.6590	0.9035	0.8637	0.9173	0.7108	0.8805	0.6709	1.0000		



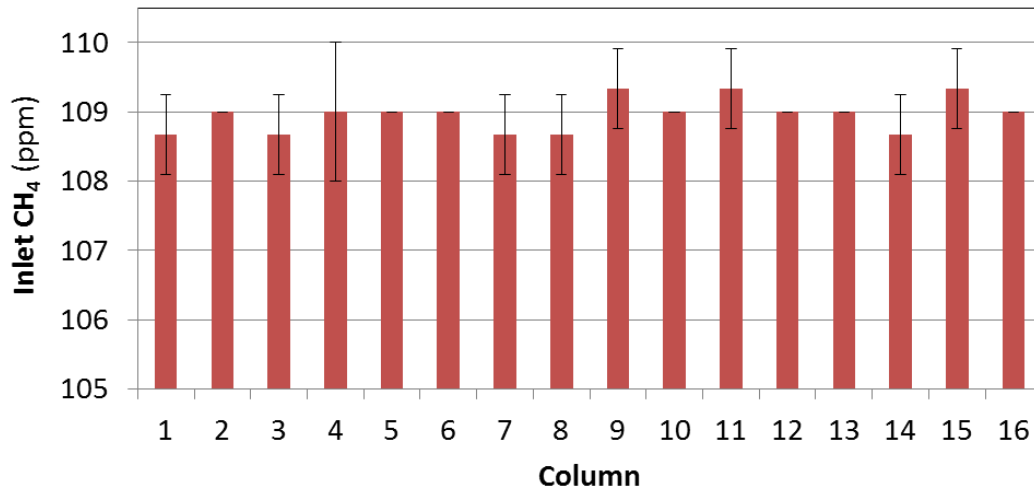
Appendix 5.5 Boxplot overlays depicting the mass remaining for averaged softwood, averaged hardwood, mulch and cob media for the control and treatment biofilter locations.



Appendix 5.6 Comparison of birch and SYP mass remaining after year 1 (June 2012-2013), year 2 (June 2013-2014) losses, and for the N treatment control (June 2013-2014) losses for both biofilter locations.

Appendix 5.7 Mean and (standard deviation) dilute alkali solubility (DAS) of tested biofilter media at time zero, 27 mo. collections, and their change over time (Δ) for both biofilter locations (n=3). DAS values were used to calculate the probability of white rot fungal decay (PWR) and brown rot fungal decay (PBR) for both biofilter locations according to the methods of Schilling et al. (2015).

Media Type	Spp.	t=0		DAS		DAS		Δ		P _{WR}	P _{BR}	P _{WR}	P _{BR}
				Control	Treatment	Control	Treatment	Control	Treatment	Control	Control	Treatment	Treatment
		%	%	%	%	%	%	%	%	%	%	%	%
Softwood	Cedar	22.6	0.9	34.7	3.0	34.0	1.9	12.0	11.4	14.7	85.3	18.6	81.4
	Pine	16.2	2.1	27.9	1.1	28.3	1.9	11.6	12.0	73.0	27.0	69.8	30.2
	SYP	13.4	0.5	29.1	1.1	27.2	0.5	15.7	13.9	69.2	30.8	83.3	16.7
Hardwood	Ash	21.7	1.0	31.5	1.4	33.3	3.0	9.7	11.5	100.0	0.0	100.0	0.0
	Aspen	18.8	2.0	40.3	4.5	37.9	7.6	21.5	19.1	41.0	59.0	94.3	5.7
	Birch	19.1	0.9	42.8	4.6	34.8	5.7	23.8	15.7	0.5	99.5	99.9	0.1
	Maple	17.1	1.0	26.5	1.2	25.0	3.1	9.4	7.9	100.0	0.0	100.0	0.0
	Oak	19.4	2.1	36.8	0.8	32.0	3.8	17.4	12.6	98.8	1.2	100.0	0.0
Byproducts	Cob	45.0	3.0	66.1	8.3	64.0	3.8	21.1	19.0	0.0	100.0	0.0	100.0
	Mulch	30.7	0.9	52.1	2.5	52.8	4.9	21.5	22.1	0.0	100.0	0.0	100.0



Appendix 6.1 Comparison of inlet emissions for the 16 lab-scale biofilter test columns (n=3).

Appendix 6.2 Basidiomycetes Selective Agar Recipe

Mix the following in a 1 L flask

10 g malt extract

7.5 g agar

1 g yeast extract

0.03 g benomyl (helps to mix in a small amount of warm ethanol; stir)

Add 500 ml water

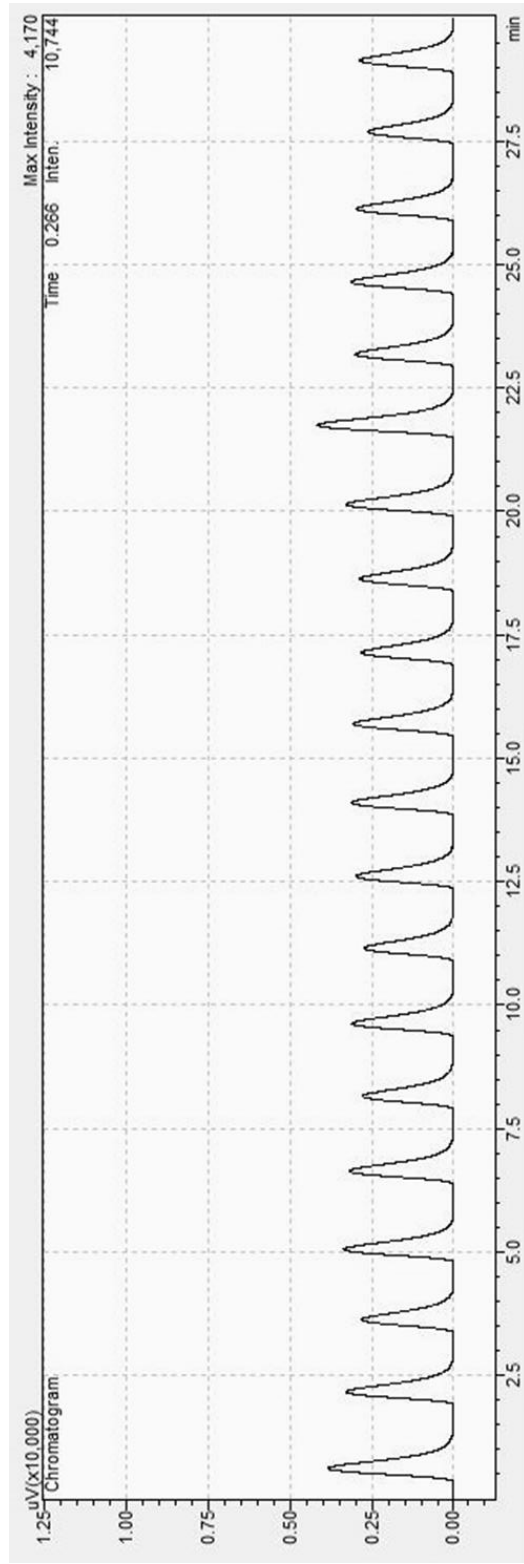
Cover and autoclave for 30 minutes at 121C/15 psi

After autoclaving add:

0.005 g streptomycin sulfate by making a stock solution and adding using a sterile 1.2
micro meter syringe filter

1 ml lactic acid

Pour plates



Appendix 6.3 Chromatogram of repeated injections shows no significant loss of sorption capacity (rise in peak height/area) with 20 repeat injections of 100ppm CH₄ into a column packed with a spore test media over a 30 min. period.